

Common Origin of $\mu - \tau$ and CP Breaking in Neutrino Seesaw, Baryon Asymmetry, and Hidden Flavor Symmetry

HONG-JIAN HE ^{a,b,c}* and FU-RONG YIN ^a†

^a Institute of Modern Physics and Center for High Energy Physics,
Tsinghua University, Beijing 100084, China

^b Center for High Energy Physics, Peking University, Beijing 100871, China

^c Kavli Institute for Theoretical Physics China,
Chinese Academy of Sciences, Beijing 100190, China

Abstract

We conjecture that all CP violations (both Dirac and Majorana types) arise from a common origin in neutrino seesaw. With this conceptually attractive and simple conjecture, we deduce that $\mu - \tau$ breaking *shares the common origin with all CP violations*. We study the common origin of $\mu - \tau$ and CP breaking in the Dirac mass matrix of seesaw Lagrangian (with right-handed neutrinos being $\mu - \tau$ blind), which uniquely leads to inverted mass-ordering of light neutrinos. We then predict a very different correlation between the two small $\mu - \tau$ breaking observables $\theta_{13} - 0^\circ$ and $\theta_{23} - 45^\circ$, *which can saturate the present experimental upper limit on θ_{13}* . This will be tested against our previous normal mass-ordering scheme by the on-going oscillation experiments. We also analyze the correlations of θ_{13} with Jarlskog invariant and neutrinoless $\beta\beta$ -decay observable. From the common origin of CP and $\mu - \tau$ breaking in the neutrino seesaw, we establish a direct link between the low energy CP violations and the cosmological CP violation for baryon asymmetry. With these we further predict a *lower bound* on θ_{13} , supporting the on-going probes of θ_{13} at Daya Bay, Double Chooz and RENO experiments. Finally, we analyze the general model-independent $\mathbb{Z}_2 \otimes \mathbb{Z}_2$ symmetry structure of the light neutrino sector, and map it into the seesaw sector, where one of the \mathbb{Z}_2 's corresponds to the $\mu - \tau$ symmetry $\mathbb{Z}_2^{\mu\tau}$ and another the hidden symmetry \mathbb{Z}_2^s (revealed in our previous work) which dictates the solar mixing angle θ_{12} . We derive the physical consequences of this \mathbb{Z}_2^s and its possible partial violation in the presence of $\mu - \tau$ breaking (*without or with neutrino seesaw*), regarding the θ_{12} determination and the correlation between $\mu - \tau$ breaking observables.

PACS numbers: 14.60.Pq, 12.15.Ff, 13.15.+g, 13.40.Em

Phys. Rev. D 84 (2011) 033009 and arXiv:1104.2654

*hjhe@tsinghua.edu.cn

†yfr@tsinghua.edu.cn

CONTENTS

1. Introduction	3
2. Common Origin of $\mu-\tau$ and CP Breaking from Neutrino Seesaw with Inverted Ordering	5
2.1. $\mu-\tau$ and CP Symmetries of Neutrino Seesaw with Inverted Ordering.....	6
2.2. Common Origin of $\mu-\tau$ and CP Breaking in the $\mu-\tau$ Blind Seesaw	9
2.3. Perturbative Expansion for $\mu-\tau$ and CP Breaking	11
3. Inverted Ordering: Reconstructing Light Neutrino Mass Matrix with $\mu-\tau$ and CP Violations at Low Energy	13
3.1. Notation Setup and Model-Independent Reconstruction	13
3.2. Reconstruction of Light Neutrino Mass Matrix with Inverted Ordering	15
4. Predictions of Common $\mu-\tau$ and CP Breaking with Inverted Ordering ...	18
4.1. Predicting Correlations of Low Energy Neutrino Observables	18
4.2. Baryon Asymmetry from $\mu-\tau$ Blind Seesaw and Direct Link to Low Energy.....	26
4.3. Extension to General Three-Neutrino Seesaw.....	33
5. Hidden Symmetry and Dictation of Solar Mixing Angle	38
5.1. $\mu-\tau$ Breaking versus θ_{12} Determination: Inverted Mass-Ordering	38
5.2. \mathbb{Z}_2^s Symmetry under General $\mu-\tau$ Breaking and General Determination of θ_{12}	40
5.2.1. \mathbb{Z}_2^s Symmetry for General Determination of Solar Angle θ_{12}	41
5.2.2. \mathbb{Z}_2^s Symmetry and Neutrino Mass-Matrix with General $\mu-\tau$ Breaking	45
5.3. Mapping $\mathbb{Z}_2 \otimes \mathbb{Z}_2$ Hidden Symmetry into Neutrino Seesaw	49
5.3.1. Neutrino Seesaw with Common Soft $\mu-\tau$ and CP Breaking.....	50
5.3.2. $\mu-\tau$ Blind Seesaw with Common $\mu-\tau$ and CP Breaking.....	52
6. Conclusion	55
Note Added in Proof	56
Note Added-2	60
Acknowledgments	62
References	63

1. Introduction

We conjecture that all CP violations (both Dirac and Majorana types) arise from a common origin in neutrino seesaw. With this conceptually attractive and simple conjecture, we deduce that $\mu-\tau$ breaking shares the common origin with all CP violations, since the $\mu-\tau$ symmetric limit enforces vanishing mixing angle θ_{13} and thus Dirac CP conservation.

In a recent work [1], we studied the common origin of soft $\mu-\tau$ and CP breaking in the neutrino seesaw, which is uniquely formulated in the dimension-3 Majorana mass term of singlet right-handed neutrinos. This formulation predicts the normal mass ordering (NMO) for light neutrinos. In this work, we study in parallel a different realization of the common origin of $\mu-\tau$ and CP breaking in the “ $\mu-\tau$ blind seesaw”, where the right-handed neutrinos are singlet under the $\mu-\tau$ transformation. We then find *the Dirac mass-matrix to be the unique place for the common origin of $\mu-\tau$ and CP breaking* in the $\mu-\tau$ blind seesaw. Since the Dirac mass-matrix arises from Yukawa interactions with Higgs boson(s), this can also provide an interesting possibility of realizing spontaneous CP violation with CP phases originating from the vacuum expectation values of Higgs fields. Different from our previous construction [1], we reveal that the common origin of $\mu-\tau$ and CP breaking in the Dirac mass-matrix uniquely leads to the inverted mass-ordering (IMO) of light neutrinos and thus different neutrino phenomenology. Hence, the present mechanism can be distinguished from the previous one [1] by the on-going and upcoming experiments on the neutrino oscillations [2] and neutrinoless double-beta decays [3].

The oscillation data from solar and atmospheric neutrinos, and from the terrestrial neutrino beams produced in the reactor and accelerator experiments, have measured two mass-squared differences (Δm_{31}^2 , Δm_{21}^2) and two large mixing angles (θ_{12} , θ_{23}) to good accuracy [4][5]. The two compelling features are [4][5]: (i) the atmospheric neutrino mixing angle θ_{23} has only small deviations from its maximal value of $\theta_{23} = 45^\circ$; (ii) the reactor neutrino mixing angle θ_{13} is found to be small, having its allowed range still consistent with $\theta_{13} = 0^\circ$ at 90% C.L. Hence, the pattern of $(\theta_{23}, \theta_{13}) = (45^\circ, 0^\circ)$ is strongly supported by the experimental data as *a good zeroth order approximation*. It is important to note that this pattern corresponds to the $\mu-\tau$ symmetry and Dirac CP conservation in the neutrino sector, where the $\mu-\tau$ symmetry is determined by both values of $(\theta_{23}, \theta_{13}) = (45^\circ, 0^\circ)$ and the Dirac CP conservation is due to $\theta_{13} = 0^\circ$. On the theory ground, it is natural and tempting to expect a common origin for all CP-violations, although the Dirac and Majorana CP-violations appear differently in the light neutrino mass-matrix of the low energy effective theory. Given such a common origin for two kinds of CP-violations, then they must vanish together in the $\mu-\tau$ symmetric limit. For the $\mu-\tau$ blind seesaw, we can uniquely formulate this common breaking in the Dirac mass matrix, leading to distinct neutrino phenomenology.

With such a conceptually attractive and simple construction of the common breaking of two discrete symmetries, we can predict the $\mu-\tau$ breaking at low energies and derive *quantitative correlations between the two small deviations*, $\theta_{23} - 45^\circ$ and $\theta_{13} - 0^\circ$, very different from that of the

previous NMO scheme [1]. Our predicted range of θ_{13} can saturate its present experimental upper limit. The improved measurements of θ_{23} will come from the Minos [7] and T2K [8] experiments, etc, while θ_{13} will be more accurately probed by the on-going reactor experiments, Daya Bay [10][11], Double Chooz [12], and RENO [13], as well as the accelerator experiments T2K [8], NO ν A [14] and LENA [15], etc. We further derive the observed baryon asymmetry via leptogenesis at seesaw scale, and analyze the correlation between the leptogenesis and the low energy neutrino observables in the present IMO scheme. Especially, we deduce a lower bound on the reactor neutrino mixing angle $\theta_{13} \gtrsim 1^\circ$, and demonstrate that most of the predicted parameter space will be probed by the on-going Double Chooz, Daya Bay, and RENO reactor experiments.

Finally, we will analyze the most general $\mathbb{Z}_2 \otimes \mathbb{Z}_2$ symmetry structure of the light neutrino sector, and map it into the seesaw sector, where one of the \mathbb{Z}_2 's is the $\mu-\tau$ symmetry $\mathbb{Z}_2^{\mu\tau}$ and another the hidden symmetry \mathbb{Z}_2^s (revealed in our recent work [1] for the NMO scheme), which dictates the solar mixing angle θ_{12} . We derive the physical consequences of the \mathbb{Z}_2^s for the most general light neutrino mass-matrix (without seesaw) and for the seesaw models (with different $\mu-\tau$ breaking mechanisms). In particular, we analyze the partial violation of \mathbb{Z}_2^s in the presence of $\mu-\tau$ breaking for the $\mu-\tau$ blind seesaw, which leads to *a modified new correlation between the $\mu-\tau$ breaking observables*, very different from that of Ref. [1]. The determination of θ_{12} is systematically studied for the current IMO scheme and the partial violation of \mathbb{Z}_2^s will be clarified.

We organize this paper as follows. In Sec. 2 we present a unique construction for the common origin of the $\mu-\tau$ and CP breakings in the neutrino seesaw with $\mu-\tau$ blind right-handed neutrinos. Then, we give in Sec. 3 a model-independent reconstruction of light neutrino mass-matrix under inverted mass-ordering and with small $\mu-\tau$ and CP violations at low energies. In Sec. 4.1, we explicitly derive the low energy $\mu-\tau$ and CP violation observables from the common breaking in the Dirac mass-matrix of the $\mu-\tau$ blind seesaw. These include the two small deviations for the mixing angles $\theta_{23} - 45^\circ$ and $\theta_{13} - 0^\circ$, the Jarlskog invariant for CP-violations, and the M_{ee} element for neutrinoless double-beta decays. In Sec. 4.2 we study the cosmological CP violation via leptogenesis in our model, this can generate the observed baryon asymmetry of the universe. Using all the existing data from neutrino oscillations and the observed baryon asymmetry [16, 17], we derive the direct link between the cosmological CP-violation and the low energy Jarlskog invariant J . We further predict a lower bound on the reactor mixing angle θ_{13} , and deduce a nonzero Jarlskog invariant J with negative range. We also establish a lower limit on the leptogenesis scale for producing the observed baryon asymmetry. In Sec. 5, we analyze the determination of solar mixing angle θ_{12} and its relation to the hidden symmetry \mathbb{Z}_2^s in the light neutrino sector (without seesaw) and in the seesaw sector (with two different realizations of $\mu-\tau$ breaking). Finally, conclusions are summarized in the last section 6.

2. Common Origin of $\mu-\tau$ and CP Breaking from Neutrino Seesaw with Inverted Ordering

The current global fit of neutrino data [4] for the three mixing angles and two mass-squared differences is summarized in Table-1. We note a striking pattern of the mixing angles, where the atmospheric angle θ_{23} has its central value slightly below the maximal mixing [18] of 45° and the reactor angle θ_{13} slightly above 0° . So the neutrino data support two small deviations $\theta_{23} - 45^\circ$ and $\theta_{23} - 0^\circ$ of the same order,

$$-7.0^\circ < (\theta_{23} - 45^\circ) < 5.5^\circ, \quad 0^\circ \leq (\theta_{13} - 0^\circ) < 9.5^\circ, \quad (2.1)$$

at 90% C.L., with the best fitted values, $(\theta_{23} - 45^\circ) = -2.2^\circ$ and $(\theta_{13} - 0^\circ) = 5.1^\circ$. This justifies a fairly good *zeroth order approximation*, $\theta_{23} = 45^\circ$ and $\theta_{13} = 0^\circ$, under which two exact discrete symmetries emerge, i.e., the $\mu-\tau$ symmetry [19] and the Dirac CP conservation in the neutrino sector. It is clear that the $\mu-\tau$ symmetry and the associated Dirac CP-invariance are well supported by all neutrino data as a good *zeroth order approximation*, and have to appear in any viable theory for neutrino mass-generation. We also note that the $\theta_{13} = 0^\circ$ limit does not remove the possible low energy Majorana CP-phases, but since the Majorana CP-violation comes from a common origin with the Dirac CP-violation in our theory construction (cf. below), it has to vanish as the Dirac CP-violation goes to zero in the $\mu-\tau$ symmetric limit.

Parameters	Best Fit	90% C.L.	99% C.L.	1σ Limits	3σ Limits
$\Delta m_{21}^2 (10^{-5} \text{eV}^2)$	7.59	7.26 – 7.92	7.00 – 8.11	7.39 – 7.79	6.90 – 8.20
$\Delta m_{31}^2 (10^{-3} \text{eV}^2)$ (NMO)	2.46	2.26 – 2.66	2.14 – 2.78	2.34 – 2.58	2.09 – 2.83
$\Delta m_{13}^2 (10^{-3} \text{eV}^2)$ (IMO)	2.36	2.18 – 2.54	2.04 – 2.68	2.25 – 2.47	1.99 – 2.73
θ_{12}	34.5°	$32.8^\circ – 36.0^\circ$	$32.1^\circ – 37.2^\circ$	$33.5^\circ – 35.5^\circ$	$31.7^\circ – 37.7^\circ$
θ_{23}	42.8°	$38.0^\circ – 50.5^\circ$	$36.5^\circ – 52.0^\circ$	$39.9^\circ – 47.5^\circ$	$35.5^\circ – 53.5^\circ$
θ_{13}	5.1°	$0^\circ – 9.5^\circ$	$0^\circ – 11.3^\circ$	$1.8^\circ – 8.1^\circ$	$0^\circ – 12.0^\circ$

Table 1: Updated global analysis [4] of solar, atmospheric, reactor and accelerator neutrino data for three-neutrino oscillations, where the AGSS09 solar fluxes and the modified Gallium capture cross-section [20] are used.

In our theory construction, we conjecture that all CP violations (both Dirac and Majorana types) have a common origin and thus they must share the common origin with the $\mu-\tau$ breaking. For the neutrino seesaw with heavy right-handed neutrinos blind to the $\mu-\tau$ symmetry, this common origin can only come from the Dirac mass-term. In the following, we first consider the minimal neutrino seesaw Lagrangian with exact $\mu-\tau$ and CP invariance, from which we will derive the seesaw mass-matrix for the light neutrinos. Diagonalizing this zeroth order mass-matrix we predict the inverted mass-ordering of light neutrinos and deduce the mixing angles, $(\theta_{23}, \theta_{13})_0 = (45^\circ, 0^\circ)$, as well as

a formula for the solar angle θ_{12} . Then we will construct the common origin for the $\mu-\tau$ and CP breaking in the Dirac mass-matrix. Finally, we systematically expand the small $\mu-\tau$ and CP breaking effects in the seesaw mass-matrix to the first nontrivial order.

2.1. $\mu-\tau$ and CP Symmetries of Neutrino Seesaw with Inverted Ordering

The right-handed neutrinos are singlets under the standard model gauge group, and thus can be Majorana fields with large masses. This naturally realizes the seesaw mechanism [21] which provides the simplest explanation for the small masses of light neutrinos. For simplicity, we consider the Lagrangian for the minimal neutrino seesaw [22, 23], with two right-handed singlet Majorana neutrinos besides the standard model (SM) particle content,

$$\begin{aligned}\mathcal{L}_{\text{ss}} &= -\overline{L} Y_\ell \Phi \ell_R - \overline{L} Y_\nu \tilde{\Phi} \mathcal{N} + \frac{1}{2} \mathcal{N}^T M_R \tilde{C} \mathcal{N} + \text{h.c.} \\ &= -\overline{\ell_L} M_\ell \ell_R - \overline{\nu_L} m_D \mathcal{N} + \frac{1}{2} \mathcal{N}^T M_R \tilde{C} \mathcal{N} + \text{h.c.} + (\text{interactions}),\end{aligned}\quad (2.2)$$

where L represents three left-handed neutrino-lepton weak doublets, $\ell = (e, \mu, \tau)^T$ denotes charged leptons, $\nu_L = (\nu_e, \nu_\mu, \nu_\tau)^T$ is the light flavor neutrinos, and $\mathcal{N} = (N_1, N_2)^T$ contains two heavy right-handed singlet neutrinos. The lepton Dirac-mass-matrix $M_\ell = v Y_\ell / \sqrt{2}$ and the neutrino Dirac-mass-matrix $m_D = \frac{v}{\sqrt{2}} Y_\nu$ arise from the Yukawa interactions after spontaneous electroweak symmetry breaking, $\langle \Phi \rangle = (0, \frac{v}{\sqrt{2}})^T \neq 0$, and the Majorana mass-term for M_R is a gauge-singlet. We can regard this minimal seesaw Lagrangian in Eq. (2.2) as an effective theory of the general three-neutrino seesaw where the right-handed singlet N_3 is much heavier than the other two (N_1, N_2) and thus can be integrated out at the mass-scales of (N_1, N_2) , leading to Eq. (2.2). As a result, the minimal seesaw generically predicts a massless light neutrino [22]; this is always a good approximation as long as one of the light neutrinos has a negligible mass in comparison with the other two (even if not exactly massless). Extension to the three-neutrino seesaw will be discussed in Sec. 4.3.

Let us integrate out the heavy neutrinos (N_1, N_2) in (2.2) and derive the seesaw formula for the 3×3 symmetric Majorana mass-matrix of the light neutrinos,

$$M_\nu \simeq m_D M_R^{-1} m_D^T, \quad (2.3)$$

where m_D is the 3×2 Dirac mass-matrix, and M_R is the 2×2 Majorana mass-matrix. The diagonalization of M_ν is achieved by unitary rotation matrix U_ν via $U_\nu^T M_\nu U_\nu = D_\nu$ with $D_\nu = \text{diag}(m_1, m_2, m_3)$.

The Lagrangian (2.2) is defined to respect both the $\mu-\tau$ and CP symmetries. Under the $\mu-\tau$ symmetry $\mathbb{Z}_2^{\mu\tau}$, we have the transformation, $\nu_\mu \leftrightarrow p \nu_\tau$, where $p = \pm$ denotes the even/odd parity assignments of the light neutrinos under $\mathbb{Z}_2^{\mu\tau}$. Since the $\mu-\tau$ symmetry has been tested at low energy via mixing angles of light neutrinos, it is logically possible that the right-handed heavy Majorana neutrinos in the seesaw Lagrangian (2.2) are singlets under $\mathbb{Z}_2^{\mu\tau}$ (called “ $\mu-\tau$ blind”), which is actually the simplest realization of $\mu-\tau$ symmetry in the neutrino seesaw. In this work we

consider that the right-handed Majorana neutrinos \mathcal{N} to be $\mu-\tau$ blind, i.e., both (N_1, N_2) are the singlets under $\mathbb{Z}_2^{\mu\tau}$, and thus can be first rotated into their mass-eigenbasis without affecting the $\mu-\tau$ symmetric structure of the Dirac mass-matrix m_D . So, in the mass-eigenbasis of (N_1, N_2) , we have $M_R = \text{diag}(M_1, M_2)$. Under the $\mu-\tau$ and CP symmetries, the Dirac mass-matrix m_D is real and obeys the invariance equation,

$$G_\nu^T m_D = m_D, \quad (2.4)$$

with

$$G_\nu = \begin{pmatrix} 1 & 0 & 0 \\ 0 & 0 & p \\ 0 & p & 0 \end{pmatrix}. \quad (2.5)$$

Next, we note that due to the large mass-splitting of μ and τ leptons, the lepton sector can exhibit, in general, a different flavor symmetry \mathbb{G}_ℓ from the $\mu-\tau$ symmetry $\mathbb{Z}_2^{\mu\tau}$ in the neutrino sector. The two symmetries $\mathbb{Z}_2^{\mu\tau}$ and \mathbb{G}_ℓ could originate from spontaneous breaking of a larger flavor symmetry \mathbb{G}_F [24]. Under the transformation of left-handed leptons $F_\ell \in \mathbb{G}_\ell$, we have the invariance equation of lepton mass-matrix, $F_\ell^\dagger M_\ell M_\ell^\dagger F_\ell = M_\ell M_\ell^\dagger$. As we will show in Sec. 4.2, we are free to choose an equivalent representation $d_\ell = U_\ell^\dagger F_\ell U_\ell$ of \mathbb{G}_ℓ from the start under which the left-handed leptons are in their mass-eigenbasis, where U_ℓ is the transformation matrix diagonalizing the lepton mass-matrix, $U_\ell^\dagger M_\ell M_\ell^\dagger U_\ell = D_\ell^2$ with $D_\ell = \text{diag}(m_e, m_\mu, m_\tau)$. This means that in the lepton mass-eigenbasis, the conventional Pontecorvo-Maki-Nakagawa-Sakata (PMNS) mixing matrix V [28] in the leptonic charged current (an analog of the CKM matrix [29] in the quark sector) is fixed by the transformation U_ν of neutrino mass-diagonalization, $V = U_\nu$. We can further rotate the right-handed leptons into their mass-eigenbasis, without affecting the PMNS matrix, except making the lepton-mass-term diagonal in the seesaw Lagrangian (2.2), i.e., $M_\ell = \text{diag}(m_e, m_\mu, m_\tau)$.

Under the $\mu-\tau$ and CP symmetries, we find the Dirac mass-matrix m_D to have the following form,

$$m_D = \begin{pmatrix} \bar{a} & \bar{a}' \\ \bar{b} & \bar{c} \\ \bar{b} & \bar{c} \end{pmatrix} = \begin{pmatrix} \sigma_1 a & \sigma_2 a' \\ \sigma_1 b & \sigma_2 c \\ \sigma_1 b & \sigma_2 c \end{pmatrix}, \quad (2.6)$$

with all elements being real, and $\sigma_1 \equiv \sqrt{\hat{m}_0 M_1}$, $\sigma_2 \equiv \sqrt{\hat{m}_0 M_2}$. As will be shown shortly, the parameter \hat{m}_0 is defined at the seesaw scale and equals the nonzero mass-eigenvalue of the light neutrinos at zeroth-order under the $\mu-\tau$ symmetric limit. In (2.6) we have also defined four dimensionless parameters,

$$(a, b) \equiv \frac{(\bar{a}, \bar{b})}{\sqrt{\hat{m}_0 M_1}}, \quad (a', c) \equiv \frac{(\bar{a}', \bar{c})}{\sqrt{\hat{m}_0 M_2}}. \quad (2.7)$$

Then, we find it convenient to define a dimensionless Dirac matrix,

$$\overline{m}_D \equiv m_D (\hat{m}_0 M_R)^{-\frac{1}{2}} = \begin{pmatrix} a & a' \\ b & c \\ b & c \end{pmatrix}. \quad (2.8)$$

Substituting the above into the seesaw equation (2.3), we derive the $\mu-\tau$ and CP symmetric mass-matrix for light neutrinos,

$$M_\nu \simeq m_D M_R^{-1} m_D^T = \hat{m}_0 (\overline{m}_D \overline{m}_D^T) = \hat{m}_0 \begin{pmatrix} a^2 + a'^2 & ab + a'c & ab + a'c \\ & b^2 + c^2 & b^2 + c^2 \\ & & b^2 + c^2 \end{pmatrix}, \quad (2.9)$$

which we call the *zeroth order mass-matrix*. In the next subsection we will further include the small $\mu-\tau$ and CP breaking effect. Note that from (2.9), we have $\det(M_\nu) = 0$, which generally holds in any minimal seesaw.

Diagonalizing the mass-matrix (2.9), we derive the mass-eigenvalues and mixing angles at zeroth order,

$$\hat{m}_{1,2} = \frac{\hat{m}_0}{2} \left[(a^2 + a'^2 + 2b^2 + 2c^2) \mp \sqrt{[(a^2 + a'^2) - 2(b^2 + c^2)]^2 + 8(ab + a'c)^2} \right], \quad (2.10a)$$

$$\hat{m}_3 = 0, \quad (2.10b)$$

$$\tan 2\theta_{12} = \frac{2\sqrt{2}|ab + a'c|}{|a^2 + a'^2 - 2(b^2 + c^2)|}, \quad \theta_{23} = 45^\circ, \quad \theta_{13} = 0^\circ, \quad (2.10c)$$

where we have made all mass-eigenvalues positive and the mixing angles $(\theta_{12}, \theta_{13}, \theta_{23})$ within the range $[0, \frac{\pi}{2}]$ by properly defining the rotation matrix. (As shown in Table-1, the solar angle θ_{12} is most precisely measured and its 3σ range is below 37.7° , so we always have $2\theta_{12} < \frac{\pi}{2}$ and $\tan 2\theta_{12} > 0$.) The mixing angles $(\theta_{23}, \theta_{13}) = (45^\circ, 0^\circ)$ are direct consequence of the $\mu-\tau$ symmetry, but this symmetry does not fix θ_{12} . Eqs.(2.10a)-(2.10b) show that the mass-spectrum of light neutrinos falls into the “inverted mass-ordering” (IMO), $\hat{m}_2 \gtrsim \hat{m}_1 \gg \hat{m}_3$.

Table-1 shows that the ratio of two mass-squared differences, $\frac{\Delta m_{21}^2}{|\Delta m_{31}^2|} \ll 1$. Since for the minimal seesaw model with IMO, the equation $\det(M_\nu) = 0$ leads to $\hat{m}_3 = 0$, so the above ratio requires the approximate degeneracy $\hat{m}_1 \simeq \hat{m}_2$ to be a good zeroth order approximation as enforced by the neutrino oscillation data. So, we will realize the exact degeneracy $\hat{m}_1 = \hat{m}_2$ for the $\mu-\tau$ and CP symmetric mass-matrix (2.9), by imposing the relations for Eq. (2.10a),

$$(a^2 + a'^2) - 2(b^2 + c^2) = 0, \quad ab + a'c = 0. \quad (2.11)$$

As will be shown in the next subsection, including the common origin of $\mu-\tau$ and CP breaking in the neutrino seesaw can produce small non-degeneracy between \hat{m}_1 and \hat{m}_2 at the next-to-leading order (NLO). Since the mass-parameter \hat{m}_0 is introduced in (2.7) for defining the dimensionless parameters (a, b, c) , we can now fix \hat{m}_0 by defining

$$\hat{m}_0 \equiv \hat{m}_1 = \hat{m}_2, \quad (2.12)$$

as the zeroth order mass-eigenvalue of light neutrinos, under the normalization condition,

$$(a^2 + a'^2) + 2(b^2 + c^2) = 2. \quad (2.13)$$

Combining this relation to Eq. (2.11), we can deduce,

$$a^2 = 2c^2 = 1 - 2b^2, \quad a'^2 = 2b^2, \quad c^2 = \frac{1}{2} - b^2, \quad a'c = -ab, \quad (2.14)$$

where we see that three of the four parameters, (a, a', c) , can all be solved in terms of b . The last equation in (2.14) is not independent, but it helps to fix a relative sign. We note that in (2.9) the $\mu-\tau$ symmetric seesaw mass-matrix M_ν contains five parameters, the mass-parameter \hat{m}_0 and the four dimensionless parameters (a, b, c, a') . The inverted mass-spectrum have imposed a LO condition $\hat{m}_1 = \hat{m}_2$, which results in two constraints in (2.11), and the normalization condition $\hat{m}_0 \equiv \hat{m}_1$ in (2.12) leads to the third constraint (2.13). In consequence, we end up with only two independent parameters, \hat{m}_0 and b .

We note that under the condition of (2.11), the mixing angle θ_{12} given by (2.10c) has no definition at the zeroth order (the $\mu-\tau$ symmetric limit) due to the vanishing numerator and denominator in the formula of $\tan 2\theta_{12}$. But including the small $\mu-\tau$ breaking effect will generate the nonzero expression of θ_{12} at the NLO even though its final formula does not depend on the $\mu-\tau$ breaking parameter (cf. Sec. 2.2). As we will show in Sec. 2.2, the $\mu-\tau$ breaking arises from deviation in the element c of m_D , so we can apply the l'Hôpital rule to the expression of $\tan 2\theta_{12}$ by taking the first-order derivatives on its numerator/denominator respect to c and deduce,

$$\tan 2\theta_{12} = \frac{|a'|}{\sqrt{2}|c|} = \frac{|\bar{a}'|}{\sqrt{2}|\bar{c}|}, \quad (2.15)$$

which is consistent with (4.5) of Sec. 4.1 from the explicit NLO analysis. For the case with $\mu-\tau$ breaking arising from deviation in the element b of m_D , we can apply the l'Hôpital rule again to infer the formula,

$$\tan 2\theta_{12} = \frac{|a|}{\sqrt{2}|b|} = \frac{\sqrt{2}|c|}{|a'|}, \quad (2.16)$$

which is *the inverse of (2.15)*. As will be shown in Sec. 5.2, the different forms of $\mu-\tau$ breaking will affect the determination of the solar mixing angle θ_{12} . But it is worth to note that the expression of θ_{12} is fixed by the $\mu-\tau$ symmetric m_D as in (2.15) or (2.16), and does not explicitly depend on the $\mu-\tau$ breaking parameter. We will systematically analyze these features in Sec. 5 and clarify the difference from our previous construction [1].

2.2. Common Origin of $\mu-\tau$ and CP Breaking in the $\mu-\tau$ Blind Seesaw

In this subsection, we will construct a unique breaking term providing a common origin for both $\mu-\tau$ and CP breaking. From this we will further derive predictions of the common $\mu-\tau$ and CP breaking for the low energy light neutrino mass-matrix, by treating the small breaking as perturbation up to the first nontrivial order (Sec. 4). We will analyze the seesaw-scale leptogenesis and its correlations with the low energy observables in Sec. 4.2.

As we have explained, the $\mu-\tau$ symmetry serves as a good zeroth order flavor symmetry of the neutrino sector, which predicts $\theta_{13} = 0$ and thus the Dirac CP-conservation. Hence, the $\mu-\tau$

symmetry breaking is generically small, and must generate all Dirac CP-violations at the same time. On the theory ground, it is natural and tempting to expect a *common origin for all CP-violations*, even though the Dirac and Majorana CP-violations appear differently in the light neutrino mass-matrix of the low energy effective theory. For the two kinds of CP-violations arising from a common origin, then they must vanish together in the $\mu-\tau$ symmetric limit.

Different from our previous study [1], we consider the heavy right-handed neutrinos to be $\mu-\tau$ blind in the neutrino seesaw. Thus the Majorana mass-matrix M_R of the right-handed neutrinos must be $\mu-\tau$ singlet. Hence, we deduce that *the unique common origin of the $\mu-\tau$ and CP breaking must arise from the Dirac mass-matrix of the seesaw Lagrangian (2.2)*. For the minimal seesaw, the most general form of m_D is

$$m_D = \begin{pmatrix} \bar{a} & \bar{a}' \\ \bar{b}_1 & \bar{c}_1 \\ \bar{b}_2 & \bar{c}_2 \end{pmatrix} = \begin{pmatrix} \sigma_1 a & \sigma_2 a' \\ \sigma_1 b_1 & \sigma_2 c_1 \\ \sigma_1 b_2 & \sigma_2 c_2 \end{pmatrix}, \quad (2.17)$$

where the scaling factors $\sigma_1 \equiv \sqrt{\hat{m}_0 M_1}$ and $\sigma_2 \equiv \sqrt{\hat{m}_0 M_2}$ are real mass-parameters as defined in Eq. (2.6). The six elements of m_D can be complex in general. But there are three rephasing degrees of freedom for the left-handed lepton-doublets. So we can always rotate the three elements in the first column of m_D to be all real, hence the remaining CP phases (associated with the $\mu-\tau$ breaking) have to appear in the elements c_1 and c_2 because a' cannot break $\mu-\tau$ symmetry and thus should be real. We have conjectured that all CP violations arise from a *common origin*, which then must originate from the $\mu-\tau$ breaking; so we can formulate such a common origin as a single phase in either c_1 or c_2 in the minimal construction, where the other two elements in the second column of m_D should be real. Hence, we present a unique minimal construction to formulate the common origin of $\mu-\tau$ and CP breaking in the Dirac mass-matrix m_D as follows,

$$m_D = \begin{pmatrix} \sigma_1 a & \sigma_2 a' \\ \sigma_1 b & \sigma_2 c(1 - \zeta') \\ \sigma_1 b & \sigma_2 c(1 - \zeta e^{i\omega}) \end{pmatrix}, \quad (2.18)$$

where the dimensionless parameters $-1 < \zeta' < 1$, $0 \leq \zeta < 1$, and the CP-phase angle $\omega \in [0, 2\pi]$. Here we have set $b_1 = b_2 \equiv b$ since (b_1, b_2) are already made real and thus cannot serve as the common source of the $\mu-\tau$ and CP breaking. Inspecting (2.18) we see that, *for any nonzero ζ and ω , the $\mu-\tau$ and CP symmetries are broken by the common source of $\zeta e^{i\omega}$* . We could also absorb the real parameter ζ' into c by defining $c' \equiv c(1 - \zeta')$. Thus we have,

$$m_D = \begin{pmatrix} \sigma_1 a & \sigma_2 a' \\ \sigma_1 b & \sigma_2 c' \\ \sigma_1 b & \sigma_2 c'(1 - \zeta'' e^{i\omega'}) \end{pmatrix}, \quad (2.19)$$

with

$$\zeta'' e^{i\omega'} = \frac{\zeta e^{i\omega} - \zeta'}{1 - \zeta'}. \quad (2.20)$$

Given the ranges of (ζ, ζ') as defined above, we see that the corresponding new parameter ζ'' of the $\mu-\tau$ breaking has a much larger range, including values within $1 \lesssim |\zeta''| \lesssim 3$ (when $|\zeta|, |\zeta'| \lesssim 0.6$ for instance), which are beyond the perturbative expansion. We find that if enforce $|\zeta''| < 1$, the parameter-space of (2.19) becomes smaller than (2.18) and insufficient for making the model fully viable. This means that our formulation of (2.18) is more general and has larger parameter-space for making theoretical predictions. Hence, we will apply (2.18) for the physical analyses below.

We note another formulation of such a breaking in the Dirac mass-matrix m_D ,

$$\hat{m}_D = \begin{pmatrix} \sigma_1 a & \sigma_2 a' \\ \sigma_1 b & \sigma_2 c(1 - \zeta e^{i\omega}) \\ \sigma_1 b & \sigma_2 c(1 - \zeta') \end{pmatrix}, \quad (2.21)$$

which is connected to (2.18) by a $\mu-\tau$ transformation for the light neutrinos $\nu = (\nu_e, \nu_\mu, \nu_\tau)$ into $\nu' = (\nu_e, \nu_\tau, \nu_\mu)$, via $\nu = G_\nu \nu'$, with $G_\nu[p=1]$ defined in Eq. (2.5). Accordingly, the mass-matrix (2.21) transforms as,

$$\hat{m}_D \rightarrow \hat{m}'_D = G_\nu^T \hat{m}_D = m_D, \quad (2.22)$$

which goes back to (2.18). So the two different formulations (2.18) and (2.21) just cause the $\mu-\tau$ asymmetric parts in the seesaw mass-matrix $M_\nu = m_D M_R^{-1} m_D^T$ to differ by an overall minus sign. As we will comment further in Sec. 4.1, this does not affect our predictions for the physical observables and their correlations. So we only need to focus on the formulation (2.18) for the rest of our analysis.

We may also first rotate the three elements in the second column of (2.17) to be real and then formulate the common origin of $\mu-\tau$ and CP breaking as follows,

$$m_D = \begin{pmatrix} \sigma_1 a & \sigma_2 a' \\ \sigma_1 b(1 - \zeta') & \sigma_2 c \\ \sigma_1 b(1 - \zeta e^{i\omega}) & \sigma_2 c \end{pmatrix}. \quad (2.23)$$

As will be clarified in Sec. 5, this will lead to the determination of solar mixing angle θ_{12} as in (2.16), in contrast to (2.18) which predicts a different θ_{12} as in (2.15). Here θ_{12} is explicitly fixed by the $\mu-\tau$ and CP symmetric parameters of m_D in either case. But, we find the predictions for all other $\mu-\tau$ and CP breaking observables and their correlations to remain the same as those from the construction in (2.18).

Finally, it is interesting to note that for an extended Higgs sector (consisting of two Higgs doublets or more) we can generate all CP-phases in the Dirac mass-matrix m_D via spontaneous CP violation [30], which is beyond the current scope and will be elaborated elsewhere [31].

2.3. Perturbative Expansion for $\mu-\tau$ and CP Breaking

Let us first consider the 3×3 mass-matrix M_ν light neutrinos, which can be generally presented as,

$$M_\nu = \begin{pmatrix} A & B_1 & B_2 \\ & C_1 & D \\ & & C_2 \end{pmatrix} \equiv \begin{pmatrix} A_0 & B_0 & B_0 \\ & C_0 & D_0 \\ & & C_0 \end{pmatrix} + \begin{pmatrix} \delta A & \delta B_1 & \delta B_2 \\ \delta C_1 & \delta D & \\ \delta C_2 & & \end{pmatrix}$$

$$\equiv M_\nu^{(0)} + \delta M_\nu = M_\nu^{(0)} + \delta M_\nu^{(1)} + \mathcal{O}(\zeta_i^2), \quad (2.24)$$

where the zeroth order matrix $M_\nu^{(0)}$ corresponds to vanishing $\mu-\tau$ breaking with $\zeta_i = 0$, and the NLO mass-matrix $\delta M_\nu^{(1)}$ includes the $\mu-\tau$ breaking to the first nontrivial order. We find it useful to further decompose $\delta M_\nu^{(1)}$ into the $\mu-\tau$ symmetric and anti-symmetric parts,

$$\delta M_\nu^{(1)} \equiv \delta M_\nu^s + \delta M_\nu^a \equiv \begin{pmatrix} \delta A & \delta B_s & \delta B_s \\ & \delta C_s & \delta D \\ & & \delta C_s \end{pmatrix} + \begin{pmatrix} 0 & \delta B_a & -\delta B_a \\ & \delta C_a & 0 \\ & & -\delta C_a \end{pmatrix}, \quad (2.25)$$

with

$$\delta B_s \equiv \frac{1}{2}(\delta B_1 + \delta B_2), \quad \delta B_a \equiv \frac{1}{2}(\delta B_1 - \delta B_2), \quad (2.26a)$$

$$\delta C_s \equiv \frac{1}{2}(\delta C_1 + \delta C_2), \quad \delta C_a \equiv \frac{1}{2}(\delta C_1 - \delta C_2). \quad (2.26b)$$

This decomposition is actually unique.

From our construction in the previous subsection, the $\mu-\tau$ and CP breaking Dirac mass-matrix m_D as well as the Majorana mass-matrix M_R is uniquely parameterized as follows,

$$m_D = \begin{pmatrix} \sigma_1 a & \sigma_2 a' \\ \sigma_1 b & \sigma_2 c_1 \\ \sigma_1 b & \sigma_2 c_2 \end{pmatrix}, \quad M_R = \text{diag}(M_1, M_2), \quad (2.27)$$

with $\sigma_{1,2} \equiv \sqrt{\hat{m}_0 M_{1,2}}$ and

$$c_1 = c(1 - \zeta'), \quad c_2 = c(1 - \zeta e^{i\omega}). \quad (2.28)$$

Thus, we can explicitly derive the seesaw mass-matrix for light neutrinos,

$$M_\nu = \hat{m}_0 \begin{pmatrix} a^2 + a'^2 & ab + a'c_1 & ab + a'c_2 \\ & b^2 + c_1^2 & b^2 + c_1c_2 \\ & & b^2 + c_2^2 \end{pmatrix}. \quad (2.29)$$

Since the neutrino data require the $\mu-\tau$ breaking to be small, we can further expand M_ν in terms of small breaking parameter ζ as,

$$M_\nu \equiv M_\nu^{(0)} + \delta M_\nu = M_\nu^{(0)} + \delta M_\nu^{(1)} + \mathcal{O}(\zeta^2), \quad (2.30)$$

with

$$M_\nu^{(0)} = \hat{m}_0 \begin{pmatrix} a^2 + a'^2 & ab + a'c & ab + a'c \\ & b^2 + c^2 & b^2 + c^2 \\ & & b^2 + c^2 \end{pmatrix} = \hat{m}_0 \begin{pmatrix} 1 & 0 & 0 \\ & \frac{1}{2} & \frac{1}{2} \\ & & \frac{1}{2} \end{pmatrix}, \quad (2.31a)$$

$$\delta M_\nu^{(1)} = \hat{m}_0 \begin{pmatrix} 0 & -a'c \zeta' & -a'c \zeta e^{i\omega} \\ & -2c^2 \zeta' & -c^2(\zeta' + \zeta e^{i\omega}) \\ & & -2c^2 \zeta e^{i\omega} \end{pmatrix}, \quad (2.31b)$$

where we have used the solution (2.14) for the second step of (2.31a) and the $\mu-\tau$ breaking expression (4.58b) for deriving (2.31b). For our current model with the expansion up to $\mathcal{O}(\zeta, \zeta')$, we deduce from (2.31a)-(2.31b) and (2.25)-(2.26),

$$A_0 = \hat{m}_0(a^2 + a'^2) = \hat{m}_0, \quad (2.32a)$$

$$B_0 = \hat{m}_0(ab + a'c) = 0, \quad (2.32b)$$

$$C_0 = D_0 = \hat{m}_0(b^2 + c^2) = \frac{1}{2}\hat{m}_0, \quad (2.32c)$$

and

$$\begin{aligned} \delta A &= 0, & \delta D &= -\hat{m}_0c^2(\zeta' + \zeta e^{i\omega}), \\ \delta B_s &= -\frac{1}{2}\hat{m}_0a'c(\zeta' + \zeta e^{i\omega}), & \delta C_s &= -\hat{m}_0c^2(\zeta' + \zeta e^{i\omega}), \\ \delta B_a &= -\frac{1}{2}\hat{m}_0a'c(\zeta' - \zeta e^{i\omega}), & \delta C_a &= -\hat{m}_0c^2(\zeta' - \zeta e^{i\omega}). \end{aligned} \quad (2.33)$$

Note that from (2.33) we can compute the ratio,

$$\frac{\delta B_a}{\delta C_a} = \frac{a'}{2c} = -\frac{b}{a}, \quad (2.34)$$

where in the last step we have used the resolution (2.14). It is interesting to note that the ratio (2.34) of the $\mu-\tau$ asymmetric parts in the light neutrino mass-matrix M_ν only depends on the $\mu-\tau$ symmetric elements of the Dirac mass-matrix m_D . This ratio just corresponds to the determination of the solar angle θ_{12} in (2.15) and will be further confirmed later by the full NLO analysis of Sec. 4.1.

3. Inverted Ordering: Reconstructing Light Neutrino Mass Matrix with $\mu-\tau$ and CP Violations at Low Energy

In this section, we give the model-independent reconstruction of the Majorana mass-matrix for light neutrinos under inverted mass-ordering (IMO), in terms of the low energy observables (mass-eigenvalues, mixings angles and CP phases). We expand this reconstruction by experimentally well-justified small parameters up to the next-to-leading order (NLO). Applying this reconstruction formulation to our model will allow us to systematically derive the physical predictions for the correlations among the low energy observables as well as for the link to the baryon asymmetry via leptogenesis at the seesaw scale.

3.1. Notation Setup and Model-Independent Reconstruction

Let us consider the general 3×3 symmetric and complex Majorana mass-matrix for the light neutrinos,

$$M_\nu \equiv \begin{pmatrix} m_{ee} & m_{e\mu} & m_{e\tau} \\ & m_{\mu\mu} & m_{\mu\tau} \\ & & m_{\tau\tau} \end{pmatrix} \equiv \begin{pmatrix} A & B_1 & B_2 \\ & C_1 & D \\ & & C_2 \end{pmatrix}. \quad (3.1)$$

In the mass-eigenbasis of charged leptons, the neutrino mass-matrix M_ν can be diagonalized by a unitary transformation $V (= U_\nu)$, i.e., $V^T M_\nu V = D_\nu \equiv \text{diag}(m_1, m_2, m_3)$, and thus we can write the reconstruction equation,

$$M_\nu = V^* D_\nu V^\dagger. \quad (3.2)$$

The mixing matrix V can be generally expressed as a product of three unitary matrices including a CKM-type mixing matrix U plus two diagonal rephasing matrices U' and U'' ,

$$V \equiv U'' U U', \quad (3.3a)$$

$$U \equiv \begin{pmatrix} c_s c_x & -s_s c_x & -s_x e^{i\delta_D} \\ s_s c_a - c_s s_a s_x e^{-i\delta_D} & c_s c_a + s_s s_a s_x e^{-i\delta_D} & -s_a c_x \\ s_s s_a + c_s c_a s_x e^{-i\delta_D} & c_s s_a - s_s c_a s_x e^{-i\delta_D} & c_a c_x \end{pmatrix}, \quad (3.3b)$$

$$U' \equiv \text{diag}(e^{i\phi_1}, e^{i\phi_2}, e^{i\phi_3}), \quad U'' \equiv \text{diag}(e^{i\alpha_1}, e^{i\alpha_2}, e^{i\alpha_3}), \quad (3.3c)$$

where δ_D is the Dirac CP-phase. For notational convenience, we have denoted the three neutrino mixing angles of the PMNS matrix as, $(\theta_{12}, \theta_{23}, \theta_{13}) \equiv (\theta_s, \theta_a, \theta_x)$, by following Ref. [23]. We will further use the notations, $(s_s, s_a, s_x) \equiv (\sin \theta_s, \sin \theta_a, \sin \theta_x)$ and $(c_s, c_a, c_x) \equiv (\cos \theta_s, \cos \theta_a, \cos \theta_x)$. For the diagonal rephasing matrix U' , only two of its three Majorana phases are measurable (such as $\phi_3 - \phi_1$ and $\phi_2 - \phi_1$) after extracting an overall phase factor. The matrix U'' contains another three phases which associate with the flavor-eigenbasis of light neutrinos and are needed for the consistency of diagonalizing a given mass-matrix M_ν .

For convenience we define the rephased mass-eigenvalues $\tilde{D}_\nu \equiv U'^* D_\nu U'^\dagger \equiv (\tilde{m}_1, \tilde{m}_2, \tilde{m}_3) = (m_1 e^{-i2\phi_1}, m_2 e^{-i2\phi_2}, m_3 e^{-i2\phi_3})$, so the reconstruction equation (3.2) becomes,

$$M_\nu = V'^* \tilde{D}_\nu V'^\dagger, \quad (V' \equiv U'' U). \quad (3.4)$$

Thus, we can fully reconstruct all elements of M_ν in terms of the rephased mass-eigenvalues $(\tilde{m}_1, \tilde{m}_2, \tilde{m}_3)$, the mixing angles $(\theta_s, \theta_a, \theta_x)$, the Dirac phase δ_D , and the rephasing phases α_i (which do not appear in physical PMNS mixing matrix),

$$m_{ee} = e^{-i2\alpha_1} \left[c_s^2 c_x^2 \tilde{m}_1 + s_s^2 c_x^2 \tilde{m}_2 + s_x^2 e^{-2i\delta_D} \tilde{m}_3 \right], \quad (3.5a)$$

$$m_{\mu\mu} = e^{-i2\alpha_2} \left[(s_s c_a - c_s s_a s_x e^{i\delta_D})^2 \tilde{m}_1 + (c_s c_a + s_s s_a s_x e^{i\delta_D})^2 \tilde{m}_2 + s_a^2 c_x^2 \tilde{m}_3 \right], \quad (3.5b)$$

$$m_{\tau\tau} = e^{-i2\alpha_3} \left[(s_s s_a + c_s c_a s_x e^{i\delta_D})^2 \tilde{m}_1 + (c_s s_a - s_s c_a s_x e^{i\delta_D})^2 \tilde{m}_2 + c_a^2 c_x^2 \tilde{m}_3 \right], \quad (3.5c)$$

$$m_{e\mu} = e^{-i(\alpha_1 + \alpha_2)} \left[c_s c_x (s_s c_a - c_s s_a s_x e^{i\delta_D}) \tilde{m}_1 - s_s c_x (c_s c_a + s_s s_a s_x e^{i\delta_D}) \tilde{m}_2 + s_a s_x c_x e^{-i\delta_D} \tilde{m}_3 \right], \quad (3.5d)$$

$$m_{e\tau} = e^{-i(\alpha_1 + \alpha_3)} \left[c_s c_x (s_s s_a + c_s c_a s_x e^{i\delta_D}) \tilde{m}_1 - s_s c_x (c_s s_a - s_s c_a s_x e^{i\delta_D}) \tilde{m}_2 - c_a s_x c_x e^{-i\delta_D} \tilde{m}_3 \right], \quad (3.5e)$$

$$m_{\mu\tau} = e^{-i(\alpha_2 + \alpha_3)} \left[(s_s c_a - c_s s_a s_x e^{i\delta_D}) (s_s s_a + c_s c_a s_x e^{i\delta_D}) \tilde{m}_1 \right]$$

$$+ (c_s c_a + s_s s_a s_x e^{i\delta_D}) (c_s s_a - s_s c_a s_x e^{i\delta_D}) \tilde{m}_2 - s_a c_a c_x^2 \tilde{m}_3 \Big], \quad (3.5f)$$

where among the Majorana phases $\phi_{1,2,3}$ (hidden in the mass-parameters $\tilde{m}_{1,2,3}$) only two are independent because an overall phase factor of U' can be absorbed into the diagonal rephasing-matrix U'' . For the case with a vanishing mass-eigenvalue (such as $m_3 = 0$ in our present model), only one independent phase combination, say $e^{i(\phi_2 - \phi_1)}$, will survive. If we impose $\mu-\tau$ symmetry on the light neutrino mass-matrix M_ν , we can deduce [1],

$$(\theta_a, \theta_x)_0 = (45^\circ, 0^\circ), \quad \alpha_{20} = \alpha_{30}. \quad (3.6)$$

The solar mixing angle θ_s is independent of the $\mu-\tau$ symmetry and is thus left undetermined. To predict θ_s , we will uncover a new flavor symmetry beyond the $\mathbb{Z}_2^{\mu\tau}$ (cf. Sec. 5).

3.2. Reconstruction of Light Neutrino Mass Matrix with Inverted Ordering

Now we are ready to apply the above general reconstruction formalism to the inverted mass-ordering (IMO), $m_2 \gtrsim m_1 \gg m_3$, with $m_3 = 0$ (as predicted by the present minimal seesaw model), in contrast to our previous model which predicts the normal mass-ordering (NMO) [1]. We introduce a small mass-ratio for light neutrinos,

$$y' \equiv \frac{m_2^2 - m_1^2}{m_1^2} = \frac{\Delta m_{21}^2}{\Delta m_{13}^2} = 0.029 - 0.036 \ll 1, \quad (3.7)$$

as constrained by the neutrino data at 90% C.L. (Table-1). So it is sufficient to make perturbative expansion in y' up to its linear order. Thus, at the zeroth order of y' , we have equal mass-eigenvalues, $m_{10} = m_{20} = m_0$. Under the y' -expansion up to next-to-leading order (NLO), $m_i = m_0 + \delta m_i$, we have

$$y' \simeq \frac{2(\delta m_2 - \delta m_1)}{m_1} = \frac{2(m_2 - m_1)}{m_1}. \quad (3.8)$$

We can define another small ratio $z \equiv \frac{\delta m_1}{m_1} = \mathcal{O}(y')$, and deduce,

$$\delta m_1 = z m_1, \quad \delta m_2 = \left(z + \frac{y'}{2}\right) m_1, \quad (3.9)$$

where $m_1 = \sqrt{\Delta m_{13}^2}$ is fixed by the neutrino data, and $m_0 = m_1 - \delta m_1 = (1 - z)m_1 \simeq \sqrt{\Delta m_{13}^2}$.

Next, we consider the mixing angles and CP-phases. Since the neutrino oscillation data strongly support the $\mu-\tau$ symmetry as a good approximate symmetry (3.6), we can define the small deviations from the general $\mu-\tau$ symmetric solution (3.6),

$$\delta_a \equiv \theta_a - \frac{\pi}{4}, \quad \delta_x \equiv \theta_x - 0, \quad (3.10)$$

which characterize the $\mu-\tau$ symmetry breaking. From the data in Table-1, we can infer the constrained 90% C.L. ranges,

$$0 \leq \delta_x^2 \leq 0.027, \quad 0 \leq \delta_a^2 \leq 0.015. \quad (3.11)$$

For our analysis we will systematically expand the small parameters $(\delta_a, \delta_x, y', z)$ up to their linear order. For the Majorana CP-phases, ϕ_3 drops due to $m_3 = 0$; we also remove an overall redundant Majorana phase ϕ_1 (from U') into the redefinition of α_j (in U''). So, the remaining independent Majorana phase is only ϕ ,

$$\bar{\alpha}_j \equiv \alpha_j + \phi_1, \quad (j = 1, 2, 3), \quad (3.12a)$$

$$\phi \equiv \phi_2 - \phi_1 = \phi_0 + \delta\phi. \quad (3.12b)$$

The expansion up to the NLO for our current reconstruction analysis will include $(\delta\bar{\alpha}_1, \delta\bar{\alpha}_2, \delta\bar{\alpha}_3, \delta\phi)$. The solar angle θ_s ($\equiv \theta_{12}$) is independent of the $\mu-\tau$ breaking and thus receives no NLO correction. Furthermore, we note that the Dirac phase $e^{i\delta_D}$ is always associated with the small mixing parameter s_x ($\simeq \delta_x$), so it only appears at the NLO and thus receive no more correction at this order of expansion.

Finally, we give a summary of all relevant NLO parameters in our reconstruction analysis,

$$(y', z, \delta_a, \delta_x, \delta\bar{\alpha}_1, \delta\bar{\alpha}_2, \delta\bar{\alpha}_3, \delta\phi), \quad (3.13)$$

Each of them is defined as the difference between its full value and zeroth-order value under the $\mu-\tau$ symmetric limit. In Sec. 4 we will derive these deviations from our seesaw model for the common origin of $\mu-\tau$ and CP breaking, and analyze their correlations.

Making the perturbative expansion of (3.13) under the inverted mass-ordering, we first deduce the LO form of the light neutrino mass-matrix (3.1),

$$m_{ee}^{(0)} \equiv A_0 = m_0 e^{-2i\bar{\alpha}_{10}} \left(c_s^2 + s_s^2 e^{-i2\phi_0} \right), \quad (3.14a)$$

$$m_{e\mu}^{(0)} = m_{e\tau}^{(0)} \equiv B_0 = \frac{1}{\sqrt{2}} m_0 s_s c_s e^{-i(\bar{\alpha}_{10} + \bar{\alpha}_{20})} \left(1 - e^{-i2\phi_0} \right), \quad (3.14b)$$

$$m_{\mu\mu}^{(0)} = m_{\tau\tau}^{(0)} \equiv C_0 = \frac{1}{2} m_0 e^{-2i\bar{\alpha}_{20}} \left(s_s^2 + c_s^2 e^{-2i\phi_0} \right) = D_0, \quad (3.14c)$$

where we have also matched to our notation of $M_\nu^{(0)}$ in (2.24). Then, we derive elements of the NLO mass-matrix $\delta M_\nu^{(1)}$ from (3.5),

$$\delta m_{ee}^{(1)} \equiv \delta A = m_0 e^{-i2\bar{\alpha}_{10}} \left[z + \frac{s_s^2}{2} y' - i2(s_s^2 \delta\phi + \delta\bar{\alpha}_1) \right], \quad (3.15a)$$

$$\delta m_{e\mu}^{(1)} \equiv \delta B_1 = \frac{m_0}{\sqrt{2}} e^{-i(\bar{\alpha}_{10} + \bar{\alpha}_{20})} \left[-\frac{c_s s_s}{2} y' - e^{i\delta_D} \delta_x + i2c_s s_s \delta\phi \right], \quad (3.15b)$$

$$\delta m_{e\tau}^{(1)} \equiv \delta B_2 = \frac{m_0}{\sqrt{2}} e^{-i(\bar{\alpha}_{10} + \bar{\alpha}_{20})} \left[-\frac{c_s s_s}{2} y' + e^{i\delta_D} \delta_x + i2c_s s_s \delta\phi \right], \quad (3.15c)$$

$$\delta m_{\mu\mu}^{(1)} \equiv \delta C_1 = m_0 e^{-i2\bar{\alpha}_{20}} \left[\frac{z}{2} + \frac{c_s^2}{4} y' - \delta_a - i(c_s^2 \delta\phi + \delta\bar{\alpha}_2) \right], \quad (3.15d)$$

$$\delta m_{\tau\tau}^{(1)} \equiv \delta C_2 = m_0 e^{-i2\bar{\alpha}_{20}} \left[\frac{z}{2} + \frac{c_s^2}{4} y' + \delta_a - i(c_s^2 \delta\phi + \delta\bar{\alpha}_3) \right], \quad (3.15e)$$

$$\delta m_{\mu\tau}^{(1)} \equiv \delta D = m_0 e^{-i2\bar{\alpha}_{20}} \left[\frac{z}{2} + \frac{c_s^2}{4} y' - \frac{i}{2} (2c_s^2 \delta\phi + \delta\bar{\alpha}_2 + \delta\bar{\alpha}_3) \right], \quad (3.15f)$$

where we have matched to our notation of $\delta M_\nu^{(1)}$ as defined in (2.24). In the above formulas, we have used the $\mu-\tau$ symmetric relations for the LO parameters, $(\theta_{a0}, \theta_{x0}) = (\frac{\pi}{4}, 0)$ and $\bar{\alpha}_{20} = \bar{\alpha}_{30}$, as well as $m_3 \equiv 0$.

From (2.25), we can uniquely decompose the elements of $\delta M_\nu^{(1)}$ in (3.15) as the $\mu-\tau$ symmetric and anti-symmetric parts, $\delta M_\nu^{(1)} \equiv \delta M_\nu^s + \delta M_\nu^a$, with their elements given by,

$$\begin{aligned} \delta B_s &\equiv \frac{\delta B_1 + \delta B_2}{2} = \frac{m_0}{\sqrt{2}} e^{-i(\bar{\alpha}_{10} + \bar{\alpha}_{20})} \left[-\frac{c_s s_s}{2} y' + i2c_s s_s \delta\phi \right], \\ \delta B_a &\equiv \frac{\delta B_1 - \delta B_2}{2} = -\frac{m_0}{\sqrt{2}} e^{-i(\bar{\alpha}_{10} + \bar{\alpha}_{20})} e^{i\delta_D} \delta_x, \\ \delta C_s &\equiv \frac{\delta C_1 + \delta C_2}{2} = m_0 e^{-i2\bar{\alpha}_{20}} \left[\frac{z}{2} + \frac{c_s^2}{4} y' - \frac{i}{2} (2c_s^2 \delta\phi + \delta\bar{\alpha}_2 + \delta\bar{\alpha}_3) \right] = \delta D, \\ \delta C_a &\equiv \frac{\delta C_1 - \delta C_2}{2} = -m_0 e^{-i2\bar{\alpha}_{20}} \left[\delta_a + \frac{i}{2} (\delta\bar{\alpha}_2 - \delta\bar{\alpha}_3) \right]. \end{aligned} \quad (3.16)$$

With these, we will be ready to apply the above reconstruction formulas (3.14), (3.15) and (3.16) to match with (2.24) in our seesaw model at the LO and NLO, respectively. We will systematically solve these matching conditions in the next section, which allows us to connect the seesaw parameters to the low energy neutrino observables and deduce our theoretical predictions.

For matching the seesaw predictions to our reconstruction formalism, we note that the latter was presented at the low energy scale so far. We need to connect the low energy neutrino parameters to the model predictions at the seesaw scale, where the possible renormalization group (RG) running effects should be taken into account in principle. Such RG effects were extensively discussed in the literature [25], and can be straightforwardly applied to the present analysis. Below the seesaw scale, heavy right-handed neutrinos can be integrated out from the effective theory and the seesaw mass-eigenvalues m_j ($j = 1, 2, 3$) for light neutrinos obey the approximate one-loop RG equation (RGE) [25],

$$\frac{dm_j}{dt} = \frac{\hat{\alpha}}{16\pi^2} m_j, \quad (3.17)$$

to good accuracy [26], where $t = \ln(\mu/\mu_0)$ with μ the renormalization scale. For the SM, the coupling-parameter $\hat{\alpha} \simeq -3g_2^2 + 6y_t^2 + \lambda$, with (g_2, y_t, λ) denoting the $SU(2)_L$ weak gauge coupling, the top Yukawa coupling and Higgs self-coupling, respectively. Hence, we can deduce the running mass-parameter m_j from scale μ_0 to μ ,

$$m_j(\mu) = \chi(\mu, \mu_0) m_j(\mu_0) \simeq \exp \left[\frac{1}{16\pi^2} \int_0^t \hat{\alpha}(t') dt' \right] m_j(\mu_0), \quad (3.18)$$

with $t = \ln(\mu/\mu_0)$. In the present analysis we will choose, $(\mu_0, \mu) = (M_Z, M_1)$, with Z boson mass M_Z representing the weak scale and the heavy neutrino-mass M_1 characterizing the seesaw scale.

Consider the minimal neutrino seesaw with inverted mass-spectrum, $m_2 \gtrsim m_1 \gg m_3 = 0$. We note that the zero-eigenvalue m_3 and the mass ratio y' do not depend on the RG running scale μ . So we can derive the running of the two nonzero mass-parameters from weak scale to seesaw scale,

$$\hat{m}_1 \equiv m_1(M_1) = \chi_1 m_1(M_Z), \quad (3.19a)$$

$$\hat{m}_2 \equiv m_2(M_1) = \chi_1 m_2(M_Z) = \sqrt{1+y'} \hat{m}_1, \quad (3.19b)$$

with $\chi_1 \equiv \chi(M_1, M_Z)$. In Sec. 4, we will compute the RG running factor $\chi_1 \equiv \chi(M_1, M_Z)$ numerically, which depends on the inputs of initial values for $\alpha_2 = g_2^2/(4\pi)$, y_t and the Higgs boson mass M_H , via the combination $\hat{\alpha}$ defined above. Using the electroweak precision data [17, 27], $\alpha_2^{-1}(M_Z) = 29.57 \pm 0.02$, $m_t = 173.1 \pm 1.4$ GeV, and the Higgs-mass range $115 \leq M_H \leq 149$ GeV [90% C.L.] for the SM, we find the running factor $\chi(M_1, M_Z) \simeq 1.3 - 1.4$ for $M_1 = 10^{13} - 10^{16}$ GeV. Other running effects due to the leptonic mixing angles and CP-phases are all negligible for the present study since their RGEs contain only flavor-dependent terms and are all suppressed by $y_\tau^2 = \mathcal{O}(10^{-4})$ at least [25]. For the analyses below (Sec. 4), we will first evolve the mass-parameters from the seesaw scale M_1 down to the low energy scale for neutrino oscillations, and then match them with those in our reconstruction formalism. Including such RG effects just requires to replace the light mass-eigenvalues (\hat{m}_1, \hat{m}_2) at seesaw scale M_1 by the corresponding (m_1, m_2) at low energy, and vice versa.

4. Predictions of Common $\mu-\tau$ and CP Breaking with Inverted Ordering

In this section we apply the reconstruction formalism (including the RG running effects) in Sec. 3.2 to our common $\mu-\tau$ and CP breaking seesaw in Sec. 2.3. Then, we systematically derive the predictions for the low energy neutrino observables. This includes the nontrivial correlation between two small $\mu-\tau$ breaking parameters $\delta_x (\equiv \theta_{13} - 0)$ and $\delta_a (\equiv \theta_{23} - \frac{\pi}{4})$. Furthermore, we study the correlations of $\theta_{23} - 45^\circ$ and θ_{13} with Jarlskog invariant J and neutrinoless $\beta\beta$ -decay observable M_{ee} . Finally, we study the matter-antimatter asymmetry (baryon asymmetry) via leptogenesis in the $\mu-\tau$ blind seesaw, and establish the direct link with low energy neutrino observables. Furthermore, we will derive a nontrivial lower bound on the reactor mixing angle, $\theta_{13} \gtrsim 1^\circ$, and restrict the Jarlskog invariant into a negative range, $-0.037 \lesssim J \lesssim -0.0035$.

4.1. Predicting Correlations of Low Energy Neutrino Observables

Both $\mu-\tau$ and CP violations arise from a common origin in the seesaw Lagrangian of our model, which is characterized by the breaking parameter $\zeta e^{i\omega}$ and shows up at the NLO of our perturbative expansion. Hence, in the light neutrino mass-matrix, the small $\mu-\tau$ breaking parameters (δ_a, δ_x) together with all CP-phases are controlled by ζ and ω . In the following, we will use the reconstruction formalism (Sec. 3.2) under IMO for diagonalizing the light neutrino mass-matrix at

the NLO. Then, we will further derive quantitative predictions for these low energy observables and their correlations.

We first inspect the reconstructed LO mass-matrix $M_\nu^{(0)}$ in (3.14). Matching (3.14) with our model prediction (2.31a) at the same order, we find the solutions,

$$\bar{\alpha}_{10} = \bar{\alpha}_{20} = \phi_0 = 0, \quad (4.1a)$$

$$m_{10} = m_{20} = m_0, \quad m_3 = 0, \quad (4.1b)$$

$$a^2 = 2c^2 = 1 - 2b^2, \quad a'^2 = 2b^2, \quad c^2 = \frac{1}{2} - b^2, \quad a'c = -ab, \quad (4.1c)$$

which is also consistent with Eq. (2.14). Here all the LO CP-phases $(\bar{\alpha}_{10}, \bar{\alpha}_{20}, \phi_0) = 0$ because the original CP-violation in the seesaw Lagrangian vanishes in the $\zeta = 0$ limit (Sec. 2.2).

Then, we analyze the NLO light neutrino mass-matrix $\delta M_\nu^{(1)}$, as given by (2.25) of our model and by the reconstruction formula (3.15). We match the two sets of equations at the low energy for the $\mu-\tau$ symmetric elements,

$$\delta A = 0 = m_0 \left[z + \frac{s_s^2}{2} y' - i2(s_s^2 \delta\phi + \delta\bar{\alpha}_1) \right], \quad (4.2a)$$

$$\delta B_s = -\frac{m_0}{2} a'c(\zeta' + \zeta e^{i\omega}) = \frac{m_0}{\sqrt{2}} \left[-\frac{c_s s_s}{2} y' + i2c_s s_s \delta\phi \right], \quad (4.2b)$$

$$\delta C_s = -m_0 c^2(\zeta' + \zeta e^{i\omega}) = \frac{m_0}{2} \left[z + \frac{c_s^2}{2} y' - i(2c_s^2 \delta\phi + \delta\bar{\alpha}_2 + \delta\bar{\alpha}_3) \right] = \delta D, \quad (4.2c)$$

and for $\mu-\tau$ anti-symmetric elements,

$$\delta B_a = -\frac{m_0}{2} a'c(\zeta' - \zeta e^{i\omega}) = -\frac{m_0}{\sqrt{2}} e^{i\delta_D} \delta_x, \quad (4.3a)$$

$$\delta C_a = -m_0 c^2(\zeta' - \zeta e^{i\omega}) = -m_0 \left[\delta_a + \frac{i}{2} (\delta\bar{\alpha}_2 - \delta\bar{\alpha}_3) \right], \quad (4.3b)$$

where using Eq. (3.19) we have run the mass-parameter \hat{m}_0 from the seesaw scale down to the corresponding m_0 at low energy for the left-hand-sides of Eqs. (4.2) and (4.3).

From the $\mu-\tau$ symmetric Eqs. (4.2a)-(4.2b), we can infer six independent conditions for the real and imaginary parts of $(\delta A, \delta B_s, \delta C_s)$, respectively,

$$z = -\frac{s_s^2}{2} y', \quad (4.4a)$$

$$\delta\bar{\alpha}_1 = -s_s^2 \delta\phi, \quad (4.4b)$$

$$\frac{c_s s_s}{\sqrt{2}} y' = a'c(\zeta' + \zeta \cos\omega), \quad (4.4c)$$

$$2\sqrt{2} c_s s_s \delta\phi = -a'c \zeta \sin\omega, \quad (4.4d)$$

$$\frac{z}{2} + \frac{c_s^2}{4} y' = -c^2(\zeta' + \zeta \cos\omega), \quad (4.4e)$$

$$-\frac{1}{2}(2c_s^2 \delta\phi + \delta\bar{\alpha}_2 + \delta\bar{\alpha}_3) = -c^2 \zeta \sin\omega. \quad (4.4f)$$

Thus, with the aid of (4.4a) we take the ratio of (4.4c) and (4.4e), and derive

$$\tan 2\theta_s = -\frac{a'}{\sqrt{2}c} = \frac{\sqrt{2}b}{a}, \quad (4.5)$$

which coincides with (2.15) in Sec. 2.1. Using Eq. (4.5), we deduce from Eq. (4.1c),

$$a = p_a \cos 2\theta_s, \quad b = p_a \frac{1}{\sqrt{2}} \sin 2\theta_s, \quad (4.6a)$$

$$a' = p_{a'} \sin 2\theta_s, \quad c = -p_{a'} \frac{1}{\sqrt{2}} \cos 2\theta_s, \quad (4.6b)$$

with $p_a, p_{a'} = \pm$ denoting the signs of (a, a') . Here we see that the four dimensionless LO parameters (a, a', b, c) in the Dirac mass-matrix (2.18) are fixed by the solar mixing angles θ_s , since the conditions in (4.1c) make three of them non-independent. Finally, we further resolve (4.4) and derive the NLO parameters,

$$y' = -2 \cos 2\theta_s (\zeta' + \zeta \cos \omega), \quad (4.7a)$$

$$z = s_s^2 \cos 2\theta_s (\zeta' + \zeta \cos \omega), \quad (4.7b)$$

$$\delta\bar{\alpha}_1 = -\frac{1}{2} s_s^2 (c_s^2 - s_s^2) \zeta \sin \omega, \quad (4.7c)$$

$$\delta\phi = \frac{1}{2} (c_s^2 - s_s^2) \zeta \sin \omega, \quad (4.7d)$$

$$\delta\bar{\alpha}_2 + \delta\bar{\alpha}_3 = s_s^2 (s_s^2 - c_s^2) \zeta \sin \omega. \quad (4.7e)$$

It is interesting to note that the present model predicts a generically small Majorana CP-phase angle at low energy, $\phi = \delta\phi = O(\zeta)$, in contrast to our soft breaking model [1] where the low energy Majorana CP-phase angle (ϕ_{23}) is not suppressed.

Next, we analyze the $\mu-\tau$ anti-symmetric equations (4.3a)-(4.3b) for $\delta M_\nu^{(1)}$. With (4.6), we can deduce from (4.3a)-(4.3b),

$$\frac{1}{2} \sin 2\theta_s \cos 2\theta_s (\zeta' - \zeta e^{i\omega}) = -e^{i\delta_D} \delta_x, \quad (4.8a)$$

$$\frac{1}{2} \cos^2 2\theta_s (\zeta' - \zeta e^{i\omega}) = \delta_a + \frac{i}{2} (\delta\bar{\alpha}_2 - \delta\bar{\alpha}_3), \quad (4.8b)$$

which decompose into

$$\cos \delta_D \delta_x = -\frac{1}{2} \sin 2\theta_s \cos 2\theta_s (\zeta' - \zeta \cos \omega), \quad (4.9a)$$

$$\sin \delta_D \delta_x = \frac{1}{2} \sin 2\theta_s \cos 2\theta_s (\zeta \sin \omega), \quad (4.9b)$$

$$\delta_a = \frac{1}{2} \cos^2 2\theta_s (\zeta' - \zeta \cos \omega), \quad (4.9c)$$

$$\delta\bar{\alpha}_2 - \delta\bar{\alpha}_3 = -\cos^2 2\theta_s (\zeta \sin \omega). \quad (4.9d)$$

Thus the Dirac CP-phase angle δ_D can be derived from the ratio of (4.9a) and (4.9b),

$$\tan \delta_D = \frac{\zeta \sin \omega}{\zeta \cos \omega - \zeta'} = \frac{\delta\bar{\alpha}_2 - \delta\bar{\alpha}_3}{2\delta_a}. \quad (4.10)$$

With Eqs. (4.7a), (4.10) and (4.9), we finally deduce,

$$\zeta' + \zeta \cos \omega = -\frac{1}{2 \cos 2\theta_s} y', \quad -\zeta \sin \omega = \frac{2 \tan \delta_D}{\cos^2 2\theta_s} \delta_a, \quad (4.11)$$

and thus

$$\cos \delta_D \delta_x = -\frac{\sin 2\theta_s}{4} (y' + 4 \cos 2\theta_s \zeta') = \frac{\sin 2\theta_s}{4} (y' + 4 \cos 2\theta_s \cos \omega \zeta), \quad (4.12a)$$

$$\delta_a = \frac{\cos 2\theta_s}{4} (y' + 4 \cos 2\theta_s \zeta') = -\frac{\cos 2\theta_s}{4} (y' + 4 \cos 2\theta_s \cos \omega \zeta), \quad (4.12b)$$

$$\delta \bar{\alpha}_2 - \delta \bar{\alpha}_3 = 2 \tan \delta_D \delta_a. \quad (4.12c)$$

From Eqs. (4.12a) and (4.12b), we derive a nontrivial correlation between the low energy $\mu - \tau$ breaking observables δ_a and δ_x ,

$$\delta_a = -\cot 2\theta_s \cos \delta_D \delta_x. \quad (4.13)$$

This shows that at the NLO the two small $\mu - \tau$ breaking parameters are *proportional to each other*, $\delta_x \propto \delta_a$. Because of $|\cos \delta_D| \leq 1$, we can infer from Eq. (4.13) a generic *lower bound* on δ_x , for any nonzero δ_a ,

$$\delta_x \geq |\delta_a| \tan 2\theta_s, \quad (4.14)$$

where we have $\delta_x \equiv \theta_{13} \in [0, \frac{\pi}{2}]$ in our convention. It is worth to note that our previous soft breaking model [1] also predicted a correlation and a lower bound,

$$\delta_a = -\cot \theta_s \cos \delta_D \delta_x, \quad (\text{Prediction of Ref. [1]}), \quad (4.15a)$$

$$\Rightarrow \delta_x \geq |\delta_a| \tan \theta_s, \quad (4.15b)$$

where the quantitative difference from the present predictions is that we have the coefficient $\cot 2\theta_s$ in Eq. (4.13) as compared to $\cot \theta_s$ in Eq. (4.15a). In fact, this is a *profound difference*. From the present oscillation data in Table-1, we observe that the deviation of the solar angle θ_s ($\equiv \theta_{12}$) from its maximal mixing value is relatively small,

$$9.0^\circ < 45^\circ - \theta_{12} < 12.2^\circ, \quad (\text{at 90\% C.L.}), \quad (4.16)$$

and this limit only relaxes slightly at 99% C.L., $7.8^\circ < 45^\circ - \theta_{12} < 12.9^\circ$. Hence, we see that the range of the deviation $45^\circ - \theta_{12}$ is at the same level as the two other small deviations $\theta_{23} - 45^\circ$ and $\theta_{13} - 0^\circ$ shown in Eq. (2.1). So, we can define a new naturally small quantity,

$$\delta_s \equiv \frac{\pi}{4} - \theta_s, \quad (4.17)$$

and make expansion for δ_s as well. Then, we immediately observe a *qualitative difference* between $\cot 2\theta_s \simeq 2\delta_s \ll 1$ in (4.13) and $\cot \theta_s \simeq 1 + 2\delta_s \gtrsim 1$ in (4.15a). Hence, we can rewrite the two correlations (4.13) and (4.15a) in the well expanded form,

$$\delta_a \simeq -2 \cos \delta_D (\delta_s \delta_x) \ll \delta_x, \quad (\text{Current Prediction}), \quad (4.18a)$$

$$\delta_a \simeq -\cos \delta_D \delta_x = O(\delta_x), \quad (\text{Prediction of Ref. [1]}). \quad (4.18b)$$

Two comments are in order. First, we deduce from (4.18) the following patterns of the three mixing angles,

$$(\theta_{12}, \theta_{23}, \theta_{13}) = \left(\frac{\pi}{4} - \delta_s, \frac{\pi}{4} - O(\delta_s \delta_x), \delta_x \right), \quad (\text{in the current model}), \quad (4.19a)$$

$$(\theta_{12}, \theta_{23}, \theta_{13}) = \left(\frac{\pi}{4} - \delta_s, \frac{\pi}{4} - \delta_a, \delta_x \right), \quad (\text{in the model of Ref. [1]}), \quad (4.19b)$$

where for the current model Eq. (4.19a) predicts a nearly maximal atmospheric angle $\theta_{23} \simeq \frac{\pi}{4}$; while for the soft-breaking model [1], Eq. (4.19b) allows all three deviations to be comparable. Second, for each given nonzero $\delta_a = \theta_{23} - \frac{\pi}{4}$, we can deduce the lower limits on $\delta_x = \theta_{13}$ from (4.18),

$$\delta_x \geq \frac{|\delta_a|}{2\delta_s} \gg |\delta_a|, \quad (\text{Current Prediction}), \quad (4.20a)$$

$$\delta_x \geq |\delta_a|, \quad (\text{Prediction of Ref. [1]}). \quad (4.20b)$$

Given the 99% C.L. range of $7.8^\circ < \delta_s < 12.2^\circ$, we derive the lower limit from (4.14) or (4.20a) for the present model,

$$\theta_{13} \geq (3.6 \sim 2.1) |\theta_{23} - 45^\circ|, \quad (4.21)$$

which allows θ_{13} to easily saturate its current upper limit. As another illustration, taking the current “best fit” values $(\theta_{12}, \theta_{23}) = (34.5^\circ, 42.8^\circ)$ as in Table-1, we derive from (4.14) or (4.20a) the lower limits $\theta_{13} \geq 6^\circ$ for the present model, and $\theta_{13} \geq 1.5^\circ$ for Ref. [1]. Hence, in contrast with Ref. [1], the present model favors a larger θ_{13} , and can saturate its current upper limit, as will be demonstrated in Fig. 2 below.

In the following, we systematically analyze the predicted parameter space and correlations in the present model (with inverted mass-ordering). We will find these to be *very different* from that in our soft breaking model (with normal mass-ordering) [1]. So, the present model can be tested against that in Ref. [1] by the on-going and upcoming neutrino experiments.

Using the neutrino data for θ_s and $(\Delta m_{21}^2, \Delta m_{13}^2)$ (Table-1), and scanning the Dirac CP phase-angle $\delta_D \in [0^\circ, 360^\circ]$, we can plot the two $\mu-\tau$ breaking mixing angles, $\theta_{13} (\equiv \delta_x)$ and $\theta_{23} - 45^\circ (\equiv \delta_a)$, from (4.12a)-(4.12b) and (4.13), as functions of the theory parameter $\zeta \cos \omega$ and δ_D . Our findings are depicted in Fig. 1(a)-(d) with the experimental inputs varied within 90% C.L. ranges and with $\zeta \cos \omega \in [-0.6, 0.6]$ in the natural perturbative region. Here we find that the theory prediction of $\theta_{23} - 45^\circ$ lies in the range,

$$-4^\circ \leq \theta_{23} - 45^\circ \leq 4^\circ, \quad (4.22)$$

which is within the current experimental bounds. On the other hand the predicted θ_{13} can saturate the current experimental limits, and has distinct distributions.

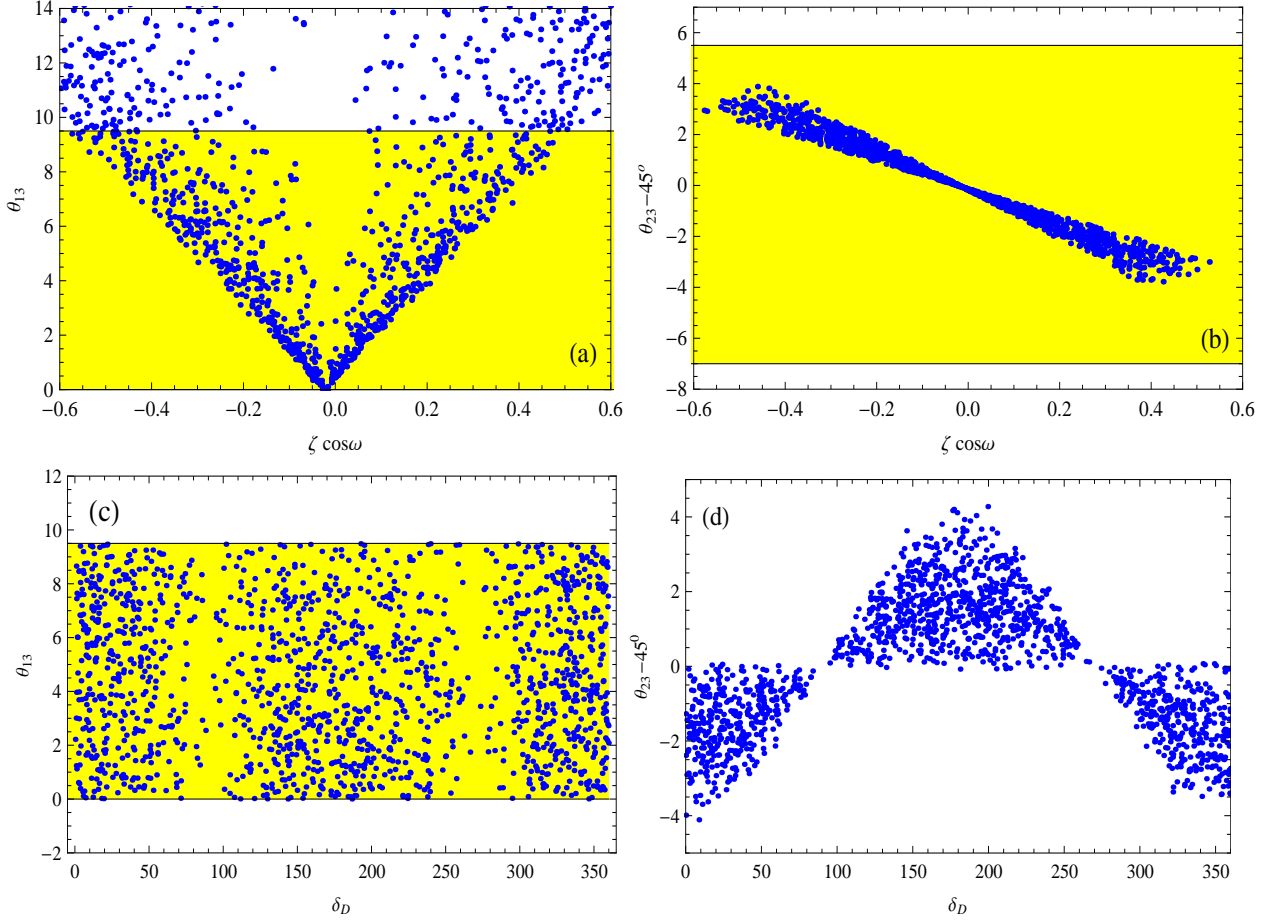


Figure 1: Predictions of θ_{13} and $\theta_{23} - 45^\circ$ as functions of the $\mu - \tau$ breaking parameter $\zeta \cos \omega$ and CP breaking parameter δ_D . The experimental inputs are scanned within 90% C.L. ranges and the Dirac phase angle $\delta_D \in [0, 2\pi)$, with 1500 samples. The shaded region (yellow) denotes the 90% C.L. limits on θ_{13} and $\theta_{23} - 45^\circ$, from Table-1.

From the theory relations (4.12a)-(4.12b), we can further explore the *correlation* between the two $\mu - \tau$ breaking mixing angles θ_{13} and $\theta_{23} - 45^\circ$. This is displayed in Fig. 2, where we have varied the measured parameters within their 90% C.L. ranges, and input the Dirac-phase angle $\delta_D \in [0, 2\pi)$ as well as $|\zeta'| \leq 0.6$. The current 90% C.L. limits on θ_{13} are shown by the shaded region (yellow), while the θ_{13} sensitivities of the on-going Double Chooz [12], RENO [13] and Daya Bay [10] experiments are depicted by the three horizontal (red) lines at 90% C.L., as 5.0° , 4.1° and 2.9° (from top to bottom), based on three years of data-taking. The horizontal dashed (red) line represents Daya Bay's future sensitivity (2.15°) with six years of running [32].

Inspecting Fig. 2, we find that the sharp edges on the two sides of the allowed parameter space are essentially determined by the lower bound given in (4.14), $\delta_x \geq |\delta_a| \tan 2\theta_s$, where the current data require, $2.2 \leq \tan 2\theta_s \leq 3.1$ at 90% C.L. (Table-1) and the lower limit $\tan 2\theta_s = 2.2$ just corresponds to the slopes of the sharp edges which are nearly straight lines. Hence, for *any measured nonzero value of $\theta_{23} - 45^\circ \neq 0$* , the Fig. 2 imposes a lower bound on θ_{13} , which will be tested by the reactor experiments such as Daya Bay, RENO and Double Chooz. The current oscillation data favor

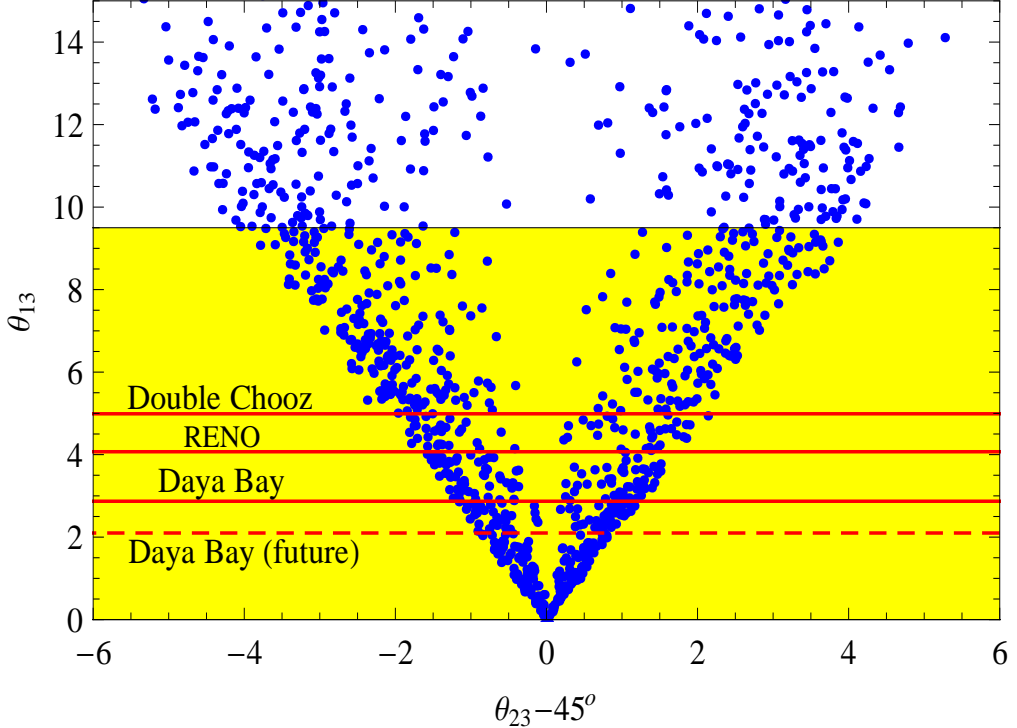


Figure 2: Correlation between θ_{13} and $\theta_{23} - 45^\circ$, based on Eqs. (4.12a)-(4.12b), where the experimental inputs are scanned within 90% C.L. ranges and the Dirac phase angle $\delta_D \in [0^\circ, 360^\circ]$, with 1500 samples. The sensitivities of Double Chooz [12], RENO [13] and Daya Bay [10] experiments to θ_{13} are shown by the three horizontal (red) solid lines at 90% C.L., as 5.0°, 4.1° and 2.9° (from top to bottom). The Daya Bay's future sensitivity (2.15°) is shown by the horizontal dashed (red) line.

the central value of θ_{23} to be smaller than 45° (Table-1) and this feature is quite robust [6]. From Fig. 2, we see that taking the current central value of $\theta_{23} - 45^\circ = -2.2^\circ$ (Table-1), the lower bound on θ_{13} is already very close to the sensitivity of Double Chooz experiment; and a minor deviation of $\theta_{23} - 45^\circ = -1.4^\circ$ will push θ_{13} up to the sensitivity of Daya Bay experiment. Hence, *the Daya Bay, RENO and Double Chooz reactor experiments hold great potential to discover a nonzero θ_{13} .* Furthermore, as shown in Fig. 2, detecting a nonzero $\theta_{13} \gtrsim 3^\circ$ will strongly favor a nonzero $\theta_{23} - 45^\circ$. Hence, we further encourage the improved measurements of θ_{23} by Minos [7] and T2K [8], as well as future neutrino factory and super-beam facility [33, 34].

Note that our previous soft breaking model [1] predicted a lower bound $\delta_x \geq |\delta_a| \tan \theta_s$ with the slope $0.64 \leq \tan \theta_s \leq 0.73$ at 90% C.L., which is about 3.4 – 4.2 times smaller than the present model. This means that given the same nonzero deviation of $\theta_{23} - 45^\circ$, the current model will place a much stronger lower bound on θ_{13} , higher than that in Ref. [1] by a factor of 3.4 – 4.2. Hence, the prediction of Fig. 2 is really encouraging for the upcoming neutrino oscillation experiments, which will probe the $\mu - \tau$ violating observables $\theta_{13} - 0^\circ$ and $\theta_{23} - 45^\circ$ to much higher precision.

Then, we analyze our model predictions for the low energy CP-violation (via Jarlskog invariant J) and the neutrinoless double-beta decays (via the element $|m_{ee}|$ of M_ν). From our theory construction

in Sec. 2.2, the original CP-phase $e^{i\omega}$ in the Dirac mass-matrix of seesaw Lagrangian is the common source of both low energy Dirac and Majorana CP-violations via the phase angles δ_D and $\delta\phi$.

The Dirac CP-violation is characterized by the Jarlskog invariant J [35] in the light neutrino sector with nonzero CP-phase δ_D and can be measured by the long baseline neutrino oscillation experiments. On the other hand, the neutrinoless double-beta decay observable $|m_{ee}|$ contains both δ_D and Majorana CP-phase $\delta\phi$. We can express the Jarlskog invariant J as follows [35],

$$J \equiv \frac{1}{8} \sin 2\theta_s \sin 2\theta_a \sin 2\theta_x \cos \theta_x \sin \delta_D = \frac{\delta_x}{4} \sin 2\theta_s \sin \delta_D + \mathcal{O}(\delta_x^2, \delta_a^2), \quad (4.23)$$

where as defined earlier, $\delta_x \equiv \theta_x$ and $\delta_a \equiv \theta_a - \frac{\pi}{4}$. The solutions (4.12a)-(4.12b) leads to the correlation (4.13). We can input the neutrino data for mixing angles, $(\theta_s, \delta_x) \equiv (\theta_{12}, \theta_{13})$, and mass-ratio, $y' \equiv \Delta m_{21}^2 / \Delta m_{13}^2$, as well as scanning the model-parameter ζ' in its perturbative range $|\zeta'| \leq 0.6$.

We then study the neutrinoless double-beta decays. Our present model predicts the inverted mass-ordering (IMO) with $m_3 = 0$, so from (3.5a) we can derive the mass-matrix element $|m_{ee}|$ for neutrinoless double-beta decays,

$$\begin{aligned} M_{ee} \equiv |m_{ee}| &= \left| \sum V_{ej}^* m_j \right| = m_1 c_x^2 \left| c_s^2 + s_s^2 \sqrt{1+y'} e^{-i2\phi} \right| \\ &\simeq m_1 \left[1 + \frac{1}{2} s_s^2 y' - \delta_x^2 - 2 s_s^2 c_s^2 \delta\phi^2 \right], \end{aligned} \quad (4.24)$$

where in the last step we have expanded δ_x and $\delta\phi$ to the second order since $y' = O(10^{-2})$ is relatively small as constrained by the current data [cf. (3.7)]. Eq. (4.24) shows that the neutrinoless $\beta\beta$ -decay observable M_{ee} only contains the second orders of the $\mu-\tau$ breaking quantity δ_x ($= \theta_{13}$) and the Majorana CP-phase angle $\delta\phi$. Hence, M_{ee} is less sensitive to the $\mu-\tau$ breaking and Majorana CP-violation at low energies.

We plot the correlation between θ_{13} and the Jarlskog invariant J in Fig. 3(a), and the neutrinoless $\beta\beta$ -decay observable M_{ee} is depicted in Fig. 3(b). For the analysis of Fig. 3(a), we have used Eq. (4.12a) where we vary the model-parameter $\zeta' \in [-0.6, 0.6]$ in its perturbative range. We scan all other measured parameters within their 90% C.L. ranges. The shaded region (yellow) in Fig. 3 is allowed by the neutrino data at 90% C.L. Fig. 3(a) shows that any nonzero J will lead to a lower bound on θ_{13} due to $\delta_x \geq 4|J| / \sin 2\theta_s$ as inferred from Eq. (4.23). Combining the current upper limit $\theta_{13} < 9.5^\circ$ (shaded region in yellow) with our parameter space in Fig. 3(b), we predict the allowed range,

$$-0.037 \lesssim J \lesssim 0.037, \quad (4.25a)$$

$$45.5 \text{ meV} \lesssim M_{ee} \lesssim 50.8 \text{ meV}, \quad (4.25b)$$

which can be probed by the on-going neutrinoless double beta decay experiments [3].

Before concluding this subsection, we compare our prediction (4.13) with a recent independent

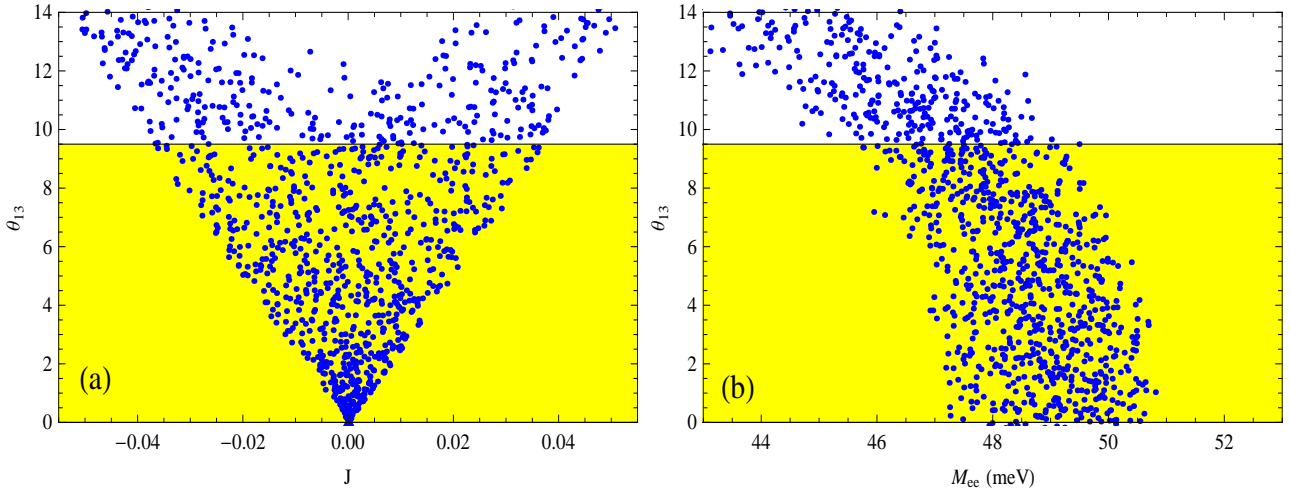


Figure 3: Correlations of θ_{13} (in degree) with the Jarlskog invariant J [plot-(a)] and with the neutrinoless $\beta\beta$ -decay observable M_{ee} [plot-(b)]. Each plot has computed 1500 samples. The shaded region (yellow) is allowed by the current data at 90% C.L.

work [36]. In Ref. [36], using a charged lepton perturbation, Friedberg and Lee derived a very interesting prediction, $\cos 2\theta_{23} = \tan^2 \theta_{13}$, leading to

$$\frac{\pi}{4} - \theta_{23} \simeq \frac{1}{2}\theta_{13}^2 \ll \theta_{13}, \quad (4.26)$$

which does not contain CP phase and predicts a nearly maximal θ_{23} . For comparison, we rewrite our predictions (4.18a)-(4.18b) in the same notations,

$$\frac{\pi}{4} - \theta_{23} \simeq 2 \cos \delta_D \left(\frac{\pi}{4} - \theta_{12} \right) \theta_{13} \ll \theta_{13}, \quad (\text{Current Prediction}), \quad (4.27a)$$

$$\frac{\pi}{4} - \theta_{23} \simeq \cos \delta_D \theta_{13} = O(\theta_{13}), \quad (\text{Prediction of Ref. [1]}), \quad (4.27b)$$

where our correlations explicitly contain the CP-phase angle δ_D . Moreover, our present model predicts a deviation $\frac{\pi}{4} - \theta_{23}$ to be significantly smaller than θ_{13} as in (4.27a), due to the suppression of $\frac{\pi}{4} - \theta_{12} = 0.16 - 0.21$ at 90% C.L. But, taking $\cos \delta_D = O(1)$, we see that the right-hand-side of (4.27a) is larger than that of (4.26) by a factor of $4(\frac{\pi}{4} - \theta_{12})/\theta_{13} = (36.0 - 48.8^\circ)/\theta_{13}$ at 90% C.L., which is clearly bigger than one. On the other hand, our previous soft breaking model [1] predicts the two small $\mu - \tau$ breaking observables to be of the same order, $\frac{\pi}{4} - \theta_{23} = O(\theta_{13})$, as in (4.27b). Hence, the predictions by Friedberg-Lee [36] and by us differ in a nontrivial and interesting way, which strongly motivate the on-going and future neutrino experiments for tests and resolution.

4.2. Baryon Asymmetry from $\mu - \tau$ Blind Seesaw and Direct Link to Low Energy

In this subsection, we study the predictions of our $\mu - \tau$ blind seesaw model for cosmological baryon asymmetry (matter-antimatter asymmetry) via thermal leptogenesis [37, 38]. We build up the direct link between leptogenesis CP-asymmetry and the low energy Dirac CP-phase, and further predict

the low energy leptonic Jarlskog invariant J [35]. Imposing the WAMP data on the baryon asymmetry [16], we predict a negative Jarlskog invariant, $J < 0$, and derive a lower bound on the reactor mixing angle, $\theta_{13} \gtrsim 1^\circ$. We also analyze the *correlations* of the leptogenesis scale with the low energy observables such as the Jarlskog-invariant J and neutrinoless $\beta\beta$ -decay parameter M_{ee} [3]. We further deduce a lower bound on the leptogenesis scale for producing the observed baryon asymmetry.

Our universe is exclusively dominated by matter rather than antimatter. The asymmetry of baryon-anti-baryon density $n_B - \bar{n}_B (\simeq n_B)$ relative to the photon density n_γ is measured to be a tiny nonzero ratio [16],

$$\eta_B \equiv \frac{n_B - \bar{n}_B}{n_\gamma} = (6.19 \pm 0.15) \times 10^{-10}. \quad (4.28)$$

The SM fails to generate the observed baryon asymmetry because of the too small CP-violations from CKM matrix and the lack of sufficiently strong first-order electroweak phase transition [39], which violate Sakharov's condition for baryogenesis [40]. It is important that the seesaw extension of the SM allows the thermal leptogenesis [37] with CP-violations originating from the neutrino sector and the lepton-number asymmetry produced during out-of-equilibrium decays of heavy Majorana neutrino N_j into the lepton-Higgs pair ℓH and its CP-conjugate $\bar{\ell}H^*$. Then, the lepton asymmetry can be partially converted to a baryon asymmetry via the nonperturbative electroweak sphaleron [41] interactions which violate $B + L$ [42] but preserve $B - L$ [43, 44], $\eta_B = \frac{\xi}{f} N_{B-L}^f = -\frac{\xi}{f} N_L^f$, where ξ is the fraction of $B - L$ asymmetry converted to baryon asymmetry via sphaleron process [43] and $\xi = 28/79$ for the SM. The dilution factor $f = N_\gamma^{\text{rec}}/N_\gamma^* = 2387/86$ is computed by considering standard photon production from the onset of leptogenesis till recombination [44]. The effect of the heavier right-handed neutrino (N_2) decays will be washed out in the thermal equilibrium, only the lightest one (N_1) can effectively generate the net lepton asymmetry for $M_1 \ll M_2$. (In the numerical analysis below, we will consider the parameter space with $M_2/M_1 \geq 5$, to ensure the full washout of lepton asymmetry from N_2 -decays.) Thus, the net lepton asymmetry N_L^f is deduced as [44], $N_L^f = \frac{3}{4} \kappa_f \epsilon_1$. Hence, we can derive the final baryon asymmetry,

$$\eta_B = -\frac{3\xi}{4f} \kappa_f \epsilon_1 = -d \kappa_f \epsilon_1, \quad (4.29)$$

where $d \equiv 3\xi/(4f) \simeq 0.96 \times 10^{-2}$, and the factor κ_f measures the efficiency of out-of-equilibrium N_1 -decays. The κ_f is determined by solving the Boltzmann equation numerically [44, 45]. In practice, useful analytical formulas for κ_f can be inferred by fitting the numerical solution of the Boltzmann equation. We find it convenient to use the following fitting formula of κ_f [45],

$$\kappa_f^{-1} \simeq \left(\frac{\bar{m}_1}{0.55 \times 10^{-3} \text{ eV}} \right)^{1.16} + \frac{3.3 \times 10^{-3} \text{ eV}}{\bar{m}_1}, \quad (4.30)$$

with $\bar{m}_1 \equiv (\underline{m}_D^\dagger \underline{m}_D)_{11}/M_1$, and $\underline{m}_D \equiv m_D U_R$ with U_R being the rotation matrix diagonalizing the mass-matrix M_R of right-handed neutrinos. In the present $\mu - \tau$ blind seesaw, it is natural to set the right-handed neutrinos in their mass-eigenbasis from the start, $M_R = \text{diag}(M_1, M_2)$, as we defined in Sec. 2.1. So we have $U_R = \mathcal{I}$ with \mathcal{I} the unit matrix, and thus $\underline{m}_D = m_D$. (Other fitting

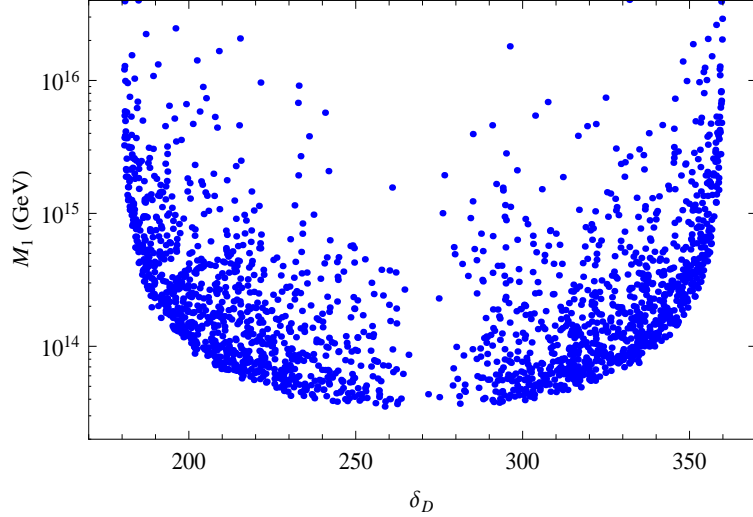


Figure 4: Leptogenesis scale M_1 is plotted as a function of Dirac CP-phase angle δ_D , where the seven years of WMAP measurement (4.28) is imposed. All experimental inputs are scanned within their 90% C.L. ranges, with 1500 samples.

formulas than (4.30) to the exact solution of κ_f in the literature [44] agree with each other quite well for the relevant range of \overline{m}_1 .) The CP asymmetry parameter ϵ_1 is defined as

$$\epsilon_1 \equiv \frac{\Gamma[N_1 \rightarrow \ell H] - \Gamma[N_1 \rightarrow \bar{\ell} H^*]}{\Gamma[N_1 \rightarrow \ell H] + \Gamma[N_1 \rightarrow \bar{\ell} H^*]} = \frac{1}{4\pi v^2} F\left(\frac{M_2}{M_1}\right) \frac{\Im\left\{[(\underline{m}_D^\dagger \underline{m}_D)_{12}]^2\right\}}{(\underline{m}_D^\dagger \underline{m}_D)_{11}}, \quad (4.31)$$

where v denotes the vacuum expectation value of the SM Higgs boson. As we constructed in Sec. 2.2, the Dirac mass-matrix \underline{m}_D is complex and provides the common origin of the $\mu-\tau$ and CP breaking; the complexity of \underline{m}_D causes the difference between the decay widths $\Gamma[N_1 \rightarrow \ell H]$ and $\Gamma[N_1 \rightarrow \bar{\ell} H^*]$, and thus a nonzero CP asymmetry $\epsilon_1 \neq 0$. For the SM, the function $F(x)$ in (4.31) takes the form,

$$F(x) \equiv x \left[1 - (1+x^2) \ln \frac{1+x^2}{x^2} + \frac{1}{1-x^2} \right] = -\frac{3}{2x} + \mathcal{O}\left(\frac{1}{x^3}\right), \quad (\text{for } x \gg 1). \quad (4.32)$$

For our numerical analysis of the thermal leptogenesis, the mass ratio $M_2/M_1 \gg 1$ and thus the above expanded formula of $F(x)$ holds with good accuracy.

Then, we proceed to compute the matrix elements,

$$(\underline{m}_D^\dagger \underline{m}_D)_{11} = \widehat{m}_0 M_1 (a^2 + 2b^2) = \widehat{m}_0 M_1, \quad (4.33a)$$

$$(\underline{m}_D^\dagger \underline{m}_D)_{12} = -\widehat{m}_0 \sqrt{M_1 M_2} bc(\zeta' + \zeta e^{i\omega}). \quad (4.33b)$$

So we can deduce the effective mass-parameter \overline{m}_1 as introduced below (4.30),

$$\overline{m}_1 = \widehat{m}_0 \simeq \chi_1 \sqrt{\Delta m_{13}^2}, \quad (4.34)$$

and the imaginary part,

$$\Im\left\{[(\underline{m}_D^\dagger \underline{m}_D)_{12}]^2\right\} = -\frac{1}{2} \widehat{m}_0^2 M_1 M_2 y' \sin 2\theta_s \sin \delta_D \delta_x, \quad (4.35)$$

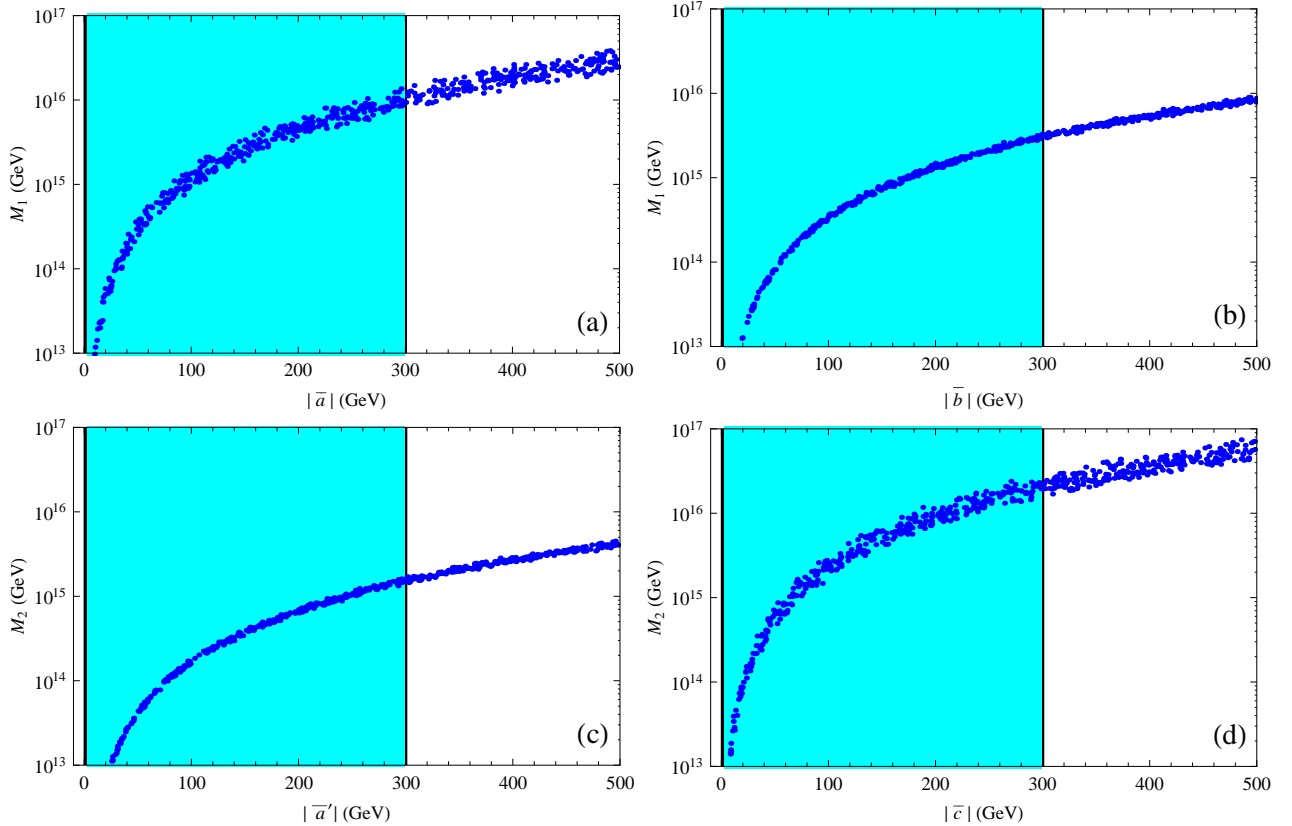


Figure 5: Seesaw scale M_1 and M_2 as functions of the elements (\bar{a}, \bar{b}) and (\bar{a}', \bar{c}) in the Dirac mass-matrix m_D , where the shaded regions correspond to the natural perturbative region $(\bar{a}, \bar{b}, \bar{a}', \bar{c}) \in [1, 300] \text{ GeV}$, and 600 samples are generated in each plot. This puts an upper bound, $M_1 \leq 3.5 \times 10^{15} \text{ GeV}$ from plot-(b), and $M_2 \leq 1.7 \times 10^{15} \text{ GeV}$ from plot-(c).

where the RG running factor $\chi_1 = \chi(M_1, m_Z)$ is defined in Eqs. (3.18)-(3.19). Using Eq. (4.34) together with the neutrino data (Table-1), we find that the light neutrino mass-parameter \overline{m}_1 lies in the 3σ range, $0.046 < \overline{m}_1/\chi_1 < 0.053 \text{ eV}$, where the RG factor $\chi_1 \simeq 1.3 - 1.4$ is evaluated numerically, as explained around the end of Sec. 3.2. So, in Eq. (4.30) the second term on the right-hand-side is negligible and κ_f is thus dominated by the first term.

With these and from (4.31), we derive the CP asymmetry parameter ϵ_1 as follows,

$$\epsilon_1 \simeq \frac{3y' \widehat{m}_0 M_1}{16\pi v^2} \sin 2\theta_s \sin \delta_D \delta_x. \quad (4.36)$$

Finally, inspecting Eqs. (4.29), (4.31) and (4.32), we can derive,

$$\frac{\eta_B}{M_1} = -d \kappa_f \frac{3y' \widehat{m}_0}{16\pi v^2} \sin 2\theta_s \sin \delta_D \delta_x. \quad (4.37)$$

Since the WMAP measurement (4.28) finds the baryon asymmetry $\eta_B > 0$, so we can infer the constraint, $\sin \delta_D < 0$, which restricts the Dirac phase angle, $\delta_D \in (\pi, 2\pi)$.

Then, from Eq. (4.37) we compute the ratio η_B/M_1 for any nonzero $\sin \delta_D$, where we vary all measured quantities within their 90% C.L. ranges. Since $0 < |\sin \delta_D| \leq 1$, we can deduce a robust numerical upper bound,

$$\frac{\eta_B}{M_1} < 1.8 \times 10^{-23} \text{ GeV}^{-1}. \quad (4.38)$$

Inspecting (4.37) we can also reexpress the leptogenesis scale M_1 in terms of baryon asymmetry η_B and other physical observables,

$$M_1 = \frac{-16\pi v^2 \eta_B}{3d \kappa_f \hat{m}_0 y' \sin 2\theta_s \sin \delta_D \delta_x}. \quad (4.39)$$

With the data of η_B from (4.28), we can plot, in Fig. 4, the leptogenesis scale M_1 as a function of Dirac CP-phase δ_D , where all experimentally measured quantities are scanned within their 90% C.L. range (with 1500 samples). Fig. 4 reveals a robust lower bound on M_1 ,

$$M_1 > 3.5 \times 10^{13} \text{ GeV}. \quad (4.40)$$

Using Eqs. (2.7) and (4.6), we connect the seesaw scale (M_1, M_2) to the elements of the Dirac mass-matrix m_D ,

$$M_1 = \frac{\bar{a}^2}{\hat{m}_0 \cos^2 2\theta_s} = \frac{2 \bar{b}^2}{\hat{m}_0 \sin^2 2\theta_s}, \quad (4.41a)$$

$$M_2 = \frac{\bar{a}'^2}{\hat{m}_0 \sin^2 2\theta_s} = \frac{2 \bar{c}^2}{\hat{m}_0 \cos^2 2\theta_s}, \quad (4.41b)$$

where the Dirac mass-parameters $(\bar{a}, \bar{b}, \bar{a}', \bar{c})$ arise from the Yukawa interactions, $(\bar{a}, \bar{b}, \bar{a}', \bar{c}) = (y_a, y_b, y_{a'}, y_c)v/\sqrt{2}$. So we can plot M_1 as a function of the magnitude of the Dirac mass-parameter $|\bar{a}|$ or $|\bar{b}|$ in Fig. 5(a)-(b), and M_2 as a function of the magnitude of the Dirac mass-parameter $|\bar{a}'|$ or $|\bar{c}|$ in Fig. 5(c)-(d), where we have varied the measured quantities in their 90% C.L. ranges. We note that the Yukawa couplings $(y_a, y_b, y_{a'}, y_c)$ cannot be too small (to avoid excessive fine-tuning) or too large (to keep valid perturbation). So, we will take the Dirac mass-parameters $(\bar{a}, \bar{b}, \bar{a}', \bar{c})$ in the natural range $[1, 300]$ GeV, corresponding to the Yukawa couplings y_j no smaller than $O(10^{-2})$ and no larger than $O(y_t)$, where $y_t = \sqrt{2}m_t/v \simeq 1$ is the top-quark Yukawa coupling in the SM. This natural perturbative range of $(\bar{a}, \bar{b}, \bar{a}', \bar{c})$ is indicated by the shaded area in Fig. 5(a)-(d), which results in an upper limit on the seesaw scale (M_1, M_2) due to the perturbativity requirement. From Fig. 5(b) we infer an upper bound $M_1 \leq 3.5 \times 10^{15}$ GeV, while Fig. 5(c) requires $M_2 \leq 1.67 \times 10^{15}$ GeV. For the above construction of natural thermal Leptogenesis we consider the parameters space $M_2/M_1 \geq 5$, so with the upper bound of Fig. 5(c) we further deduce a stronger limit $M_1 \leq 3.3 \times 10^{14}$ GeV.

With the above constraint on the parameter space from realizing successful thermal leptogenesis, we can rederive the correlation between θ_{13} and $\theta_{23} - 45^\circ$, as shown in the new Fig. 6, which should be compared with Fig. 2 in Sec. 4.1 (without requiring leptogenesis). We note that the realization of successful thermal leptogenesis puts a general *lower bound* on the mixing angle θ_{13} ,

$$\theta_{13} \gtrsim 1^\circ, \quad (4.42)$$

even for the region around $\theta_{23} = 45^\circ$.

Under successful leptogenesis, the correlations of θ_{13} with the Jarlskog invariant J and the neutrinoless double beta decay observable M_{ee} are plotted in Fig. 7(a) and (b), respectively. This

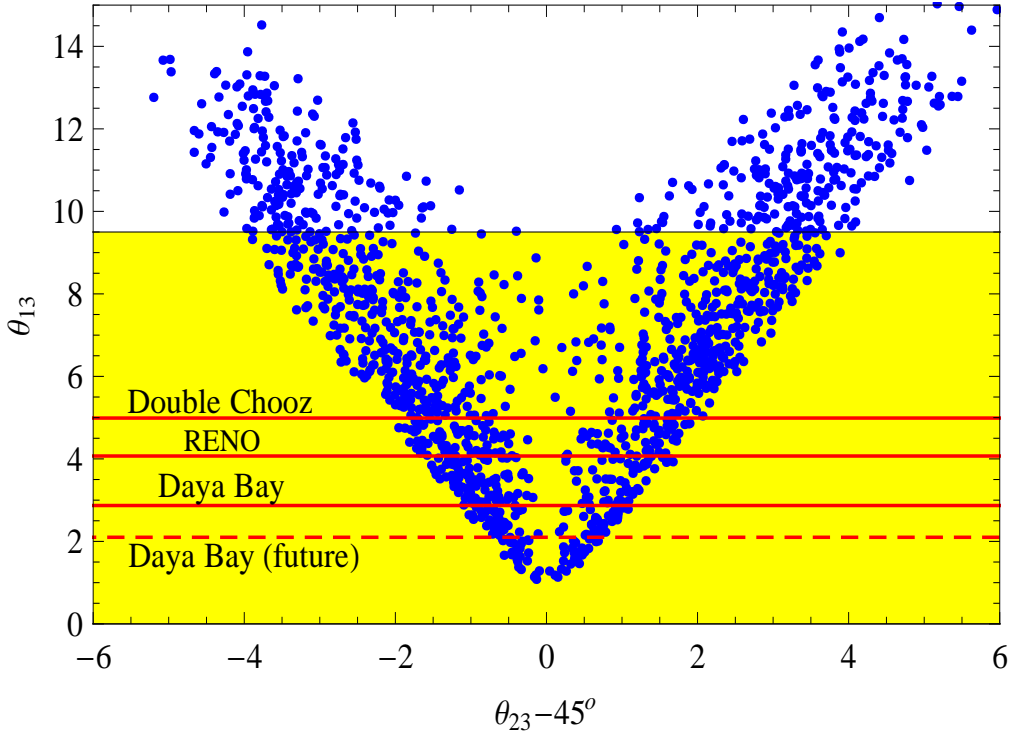


Figure 6: Correlation between θ_{13} and $\theta_{23} - 45^\circ$, where all the inputs are the same as Fig. 2, except requiring successful leptogenesis in the present analysis, with 1500 samples.

should be compared to Fig. 3 where leptogenesis is not required. We see that due to the constraint from the observed baryon asymmetry, the parameter space of $J > 0$ is forbidden in Fig. 7(a). On the other hand, the constrained range for M_{ee} in Fig. 7(b) is almost the same as Fig. 3(b), since Eq. (4.24) shows that the observable M_{ee} has rather weak dependence on small NLO parameters δ_x ($= \theta_{13}$) and $\delta\phi$ via their squared terms. Thus, from Fig. 7(a)-(b), we infer the following constraints on J and M_{ee} ,

$$-0.037 \lesssim J \lesssim -0.0035, \quad (4.43a)$$

$$45.5 \text{ meV} \lesssim M_{ee} \lesssim 50.7 \text{ meV}, \quad (4.43b)$$

which should be compared to Eqs. (4.25a)-(4.25b) in Sec. 4.1 without requiring the successful leptogenesis.

We further analyze the correlations of the neutrinoless $\beta\beta$ -decay observable M_{ee} with the Jarlskog invariant J and the light neutrino mass m_1 ($\simeq m_2$), in Fig. 8(a-b) and Fig. 8(c-d), respectively. The two left plots in Fig. 8(a) and (c) show the correlations of M_{ee} with J and with m_1 after imposing the leptogenesis. For the two right plots in Fig. 8(b)(d), we have replotted the same model-predictions as in the two corresponding left plots of Fig. 8(a)(c) (all in blue color). For comparison, we have further plotted, in Fig. 8(b)(d) with green color, the model-independent parameter space of M_{ee} [cf. (4.24)] versus J [cf. (4.23)] or m_1 ($= \sqrt{\Delta m_{13}^2}$), for the IMO scheme with $m_3 \simeq 0$, where the relevant observables are varied within their 90% C.L. ranges and $\delta_D \in (0, 2\pi]$. This comparison

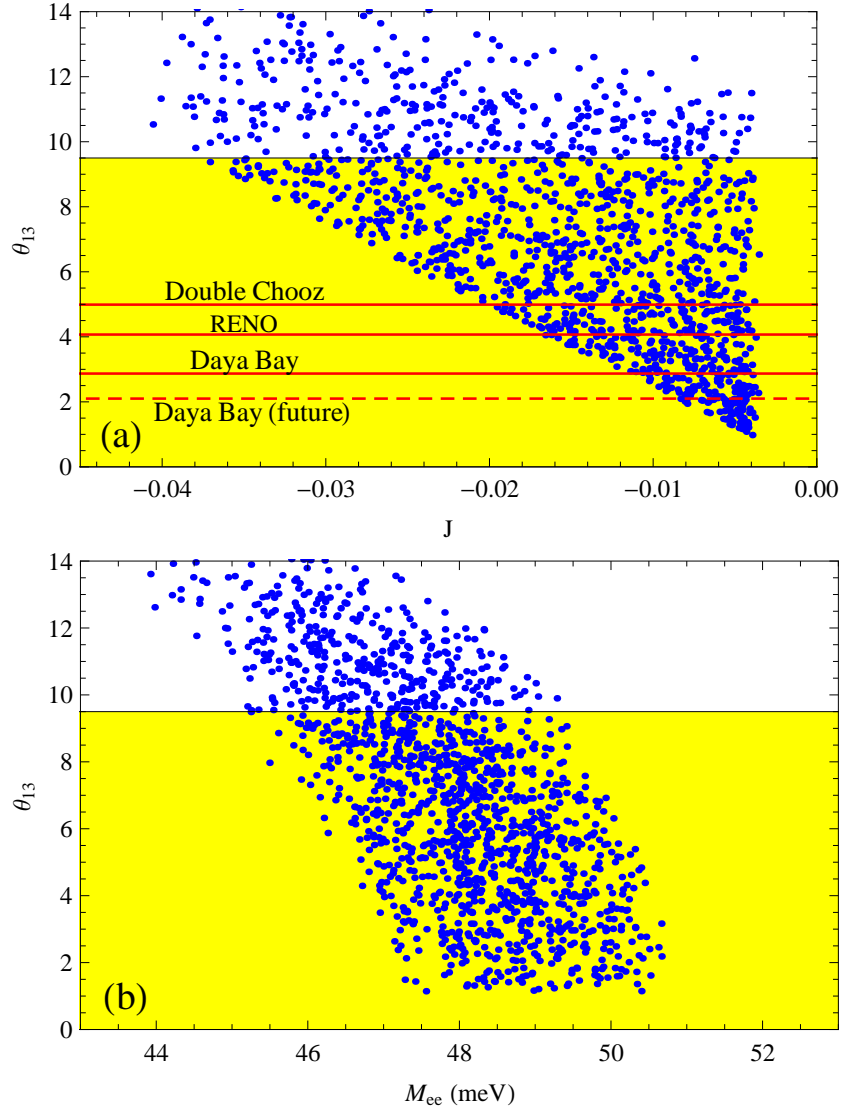


Figure 7: Correlations of θ_{13} with Jarlskog invariant J in plot-(a) and with neutrinoless double beta decay observable M_{ee} in plot-(b), where all inputs are the same as Fig. 3, except requiring the successful leptogenesis in the present figure, with 1500 samples for each plot.

shows that our model predictions are located at the *upper boundaries* of the whole parameter space, giving rise to the largest allowed M_{ee} . This is very distinctive and highly testable. Furthermore, in Fig. 8(b)(d), we have compared our predictions with the sensitivities of the future neutrinoless $\beta\beta$ -decay experiments CUORE (CU) [46] and Majorana [47]/GERDA III [48] (M/G), which are depicted by the horizontal dashed lines at 15 meV (black) and 20 meV (red), respectively.

The leptogenesis scale M_1 can be determined from the baryon asymmetry η_B , the reactor angle θ_{13} , the Dirac phase $\sin \delta_D$ and other neutrino observables as in Eq. (4.39). Since the low energy parameter J in Eq. (4.23) is also predicted as a function of θ_{13} and $\sin \delta_D$, so it will correlate with the leptogenesis scale M_1 . Hence, we can plot the correlations of the leptogenesis scale M_1 with the reactor angle θ_{13} in Fig. 9(a), and with the Jarlskog invariant J in Fig. 9(b). Inspecting Eqs. (4.23) and (4.39), we deduce, $J \propto \delta_x \sin \delta_D$ and $M_1 \propto (\delta_x \sin \delta_D)^{-1}$, from which we arrive

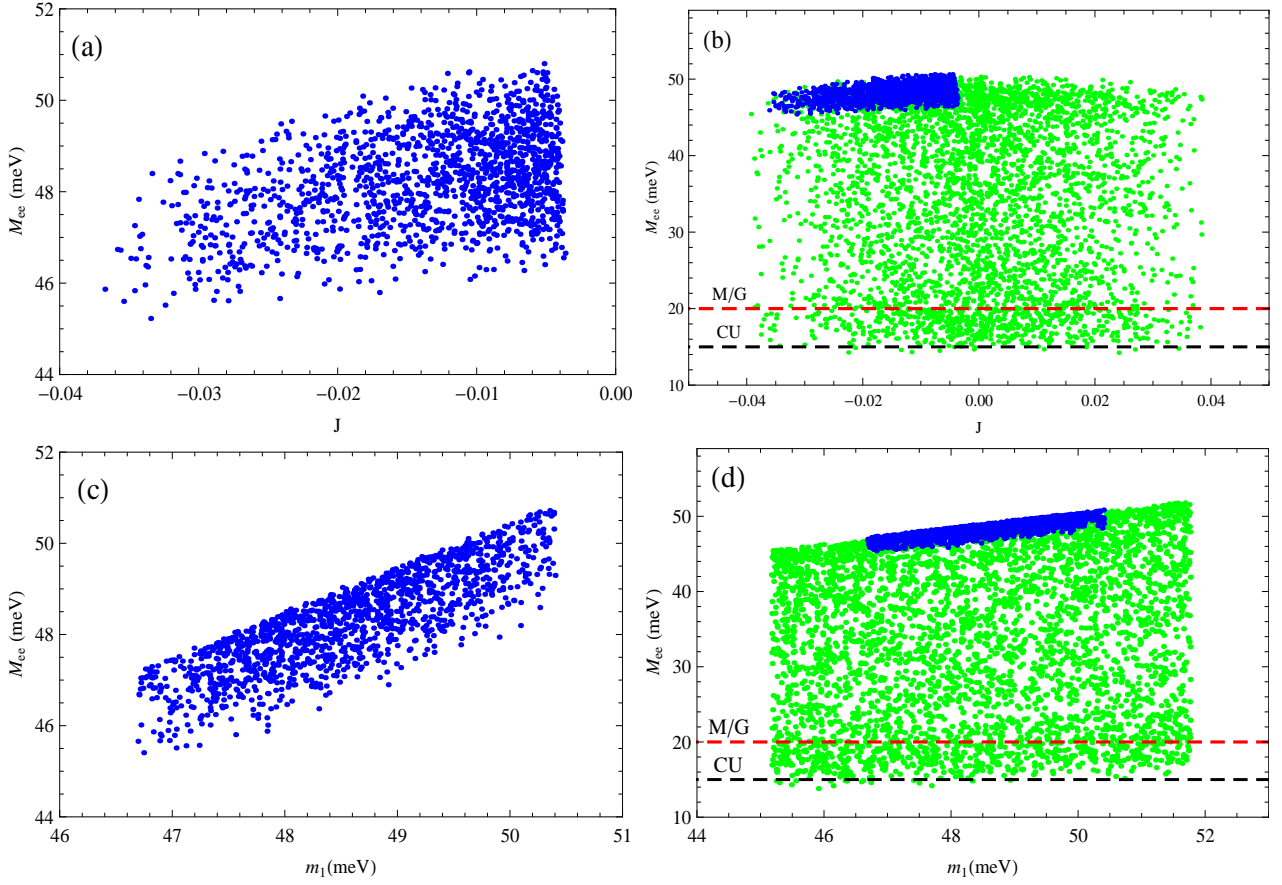


Figure 8: Upper plots (a)-(b) show the correlations between the neutrinoless $\beta\beta$ -decay observable M_{ee} and the Jarlskog invariant J with successful leptogenesis. Lower plots (c)-(d) depict the correlations between M_{ee} and light neutrino mass $m_1 (\simeq m_2)$ with successful leptogenesis. All experimental inputs are varied within 90% C.L. ranges, for 1500 samples. The background (green) regions in plots (b) and (d) represent the model-independent parameter space of the IMO scheme with $m_3 \simeq 0$. The horizontal dashed lines in (b) and (d) depict the sensitivities of the future neutrinoless $\beta\beta$ -decay experiments CUORE (CU) [46] and Majorana [47]/GERDA III [48] (M/G), at 15 meV (black) and 20 meV (red), respectively.

at, $M_1 \propto 1/|J|$. This behavior is impressively reflected in Fig. 9(b), as expected. In addition, the relation, $M_1 \propto (\delta_x \sin \delta_D)^{-1} \geq \theta_{13}^{-1}$, nicely explains the lower arched edge in Fig. 9(a).

4.3. Extension to General Three-Neutrino Seesaw

In this subsection, we analyze the extension to the general neutrino seesaw with three right-handed neutrinos $\mathcal{N}' = (N_1, N_2, N_3)^T$, where \mathcal{N}' is $\mu-\tau$ blind. Then, in the $\mu-\tau$ and CP symmetric limit, the mass-matrices m_D and M_R are extended to 3×3 matrices,

$$m_D = \begin{pmatrix} \bar{a} & \bar{a}' & \bar{a}'' \\ \bar{b} & \bar{c} & \bar{d} \\ \bar{b} & \bar{c} & \bar{d} \end{pmatrix} \equiv \begin{pmatrix} \sigma_1 a & \sigma_2 a' & \sigma_3 a'' \\ \sigma_1 b & \sigma_2 c & \sigma_3 d \\ \sigma_1 b & \sigma_2 c & \sigma_3 d \end{pmatrix}, \quad M_R = \text{diag}(M_1, M_2, M_3), \quad (4.44)$$

with $\sigma_1 \equiv \sqrt{\hat{m}_0 M_1}$, $\sigma_2 \equiv \sqrt{\hat{m}_0 M_2}$, and $\sigma_3 \equiv \sqrt{\hat{m}_0 M_3}$, where the $\mu-\tau$ blind right-handed neutrinos \mathcal{N}' can always be rotated into their mass-eigenbasis without affecting the structure of

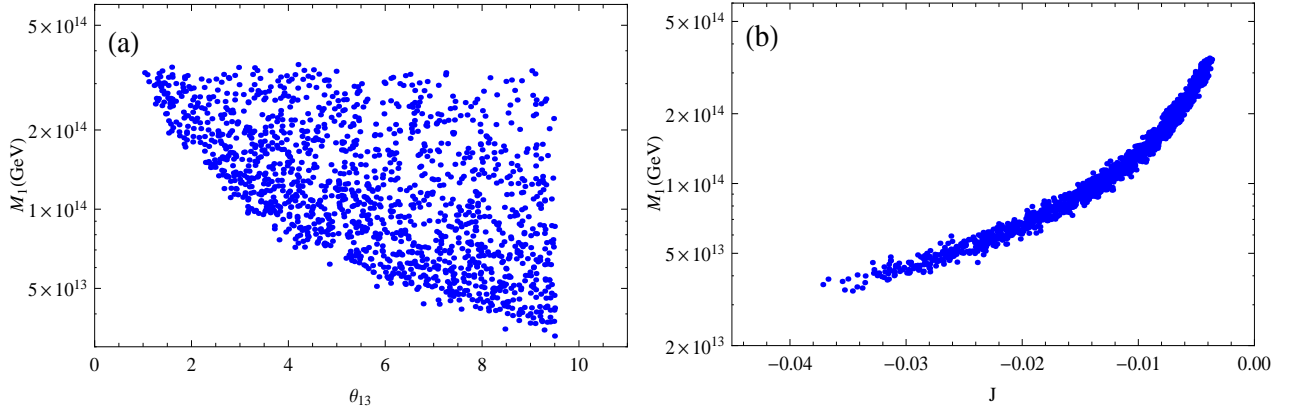


Figure 9: Correlations of leptogenesis scale M_1 with the reactor mixing angle θ_{13} in plot-(a), and with the low energy Jarlskog invariant J in plot-(b). Each plot contains 1500 samples.

m_D . Thus, we rederive the $\mu-\tau$ and CP symmetric seesaw mass-matrix for the light neutrinos,

$$M_\nu = \hat{m}_0 \begin{pmatrix} a^2 + a'^2 + a''^2 & ab + a'c + a''d & ab + a'c + a''d \\ & b^2 + c^2 + d^2 & b^2 + c^2 + d^2 \\ & & b^2 + c^2 + d^2 \end{pmatrix} \equiv \begin{pmatrix} A & B_s & B_s \\ C_s & C_s & C_s \end{pmatrix}, \quad (4.45)$$

from which we deduce the mass-eigenvalues and mixing angles,

$$\begin{aligned} \hat{m}_{1,2} &= \frac{1}{2} \left[(A + 2C_s) \mp \sqrt{(A - 2C_s)^2 + 8B_s^2} \right] \\ &= \frac{\hat{m}_0}{2} \left[(a^2 + a'^2 + a''^2 + 2b^2 + 2c^2 + 2d^2) \right. \\ &\quad \left. \mp \sqrt{[(a^2 + a'^2 + a''^2) - 2(b^2 + c^2 + d^2)]^2 + 8(ab + a'c + a''d)^2} \right], \end{aligned} \quad (4.46a)$$

$$\hat{m}_3 = C_s - C_s = 0, \quad (4.46b)$$

$$\tan 2\theta_{12} = \frac{2\sqrt{2}B_s}{A - 2C_s} = \frac{2\sqrt{2}|ab + a'c + a''d|}{|a^2 + a'^2 + a''^2 - 2(b^2 + c^2 + d^2)|}, \quad (4.46c)$$

$$\theta_{23} = 45^\circ, \quad \theta_{13} = 0^\circ, \quad (4.46d)$$

where the mass-spectrum remains the inverted mass-ordering (IMO). The third mass-eigenvalue \hat{m}_3 vanishes because our $\mu-\tau$ blind seesaw (4.44) predicts the seesaw mass-matrix (4.45) with its 23-element equal to the 22-element and 33-element. This is also a general feature of any $\mu-\tau$ symmetric IMO scheme at the LO, as to be shown in (5.5) of Sec. 5.1. Furthermore, we will demonstrate shortly that the third mass-eigenvalue $\hat{m}_3 = 0$ actually holds up to the NLO after including the $\mu-\tau$ and CP breaking in our analysis. So this resembles very much the minimal seesaw we studied earlier.

Similar to Eqs. (2.11) and (2.13) in Sec. 2.1, we can realize the IMO at the LO of three-neutrino seesaw, $\hat{m}_1 = \hat{m}_2 = \hat{m}_0$, which leads to the three extended conditions,

$$(a^2 + a'^2 + a''^2) + 2(b^2 + c^2 + d^2) = 2, \quad (4.47a)$$

$$(a^2 + a'^2 + a''^2) - 2(b^2 + c^2 + d^2) = 0, \quad (4.47b)$$

$$ab + a'c + a''d = 0. \quad (4.47c)$$

With these we deduce from (4.45) the generic LO seesaw mass-matrix for the IMO,

$$M_\nu^{(0)} = \hat{m}_0 \begin{pmatrix} a^2 + a'^2 + a''^2 & ab + a'c + a''d & ab + a'c + a''d \\ & b^2 + c^2 + d^2 & b^2 + c^2 + d^2 \\ & & b^2 + c^2 + d^2 \end{pmatrix} = \hat{m}_0 \begin{pmatrix} 1 & 0 & 0 \\ & \frac{1}{2} & \frac{1}{2} \\ & & \frac{1}{2} \end{pmatrix}, \quad (4.48)$$

which is the same as the LO mass-matrix (2.31a) we derived earlier for the minimal seesaw. Hence, despite that the LO mass-matrix $M_\nu^{(0)}$ contains two new parameters (a'', d) at the beginning, the realization of IMO eliminates them all and reduces $M_\nu^{(0)}$ to the universal LO mass-matrix as shown in the final form of (4.48) which is parameter-free except an overall mass-scale. As a result of the IMO conditions (4.47), we note that the solar angle formula (4.46c) gives $\tan 2\theta_{12} = \frac{0}{0}$ at the LO, which is now undetermined. So, the θ_{12} has to be derived from the NLO contributions related to $\mu - \tau$ breaking terms. Before getting into detail, it is convenient to infer θ_{12} by using the l'Hôpital rule, similar to what we did in Sec. 2.1 for the minimal seesaw. Thus we have,

$$\tan 2\theta_{12} = \frac{|a|}{\sqrt{2}|b|}, \quad (4.49a)$$

for $\mu - \tau$ breaking arising from the deviation in the element b of m_D , or

$$\tan 2\theta_{12} = \frac{|a'|}{\sqrt{2}|c|}, \quad (4.49b)$$

for $\mu - \tau$ breaking arising from the deviation in the element c of m_D , or

$$\tan 2\theta_{12} = \frac{|a''|}{\sqrt{2}|d|}, \quad (4.49c)$$

for $\mu - \tau$ breaking arising from the deviation in the element d of m_D .

As noted in Sec. 2.2, we can always rotate the first column in m_D to be all real by rephasing. For the convenience of comparison with the minimal neutrino seesaw, we will thus formulate the common origin of $\mu - \tau$ and CP breaking in the element c of m_D . It is possible to construct such a breaking in the element d of m_D , but this does not affect our physical conclusions as will be clarified below, after Eq.(4.57). [Since we are constructing a common origin of $\mu - \tau$ and CP breaking from a single source in m_D , we do not consider this breaking to occur in both c and d elements of m_D at the same time.] So, we build the Dirac mass-matrix m_D with the common $\mu - \tau$ and CP breaking in the following form,

$$m_D = \begin{pmatrix} \sigma_1 a & \sigma_2 a' & \sigma_3 a'' \\ \sigma_1 b & \sigma_2 c_1 & \sigma_3 d \\ \sigma_1 b & \sigma_2 c_2 & \sigma_3 d \end{pmatrix}, \quad (4.50a)$$

$$c_1 = c(1 - \zeta'), \quad c_2 = c(1 - \zeta e^{i\omega}). \quad (4.50b)$$

Thus we can deduce the NLO part of the seesaw mass-matrix $M_\nu = M_\nu^{(0)} + \delta M_\nu^{(1)}$ for light neutrinos,

$$\delta M_\nu^{(1)} = \hat{m}_0 \begin{pmatrix} 0 & -a'c\zeta' & -a'c\zeta e^{i\omega} \\ & -2c^2\zeta' & -c^2(\zeta' + \zeta e^{i\omega}) \\ & & -2c^2\zeta e^{i\omega} \end{pmatrix}, \quad (4.51)$$

which equals (2.31b) as expected, since the new parameters (a'', d) appear in the seesaw mass-matrix M_ν only via the products $(a''^2, d^2, a''d)$ with no crossing terms like $c_{1,2}a''$ or $c_{1,2}d$. With these, we deduce the $\mu-\tau$ symmetric and antisymmetric elements of $\delta M_\nu^{(1)}$ to be the same as Eq. (2.33).

Using the formalism of Sec. 3.1 and extending Sec. 3.2, we can reconstruct the light neutrino mass-matrix M_ν for the IMO with $m_3 \neq 0$, via the NLO parameters,

$$(y', z, z', \delta_a, \delta_x, \delta\bar{\alpha}_1, \delta\bar{\alpha}_2, \delta\bar{\alpha}_3, \delta\phi, \delta\phi'), \quad (4.52)$$

where we have defined $z' \equiv \frac{m_3}{m_1}$ and $\phi' \equiv \phi_3 - \phi_1 = \phi'_0 + \delta\phi'$. Note that the LO phases vanish, $\bar{\alpha}_{i0} = \phi_0 = \phi'_0 = 0$. So the NLO elements of M_ν are reconstructed as follows,

$$\delta A = m_0 \left[z + \frac{s_s^2}{2} y' - i2(s_s^2 \delta\phi + \delta\bar{\alpha}_1) \right], \quad (4.53a)$$

$$\delta B_s = \frac{m_0}{2\sqrt{2}} \sin 2\theta_s \left[-\frac{1}{2} y' + i2\delta\phi \right], \quad (4.53b)$$

$$\delta C_s = \frac{m_0}{2} \left[z + z' + \frac{c_s^2}{2} y' - i(2c_s^2 \delta\phi + \delta\bar{\alpha}_2 + \delta\bar{\alpha}_3) \right], \quad (4.53c)$$

$$\delta D = \frac{m_0}{2} \left[z - z' + \frac{c_s^2}{2} y' - i(2c_s^2 \delta\phi + \delta\bar{\alpha}_2 + \delta\bar{\alpha}_3) \right], \quad (4.53d)$$

$$\delta B_a = -\frac{m_0}{\sqrt{2}} e^{i\delta_D} \delta_x, \quad (4.53e)$$

$$\delta C_a = -m_0 \left[\delta_a + \frac{i}{2} (\delta\bar{\alpha}_2 - \delta\bar{\alpha}_3) \right], \quad (4.53f)$$

where we note that the Majorana phase $\delta\phi'$ does not appear at the NLO because it is always suppressed by another NLO parameter $z' = \frac{m_3}{m_1}$. Moreover, since the $\mu-\tau$ and CP breaking matrix (4.51) gives Eq. (2.33) with the equality $\delta C_s = \delta D$, we deduce $z' = \frac{m_3}{m_1} = 0$ by comparing (4.53c) with (4.53d), and thus $m_3 = 0$ holds up to the NLO. Hence, we have shown that our model with the general three-neutrino seesaw under IMO does share the essential feature of $m_3 = 0$ with the minimal seesaw.

Then, with the NLO $\mu-\tau$ symmetric parts from (2.33) and (4.53), we deduce the solar angle θ_{12} ,

$$\tan 2\theta_s = -\frac{a'}{\sqrt{2}c}, \quad (4.54)$$

which coincides with Eq. (4.5) as we derived earlier for the minimal seesaw.

Next, connecting the $\mu-\tau$ anti-symmetric parts in (2.33) and (4.53) gives,

$$\frac{m_0}{2} a' c (\zeta' - \zeta e^{i\omega}) = -\frac{m_0}{\sqrt{2}} e^{i\delta_D} \delta_x, \quad (4.55a)$$

$$-m_0 c^2 (\zeta' - \zeta e^{i\omega}) = -m_0 \left[\delta_a + \frac{i}{2} (\delta \bar{\alpha}_2 - \delta \bar{\alpha}_3) \right], \quad (4.55b)$$

from which we arrive at

$$\cos \delta_D \delta_x = \frac{a' c}{\sqrt{2}} (\zeta' - \zeta \cos \omega), \quad (4.56a)$$

$$\sin \delta_D \delta_x = -\frac{a' c}{\sqrt{2}} (\zeta \sin \omega), \quad (4.56b)$$

$$\delta_a = c^2 (\zeta' - \zeta \cos \omega), \quad (4.56c)$$

$$\delta \bar{\alpha}_2 - \delta \bar{\alpha}_3 = -2c^2 (\zeta \sin \omega). \quad (4.56d)$$

Here for the left-hand-sides of (4.55a)-(4.55b) we have used the Eq. (3.19) to evolve the overall mass-parameter \hat{m}_0 from seesaw scale down to the corresponding m_0 at low energy.

Finally, using Eqs. (4.54), (4.56a) and (4.56c), we derive the key correlation between two low energy $\mu-\tau$ breaking observables δ_a and δ_x ,

$$\delta_a = -\cot 2\theta_s \cos \delta_D \delta_x, \quad (4.57)$$

which coincides with (4.13) as we derived earlier for the minimal seesaw.

We note that it is also possible to construct the common origin of $\mu-\tau$ and CP breaking in the element d of m_D , instead of the element c . Then we can rewrite the Dirac mass-matrix (4.50) as

$$m_D = \begin{pmatrix} \sigma_1 a & \sigma_2 a' & \sigma_3 a'' \\ \sigma_1 b & \sigma_2 c & \sigma_3 d_1 \\ \sigma_1 b & \sigma_2 c & \sigma_3 d_2 \end{pmatrix}, \quad (4.58a)$$

$$d_1 = d (1 - \zeta'), \quad d_2 = d (1 - \zeta e^{i\omega}). \quad (4.58b)$$

This results in the following NLO seesaw mass-matrix,

$$\delta M_\nu^{(1)} = \hat{m}_0 \begin{pmatrix} 0 & -a'' d \zeta' & -a'' d \zeta e^{i\omega} \\ -2d^2 \zeta' & -d^2 (\zeta' + \zeta e^{i\omega}) & -2d^2 \zeta e^{i\omega} \end{pmatrix}, \quad (4.59)$$

from which we derive the solar angle,

$$\tan 2\theta_s = -\frac{a''}{\sqrt{2} d}, \quad (4.60)$$

and the reconstruction conditions,

$$\cos \delta_D \delta_x = \frac{a'' d}{\sqrt{2}} (\zeta' - \zeta \cos \omega), \quad (4.61a)$$

$$\sin \delta_D \delta_x = -\frac{a'' d}{\sqrt{2}} (\zeta \sin \omega), \quad (4.61b)$$

$$\delta_a = d^2 (\zeta' - \zeta \cos \omega), \quad (4.61c)$$

$$\delta\bar{\alpha}_2 - \delta\bar{\alpha}_3 = -2d^2 (\zeta \sin \omega). \quad (4.61d)$$

So, from Eqs. (4.60), (4.61a) and (4.61c), we can readily derive the correlation between two $\mu - \tau$ breaking observables,

$$\delta_a = -\cot 2\theta_s \cos \delta_D \delta_x, \quad (4.62)$$

which coincides with (4.57).

In summary, the general three-neutrino seesaw (with right-handed neutrinos being $\mu - \tau$ blind) still predicts the inverted mass-ordering (IMO) for light neutrinos [cf. Eqs. (4.46a)-(4.46b)]. Despite that the LO conditions (4.47) for the IMO contains two new parameters (a'', d), the LO seesaw mass-matrix (4.48) is shown to take the same form as in the minimal seesaw. Furthermore, the NLO $\mu - \tau$ and CP breaking part of our seesaw mass-matrix (4.51) or (4.59) exhibits the same structure as in the minimal seesaw. This makes our final physical prediction of the correlation (4.57) or (4.62) coincides with (4.13).

5. Hidden Symmetry and Dictation of Solar Mixing Angle

So far, by analyzing the $\mu - \tau$ symmetry and its breaking, we have studied the atmospheric mixing angle θ_{23} and the reactor mixing angle θ_{13} in great detail. As shown in Table-1, the solar mixing angle θ_{12} is best measured [49, 50] among the three mixing angles. In this section we will clarify the connection between $\mu - \tau$ breaking and the determination of the solar mixing angle θ_{12} for both inverted mass-ordering (IMO) (cf. Sec. 2) and normal mass-ordering (NMO) [1]. Then, we analyze the general model-independent $\mathbb{Z}_2 \otimes \mathbb{Z}_2$ symmetry structure in the light neutrino sector, and map it into the seesaw sector, where one of the \mathbb{Z}_2 symmetries corresponds to the $\mu - \tau$ symmetry $\mathbb{Z}_2^{\mu\tau}$ and another the hidden symmetry \mathbb{Z}_2^s (which we revealed in [1] for the NMO of light neutrinos and is supposed to dictate θ_{12}). We will further derive the general consequences of this \mathbb{Z}_2^s and its possible violation in the presence of $\mu - \tau$ breaking for cases either with or without neutrino seesaw, regarding the θ_{12} determination.

5.1. $\mu - \tau$ Breaking versus θ_{12} Determination: Inverted Mass-Ordering

In Ref. [1] we proved that the solar mixing angle $\theta_{12} (\equiv \theta_s)$ is not affected by the soft $\mu - \tau$ breaking from the neutrino seesaw, and we revealed a hidden symmetry \mathbb{Z}_2^s for both the seesaw Lagrangian and the light neutrino mass-matrix which dictates θ_s , where the normal mass-ordering (NMO) is realized. In this subsection, we generally analyze mass-eigenvalues and mixing angles for the $\mu - \tau$ symmetric mass-matrix of light neutrinos under the inverted mass-ordering (IMO). Then we explain why the $\mu - \tau$ breaking is invoked for the θ_s determination and why the hidden symmetry \mathbb{Z}_2^s will be violated. The $\mu - \tau$ blind seesaw constructed in Sec. 2 belongs to an explicit realization of the IMO scheme.

Let us start with the general $\mu-\tau$ symmetric mass-matrix for light neutrinos,

$$M_\nu^{(s)} = \begin{pmatrix} A & B_s & B_s \\ & C_s & D \\ & & C_s \end{pmatrix}, \quad (5.1a)$$

which can be diagonalized as follows [1, 53],

$$m_{1,2} = \frac{1}{2} \left[[A + (C_s + D)] \mp \sqrt{[A - (C_s + D)]^2 + 8B_s^2} \right], \quad (5.2a)$$

$$m_3 = C_s - D, \quad (5.2b)$$

$$\tan 2\theta_s = \frac{2\sqrt{2}B_s}{A - (C_s + D)}, \quad \theta_a = 45^\circ, \quad \theta_x = 0^\circ. \quad (5.2c)$$

Substituting (5.2c) into (5.2a), we arrive at

$$m_{1,2} = \frac{1}{2} \{ [A + (C_s + D)] \mp |A - (C_s + D)| \sec 2\theta_s \}. \quad (5.3)$$

For the IMO scheme, we have the mass-spectrum $m_2 \gtrsim m_1 \gg m_3$, where a small $m_3 \neq 0$ is also generally allowed for the analysis below. So we can derive, for the general IMO scheme,

$$\left| \frac{A - (C_s + D)}{A + (C_s + D)} \right| = \frac{m_2 - m_1}{m_2 + m_1} \cos 2\theta_s \simeq \frac{\Delta m_{21}^2}{4\Delta m_{13}^2} \cos 2\theta_s = (2.1 - 3.8) \times 10^{-3}, \quad (5.4)$$

where in the last step we have used the neutrino data (Table-1) to estimate the allowed range of this ratio at 90%C.L. Literally, Eq.(5.4) shows a fine-tuned cancellation between the mass-matrix elements A and $(C_s + D)$ down to the level of 10^{-3} . As will be clear in Sec. 5.2. 2 by using the general reconstruction formalism for the IMO scheme, we find that the LO form of the $\mu-\tau$ symmetric mass-matrix $M_\nu^{(0)}$ predicts the exact relations [cf. Eq.(5.44)],

$$A^{(0)} - (C_s^{(0)} + D^{(0)}) = \left[1 - \left(\frac{1}{2} + \frac{1}{2} \right) \right] m_0 = 0, \quad (5.5)$$

$$B_s^{(0)} = 0, \quad C_s^{(0)} - D^{(0)} = 0,$$

which ensures $m_1 = m_2$ and $m_3 = 0$ at the LO. So, the small ratio (5.4) naturally arises from the NLO elements $[\delta A - (\delta C_s + \delta D)] \neq 0$, and thus there is no real fine-tuning in (5.4). This also means that at the LO the solar angle θ_s is undetermined from the formula (5.2c), $\tan 2\theta_s = 0$, and the real determination of θ_s is given by the NLO elements of $M_\nu^{(s)}$,

$$\tan 2\theta_s = \frac{2\sqrt{2}\delta B_s}{\delta A - (\delta C_s + \delta D)}, \quad (5.6)$$

as we will explicitly verify in the next subsection for the general IMO scheme [cf. Eqs.(5.46)-(5.47a)].

For the $\mu-\tau$ blind seesaw defined in Sec. 2.1, we find that the light neutrino mass-spectrum must be inverted ordering, as given in Eqs.(2.10a)-(2.10b). So, following the consistency with neutrino data (5.4) and matching the reconstruction formalism (5.5) for the IMO scheme, we can explicitly realize the degeneracy $m_1 = m_2$ at the LO by imposing the condition (2.11) on the elements of m_D .

(Here $m_3 = 0$ is an outcome of the minimal seesaw.) Thus, as expected, we find a problem for the θ_s determination in the $\mu-\tau$ symmetric limit,

$$\tan 2\theta_s = \frac{2\sqrt{2}|ab + a'c|}{|a^2 + a'^2 - 2(b^2 + c^2)|} = \frac{0}{0}, \quad (5.7)$$

which is just an explicit realization of our above general IMO analysis [cf. (5.5)]. Hence, it is clear that θ_s must be inferred from the NLO formula (5.6), where the NLO elements will be predicted by a given model, *e.g.*, by the first four expressions in Eq. (2.33) in the $\mu-\tau$ blind seesaw with all NLO corrections arising from the $\mu-\tau$ breaking [51]. Thus the explicit expression of θ_s from such underlying models will depend on how the $\mu-\tau$ breaking is constructed. This is contrary to the neutrino seesaw with normal mass-ordering (NMO) of light neutrinos as studied in Ref. [1], where we find that the formula of $\tan 2\theta_s$ [cf. (5.2c) above] is well defined in the $\mu-\tau$ symmetric limit.

As we noted in Sec. 2.1, the structure $\frac{0}{0}$ in Eq. (5.7) allows us to use the l'Hôpital rule on (5.7) by taking the first derivatives on both its numerator and denominator. We need to decide for which parameter in (5.7) the derivatives should be taken. There are only two possible choices, either c or b , since the $\mu-\tau$ breaking under the $\mu-\tau$ blind seesaw could appear in either c or b element of m_D , as we explicitly constructed in Eqs. (2.18) and (2.23). Thus, applying the l'Hôpital rule to (5.7) we have

$$\tan 2\theta_s = \begin{cases} \frac{|a'|}{\sqrt{2}|c|}, & (\mu-\tau \text{ breaking in } c), \\ \frac{|a|}{\sqrt{2}|b|}, & (\mu-\tau \text{ breaking in } b), \end{cases} \quad (5.8)$$

which, as expected, gives finite expressions for θ_s , depending only on the LO parameters of the Dirac mass-matrix m_D . This also agrees to Eqs. (2.15)-(2.16) in Sec. 2.1. But Eq. (5.8) shows that θ_s does depend on how the $\mu-\tau$ breaking is built in the seesaw Lagrangian, and the two different constructions of $\mu-\tau$ breaking for m_D lead to two different θ_s formulas above. This is an essential difference from the soft $\mu-\tau$ breaking model in Ref. [1], where θ_s is dictated by the hidden symmetry \mathbb{Z}_2^s under which the soft $\mu-\tau$ breaking term in M_R is an exact singlet. In the next subsections we will analyze the general model-independent $\mathbb{Z}_2 \otimes \mathbb{Z}_2$ symmetry in the light neutrino sector, and then map it into the seesaw sector. This allows us to explore, *at a deeper level, the \mathbb{Z}_2^s symmetry and its possible partial violation under the $\mu-\tau$ breaking in a unified way, concerning θ_s determination.*

5.2. \mathbb{Z}_2^s Symmetry under General $\mu-\tau$ Breaking and General Determination of θ_{12}

This subsection consists of two parts. In Sec. 5.2.1, we analyze the general model-independent $\mathbb{Z}_2 \otimes \mathbb{Z}_2$ symmetry structure of the light neutrino sector, in both the mass and flavor eigenbases. We will show that, in the flavor eigenbasis of light neutrinos, one of the \mathbb{Z}_2 's is the $\mathbb{Z}_2^{\mu\tau}$ symmetry which predicts the mixing angles $(\theta_{23}, \theta_{13}) = (45^\circ, 0^\circ)$, and another is the \mathbb{Z}_2^s symmetry which generally dictates the solar angle θ_{12} by its group parameter (allowing deviations from the conventional tri-bimaximal

mixing ansatz). With general $\mu - \tau$ breaking parameters, we will derive a nontrivial correlation between the two $\mu - \tau$ breaking observables which is *necessary for holding the \mathbb{Z}_2^s symmetry*. In Sec. 5.2.2, we will further analyze the general $\mu - \tau$ breaking in the light neutrino mass-matrix M_ν and derive a nontrivial consistency condition to hold the \mathbb{Z}_2^s symmetry. From this condition and using the general reconstruction formalism of Sec. 3.1, we will deduce the *same correlation* between the $\mu - \tau$ breaking observables, for both the normal mass-ordering and inverted mass-ordering of light neutrinos (*without* approximating the lightest neutrino mass to zero) [52].

5.2.1. \mathbb{Z}_2^s Symmetry for General Determination of Solar Angle θ_{12}

Let us inspect the flavor symmetries in the lepton and neutrino sectors. In general, the lepton and neutrino sectors are expected to obey different flavor symmetries. After spontaneous symmetry breaking, the residual symmetry groups for the lepton and neutrino mass-matrices may be denoted as \mathbb{G}_ℓ and \mathbb{G}_ν , respectively. Consider the symmetry transformations $F_j \in \mathbb{G}_\ell$ and $G_j \in \mathbb{G}_\nu$ for left-handed leptons and neutrinos. Thus the mass-matrices of leptons (M_ℓ) and light neutrinos (M_ν) will satisfy the invariance equations [57],

$$F_j^\dagger M_\ell M_\ell^\dagger F_j = M_\ell M_\ell^\dagger, \quad G_j^T M_\nu G_j = M_\nu. \quad (5.9)$$

The above mass-matrices can be diagonalized by unitary rotations for left-handed leptons and neutrinos,

$$U_\ell^\dagger M_\ell M_\ell^\dagger U_\ell = D_\ell \equiv \text{diag}(m_e^2, m_\mu^2, m_\tau^2), \quad U_\nu^T M_\nu U_\nu = D_\nu \equiv \text{diag}(m_1, m_2, m_3). \quad (5.10)$$

Then, combining the invariance equations (5.9) and diagonalization equations (5.10) result in

$$U_\ell^\dagger F_j^\dagger M_\ell M_\ell^\dagger F_j U_\ell = d_\ell^\dagger D_\ell d_\ell = D_\ell, \quad U_\nu^T G_j^T M_\nu G_j U_\nu = d_\nu^T D_\nu d_\nu = D_\nu, \quad (5.11)$$

where d_ℓ and d_ν are diagonal phase-matrices obeying $d_\ell^\dagger d_\ell = \mathcal{I}_3$ and $d_\nu^2 = \mathcal{I}_3$ (with \mathcal{I}_3 the 3×3 unit matrix), which require $d_\ell = \text{diag}(e^{i\gamma_1}, e^{i\gamma_2}, e^{i\gamma_3})$ and $d_\nu = \text{diag}(\pm 1, \pm 1, \pm 1)$. So, up to an overall phase factor, the $\{d_\ell^{(j)}\}$ forms the generic Abelian group $U(1) \otimes U(1) = \mathbb{G}_\ell$ for leptons, and $\{d_\nu^{(j)}\}$ has only two independent d_ν ,

$$d_\nu^{(1)} = \text{diag}(1, 1, -1), \quad d_\nu^{(2)} = \text{diag}(-1, 1, 1), \quad (5.12)$$

forming the generic discrete group $\mathbb{Z}_2 \otimes \mathbb{Z}_2 = \mathbb{G}_\nu$ for neutrinos. From Eq. (5.11) the following consistency solutions are deduced,

$$F_j = U_\ell d_\ell^{(j)} U_\ell^\dagger, \quad G_j = U_\nu d_\nu^{(j)} U_\nu^\dagger. \quad (5.13)$$

This proves that $\{F_j\}$ and $\{d_\ell^{(j)}\}$ are just connected by the similarity transformations, and are thus two *equivalent representations* of the same group \mathbb{G}_ℓ ; similarly, $\{G_j\}$ and $\{d_\nu^{(j)}\}$ are two *equivalent representations* of the same group \mathbb{G}_ν . We may call the representation $\{d_\ell^{(j)}\}$ and $\{d_\nu^{(j)}\}$ the “kernel

representations”, with which the equivalent “flavor representations” $\{F_j\}$ and $\{G_j\}$ can be generated as in (5.13) via the diagonalization matrices U_ℓ and U_ν , respectively. Hence, we are free to choose an equivalent lepton symmetry group representation $\{F_j\} = \{d_\ell^{(j)}\}$ with $U_\ell = \mathcal{I}_3$, and accordingly, rewrite the representation of neutrinos symmetry group,

$$G_j = V d_\nu^{(j)} V^\dagger, \quad (5.14)$$

with $V = U_\ell^\dagger U_\nu = U_\nu$ equal to the physical PMNS mixing matrix as defined in Eq. (3.3) of Sec. 3[54]. Let us rewrite the PMNS matrix (3.3), $V = U'' U U' = V' U'$, with $V' \equiv U'' U$ as introduced in Eq. (3.4). So we see that the Majorana phase-matrix U' cancels in G_j ,

$$G_j = V' d_\nu^{(j)} V'^\dagger. \quad (5.15)$$

According to the most general reconstruction formulation in Sec. 3.1, we can expand the matrix V' to NLO in terms of the small parameters, $(\delta_a, \delta_x, \delta\alpha_i)$, where (δ_a, δ_x) characterizes the low energy $\mu-\tau$ breaking and the CP-angle $\delta\alpha_i$ arises from the phase matrix U'' (which is not directly observable and only needed for the consistency of diagonalizing the mass matrix M_ν). There is no need to expand the Dirac CP-phase $e^{i\delta_D}$ itself since it is always associated with the small $\mu-\tau$ breaking parameter δ_x . So, under this expansion we derive

$$V' = V_s + \delta V', \quad (5.16)$$

with

$$V_s = \begin{pmatrix} c_s & -s_s & 0 \\ \frac{s_s}{\sqrt{2}} & \frac{c_s}{\sqrt{2}} & -\frac{1}{\sqrt{2}} \\ \frac{s_s}{\sqrt{2}} & \frac{c_s}{\sqrt{2}} & \frac{1}{\sqrt{2}} \end{pmatrix}, \quad (5.17a)$$

$$\delta V' = \begin{pmatrix} i c_s \delta\alpha_1 & i s_s \delta\alpha_1 & -\delta_x e^{-i\delta_D} \\ -\frac{s_s \delta_a + c_s \delta_x e^{i\delta_D} + i s_s \delta\alpha_2}{\sqrt{2}} & \frac{-c_s \delta_a + s_s \delta_x e^{i\delta_D} - i c_s \delta\alpha_2}{\sqrt{2}} & \frac{-\delta_a - i \delta\alpha_2}{\sqrt{2}} \\ \frac{s_s \delta_a + c_s \delta_x e^{i\delta_D} - i s_s \delta\alpha_3}{\sqrt{2}} & \frac{c_s \delta_a - s_s \delta_x e^{i\delta_D} - i c_s \delta\alpha_3}{\sqrt{2}} & \frac{-\delta_a + i \delta\alpha_3}{\sqrt{2}} \end{pmatrix}. \quad (5.17b)$$

Let us first consider the $\mu-\tau$ symmetric limit with $V' = V_s$. So substituting V_s into Eq. (5.15) we deduce,

$$G_{\mu\tau} \equiv G_1 = V_s d_\nu^{(1)} V_s^\dagger = \begin{pmatrix} 1 & 0 & 0 \\ 0 & 0 & 1 \\ 0 & 1 & 0 \end{pmatrix}, \quad (5.18)$$

which, as expected, just gives the $\mathbb{Z}_2^{\mu\tau}$ symmetry-transformation matrix G_ν for light neutrinos as we explicitly constructed in (2.5) earlier for the seesaw Lagrangian (2.2).

Next, we derive the symmetry-transformation matrix G_s^0 corresponding to $d_\nu^{(2)}$ of (5.12) in the $\mu-\tau$ symmetric limit with $(\delta V' = 0)$,

$$G_s^0 = V_s d_\nu^{(2)} V_s^\dagger = \begin{pmatrix} s_s^2 - c_s^2 & -\sqrt{2} s_s c_s & -\sqrt{2} s_s c_s \\ c_s^2 & -s_s^2 & c_s^2 \\ c_s^2 & c_s^2 & c_s^2 \end{pmatrix} \quad (5.19a)$$

$$= \frac{1}{1+k^2} \begin{pmatrix} k^2-1 & -\sqrt{2}k & -\sqrt{2}k \\ & 1 & -k^2 \\ & & 1 \end{pmatrix}, \quad (5.19b)$$

which is symmetric since V_s and $d_\nu^{(j)}$ are real. (For the same reason $G_{\mu\tau}$ is also symmetric.) In the last step, for convenience we have defined,

$$(s_s, c_s) = \frac{(k, 1)}{\sqrt{1+k^2}}, \quad (5.20)$$

with k (or equivalently, $\tan \theta_s$) serving as the group parameter of \mathbb{Z}_2^s ,

$$\tan \theta_s = k, \quad (5.21)$$

where we can always choose the convention of $\theta_s \in [0, \frac{\pi}{2}]$ such that, $\tan \theta_s = k \geq 0$. Noting $(d_\nu^{(j)})^2 = \mathcal{I}_3$ and using the relation $G_s^0 = V_s d_\nu^{(2)} V_s^\dagger$, we can readily verify $(G_s^0)^2 = \mathcal{I}_3$ and thus indeed $G_s^0 \in \mathbb{Z}_2^s$. Hence, the solar angle θ_s is dictated by the group parameter k of the 3-dimensional representation of the hidden symmetry \mathbb{Z}_2^s [55]. We stress that the G_s^0 in (5.19b), as the 3d representation of \mathbb{Z}_2^s , is uniquely fixed by the $\mu-\tau$ symmetric matrix V_s ; we call \mathbb{Z}_2^s a *hidden symmetry* since it generally exists for any $\mu-\tau$ symmetric neutrino mass-matrix $M_\nu^{(s)}$ [cf. Eq. (5.29a) below], i.e., *any $\mu-\tau$ symmetric neutrino sector must automatically contain the hidden \mathbb{Z}_2^s symmetry which dictates the solar angle θ_s as in (5.21)*.

As pointed out in Ref. [1], a particular choice of $k = \frac{1}{\sqrt{2}}$ gives the conventional tri-bimaximal ansatz [56] $\tan \theta_s = \frac{1}{\sqrt{2}}$ ($\theta_s \simeq 35.3^\circ$), but *other choices of the group parameter k allow deviations from the conventional tri-bimaximal mixing*, e.g., we can make a very simple choice of $k = \frac{2}{3}$, leading to $\tan \theta_s = \frac{2}{3}$ ($\theta_s \simeq 33.7^\circ$), which agrees to the neutrino data equally well (cf. Table-1 in Sec. 2) or even better (cf. Table-2 in ‘‘Note Added in Proof’’). The \mathbb{Z}_2^s itself, as *the minimal hidden symmetry for θ_s* , is not restrictive enough to fix its group parameter k . But, extending the $\mathbb{Z}_2^{\mu\tau} \otimes \mathbb{Z}_2^s$ symmetry into a larger simple group can fix a particular k value and thus the solar angle θ_s . As we demonstrated in Sec. 6.3 of Ref. [1], a simple example is to enlarge $\mathbb{Z}_2^{\mu\tau} \otimes \mathbb{Z}_2^s$ to the permutation group S_4 [57], under which we can infer $k = \frac{1}{\sqrt{2}}$, corresponding to the tri-bimaximal mixing $\theta_s = \arctan \frac{1}{\sqrt{2}}$.

Then, we examine how such a \mathbb{Z}_2^s symmetry could possibly survive after including general $\mu-\tau$ breaking terms in $V' = V_s + \delta V'$. Expanding the small $\mu-\tau$ breaking parameters up to NLO, we can derive the symmetry-transformation matrix G_s corresponding to $d_\nu^{(2)}$ of (5.12),

$$\begin{aligned} G_s &\equiv G_2 = V' d_\nu^{(2)} V'^\dagger = V_s d_\nu^{(2)} V_s^\dagger + (V_s d_\nu^{(2)} \delta V'^\dagger + \delta V' d_\nu^{(2)} V_s^\dagger) \\ &\equiv G_s^0 + \delta G_s, \end{aligned} \quad (5.22)$$

where $\delta G_s = \text{Re}[\delta G_s] + i\text{Im}[\delta G_s]$ with

$$\text{Re}[\delta G_s] = \begin{pmatrix} 0 & -\frac{s_{2s}\delta_a+2c_s^2\cos\delta_D\delta_x}{\sqrt{2}} & \frac{s_{2s}\delta_a+2c_s^2\cos\delta_D\delta_x}{\sqrt{2}} \\ -\frac{s_{2s}\delta_a+2c_s^2\cos\delta_D\delta_x}{\sqrt{2}} & -2s_s^2\delta_a-s_{2s}\cos\delta_D\delta_x & 0 \\ \frac{s_{2s}\delta_a+2c_s^2\cos\delta_D\delta_x}{\sqrt{2}} & 0 & 2s_s^2\delta_a+s_{2s}\cos\delta_D\delta_x \end{pmatrix}, \quad (5.23a)$$

$$\text{Im}[\delta G_s] = \begin{pmatrix} 0 & \frac{s_{2s}(\delta\alpha_1 - \delta\alpha_2) - 2c_s^2 \sin \delta_D \delta_x}{\sqrt{2}} & \frac{s_{2s}(\delta\alpha_1 - \delta\alpha_3) + 2c_s^2 \sin \delta_D \delta_x}{\sqrt{2}} \\ -\frac{s_{2s}(\delta\alpha_1 - \delta\alpha_2) - 2c_s^2 \sin \delta_D \delta_x}{\sqrt{2}} & 0 & s_s^2(\delta\alpha_2 - \delta\alpha_3) + s_{2s} \sin \delta_D \delta_x \\ -\frac{s_{2s}(\delta\alpha_1 - \delta\alpha_3) + 2c_s^2 \sin \delta_D \delta_x}{\sqrt{2}} & -s_s^2(\delta\alpha_2 - \delta\alpha_3) - s_{2s} \sin \delta_D \delta_x & 0 \end{pmatrix}, \quad (5.23b)$$

where $s_{2s} \equiv \sin 2\theta_s$. Because the symmetry transformation $G_s \in \mathbb{Z}_2^s$, we have the condition $G_s^2 = \mathcal{I}_3$. Then, expanding this up to the NLO, we have verified the consistency condition,

$$\{G_s^0, \delta G_s\} = 0. \quad (5.24)$$

Requiring that the \mathbb{Z}_2^s symmetry persists under $\mu-\tau$ breaking, i.e., the form of G_s remains unaffected by the $\mu-\tau$ violation, we have the condition,

$$G_s = G_s^0, \quad \text{or,} \quad \delta G_s = 0. \quad (5.25)$$

Thus, with (5.23a)-(5.23b), we can derive the following solutions,

$$\frac{\delta_a}{\delta_x} = -\cot \theta_s \cos \delta_D, \quad (5.26)$$

from the real part condition $\text{Re}[\delta G_s] = 0$, and

$$2\delta\alpha_1 = \delta\alpha_2 + \delta\alpha_3, \quad (5.27a)$$

$$\delta\alpha_2 - \delta\alpha_3 = -2 \cot \theta_s \sin \delta_D \delta_x = 2 \tan \delta_D \delta_a, \quad (5.27b)$$

from the imaginary part condition $\text{Im}[\delta G_s] = 0$, where in the last step of (5.27b) we have made use of (5.26) for simplification. Note that the correlation (5.26) precisely agrees to what derived from our soft breaking model in Eq. (4.12a) of Ref. [1]; but now it is re-derived by *requiring that the \mathbb{Z}_2^s symmetry persists in the presence of general low energy $\mu-\tau$ breaking*. In addition, the above Eq. (5.27b) also coincides with Eq. (4.12b) of Ref. [1]. As we will demonstrate in the next subsection, the \mathbb{Z}_2^s symmetry is independent of the soft $\mu-\tau$ breaking in the seesaw model of Ref. [1]. We note that in the current construction of common $\mu-\tau$ and CP breaking with seesaw mechanism (Sec. 2.2), such a \mathbb{Z}_2^s symmetry is not fully respected, hence the correlation (5.26) no longer holds and we have predicted a *modified correlation* (4.13), which can be tested against (5.26) by the on-going and upcoming neutrino oscillation experiments.

To summarize, as we have demonstrated above from general low energy reconstruction formulation, the transformations $G_{\mu\tau} = G_1$ and $G_s = G_2$ in the $\mu-\tau$ symmetric limit correspond to the discrete groups $\mathbb{Z}_2^{\mu\tau} \otimes \mathbb{Z}_2^s$, which are *equivalent to* and *originate from* the generic symmetry $\mathbb{Z}_2 \otimes \mathbb{Z}_2$ in the neutrino mass-eigenbasis because they are connected by the similarity transformations via (5.13). The $\mu-\tau$ symmetry $\mathbb{Z}_2^{\mu\tau}$ has been known before, and the hidden symmetry \mathbb{Z}_2^s (as the *minimal group dictating the solar angle θ_s*) was revealed by Ref. [1] in the context of neutrino seesaw. In this work, we further find that requiring the symmetry \mathbb{Z}_2^s to persist in the presence of most

general $\mu-\tau$ breaking terms will predict a new correlation (5.26) between the small $\mu-\tau$ breaking parameters (δ_a, δ_x) . As we will prove below, the \mathbb{Z}_2^s symmetry is respected by a class of soft $\mu-\tau$ breaking seesaw models in Ref. [1], but is *partially violated* in the present $\mu-\tau$ breaking seesaw model (Sec. 2.2).

5.2.2. \mathbb{Z}_2^s Symmetry and Neutrino Mass-Matrix with General $\mu-\tau$ Breaking

In this subsection, we directly analyze the generally reconstructed light neutrino mass-matrix M_ν under the hidden symmetry \mathbb{Z}_2^s and the determination of solar angle θ_s . The mass-matrix (3.1) can be *uniquely* decomposed into the $\mu-\tau$ symmetric and anti-symmetric parts,

$$M_\nu = M_\nu^{(s)} + \delta M_\nu^{(a)}, \quad (5.28)$$

with

$$M_\nu^{(s)} = \begin{pmatrix} A & B_s & B_s \\ & C_s & D \\ & & C_s \end{pmatrix}, \quad \delta M_\nu^{(a)} = \begin{pmatrix} 0 & \delta B_a & -\delta B_a \\ & \delta C_a & 0 \\ & & -\delta C_a \end{pmatrix}, \quad (5.29a)$$

$$B_s \equiv \frac{1}{2}(B_1 + B_2), \quad C_s \equiv \frac{1}{2}(C_1 + C_2), \quad (5.29b)$$

$$\delta B_a \equiv \frac{1}{2}(B_1 - B_2), \quad \delta C_a \equiv \frac{1}{2}(C_1 - C_2), \quad (5.29c)$$

where we generally allow $m_1 m_2 m_3 \neq 0$. Then, from (5.9), the invariance equation of M_ν under G_s corresponds to

$$G_s^\dagger (M_\nu^{(s)} + \delta M_\nu^{(a)}) G_s = M_\nu^{(s)} + \delta M_\nu^{(a)}, \quad (5.30)$$

which uniquely gives,

$$G_s^\dagger M_\nu^{(s)} G_s = M_\nu^{(s)}, \quad (5.31a)$$

$$G_s^\dagger \delta M_\nu^{(a)} G_s = \delta M_\nu^{(a)}. \quad (5.31b)$$

Note that two possibilities may exist: **(i)**. The \mathbb{Z}_2^s symmetry is a *full symmetry* of the light neutrino mass-matrix M_ν if *both* (5.31a) and (5.31b) hold. **(ii)**. The \mathbb{Z}_2^s symmetry is a *partial symmetry* of M_ν if the $\mu-\tau$ anti-symmetric part $M_\nu^{(a)}$ breaks (5.31b).

We can prove that the \mathbb{Z}_2^s is always a symmetry of the $\mu-\tau$ symmetric part $M_\nu^{(s)}$ and generally holds (5.31a). Substituting (5.16) into (3.4) and noting that the decomposition (5.28) is unique, we can reconstruct the $\mu-\tau$ symmetric and anti-symmetric parts of M_ν , respectively,

$$M_\nu^{(s)} = V_s^* \tilde{D}_\nu V_s^\dagger, \quad (5.32a)$$

$$\begin{aligned} \delta M_\nu^{(a)} &= V_s^* \tilde{D}_\nu \delta V'^\dagger + \delta V'^* \tilde{D}_\nu V_s^\dagger + \delta V'^* \tilde{D}_\nu \delta V'^\dagger \\ &= V_s^* \tilde{D}_\nu \delta V'^\dagger + \delta V'^* \tilde{D}_\nu V_s^\dagger + O(\delta_j^2), \end{aligned} \quad (5.32b)$$

where δ_j denotes all possible NLO parameters under consideration (such as δ_x , δ_a and y' , etc). This shows that the $\mu-\tau$ symmetric part $M_\nu^{(s)}$ is diagonalized by V_s . Hence, the corresponding \mathbb{Z}_2^s transformation matrix is just G_s^0 , as given by (5.19). The G_s^0 must be the symmetry of $M_\nu^{(s)}$ and thus always holds the invariance equation (5.31a). This proves that the *solar mixing angle* θ_s (as contained in the rotation matrix V_s and symmetry transformation matrix G_s^0) is generally dictated by the \mathbb{Z}_2^s symmetry, independent of any specific model.

On the other hand, the validity of (5.31b) is highly nontrivial because the requirement of $G_s = G_s^0$ [cf. (5.25)] does not generally hold under $\mu-\tau$ breaking, and it has to be checked case by case. As we will prove in Sec. 5.3, the $\mu-\tau$ anti-symmetric part $M_\nu^{(a)}$ will break \mathbb{Z}_2^s in the current $\mu-\tau$ blind seesaw (Sec. 2), while it preserves \mathbb{Z}_2^s in the soft $\mu-\tau$ breaking seesaw of Ref. [1].

Using the expression of G_s [Eqs. (5.19a) and (5.25)], we can derive the solution from (5.31a) for the $\mu-\tau$ symmetric part,

$$\tan 2\theta_s = \frac{2\sqrt{2} B_s}{A - (C_s + D)}, \quad (5.33)$$

and another solution from (5.31b) for the $\mu-\tau$ anti-symmetric part,

$$\tan \theta_s = -\sqrt{2} \frac{\delta B_a}{\delta C_a}, \quad (5.34)$$

which further leads to,

$$\tan 2\theta_s = -\frac{2\sqrt{2} \delta B_a \delta C_a}{\delta C_a^2 - 2\delta B_a^2}. \quad (5.35)$$

Hence, if the \mathbb{Z}_2^s would be a full symmetry of M_ν (including its $\mu-\tau$ breaking part), the two solutions (5.33) and (5.35) for the solar angle θ_s must be identical, leading to a *nontrivial consistency condition*,

$$\tan 2\theta_s = \frac{2\sqrt{2} B_s}{A - (C_s + D)} \doteq -\frac{2\sqrt{2} \delta B_a \delta C_a}{\delta C_a^2 - 2\delta B_a^2}. \quad (5.36)$$

An explicit counter example to this condition will be given in Sec. 5.3.2.

In the following, we apply the most general reconstruction formalism (Sec. 3.1) to compute the $\mu-\tau$ symmetric and anti-symmetric parts of light neutrino mass-matrix $M_\nu = M_\nu^{(s)} + M_\nu^{(a)}$. With these, we will explicitly verify Eq. (5.33) by using the elements of $\mu-\tau$ symmetric $M_\nu^{(s)}$, and we further derive physical consequences of the consistency condition (5.36) by using the elements of $\mu-\tau$ anti-symmetric $M_\nu^{(a)}$.

◆ Reconstruction Analysis for General Normal Mass-Ordering Scheme

Eq. (3.5) reconstructs all the elements of M_ν in terms of three mass-eigenvalues, three mixing angles and relevant CP-phases. The normal mass-ordering (NMO) has the spectrum $m_1 < m_2 \ll m_3$, so we can define the small ratios,

$$y_1 \equiv \frac{m_1}{m_3}, \quad y_2 \equiv \frac{m_2}{m_3}, \quad y_3 \equiv \frac{m_3 - m_{30}}{m_3}. \quad (5.37)$$

Thus we have the independent NLO parameters for the NMO analysis, $(y_1, y_2, z, \delta_a, \delta_x, \delta\alpha_i, \delta\phi_i)$. Expanding them perturbatively, we derive the LO form of the $\mu-\tau$ symmetric mass-matrix M_ν ,

$$M_\nu^{(0)} = m_{30} \begin{pmatrix} 0 & 0 & 0 \\ \frac{1}{2} & -\frac{1}{2} & \frac{1}{2} \\ \frac{1}{2} & \frac{1}{2} & \frac{1}{2} \end{pmatrix}, \quad (5.38)$$

with $\alpha_{10} = \alpha_{20} = \alpha_{30} \equiv \alpha_0$, $\alpha_{30} + \phi_{30} = n\pi$, and the NLO elements in δM_ν ,

$$\delta A = e^{-i2\alpha_0} (e^{-i2\phi_{10}} c_s^2 y_1 + e^{-i2\phi_{20}} s_s^2 y_2) m_{30}, \quad (5.39a)$$

$$\delta B_s = \frac{1}{2\sqrt{2}} e^{-i2\alpha_0} (e^{-i2\phi_{10}} y_1 - e^{-i2\phi_{20}} y_2) \sin 2\theta_s m_{30}, \quad (5.39b)$$

$$\delta C_s + \delta D = e^{-i2\alpha_0} (e^{-i2\phi_{10}} s_s^2 y_1 + e^{-i2\phi_{20}} c_s^2 y_2) m_{30}, \quad (5.39c)$$

$$\delta B_a = \frac{1}{\sqrt{2}} e^{-i\delta_D} \delta_x m_{30}, \quad (5.39d)$$

$$\delta C_a = \frac{1}{2} [2\delta_a - i(\delta\alpha_2 - \delta\alpha_3)] m_{30}. \quad (5.39e)$$

From (5.38), we have $A_s^{(0)} = B_s^{(0)} = C_s^{(0)} + D^{(0)} = 0$. Thus, using the $\mu-\tau$ symmetric NLO elements (5.39a)-(5.39c), we can compute the ratio,

$$\frac{2\sqrt{2} B_s}{A_s - (C_s + D)} = \frac{(e^{-i2\phi_{10}} y_1 - e^{-i2\phi_{20}} y_2) \sin 2\theta_s}{(e^{-i2\phi_{10}} y_1 - e^{-i2\phi_{20}} y_2)(c_s^2 - s_s^2)} = \tan 2\theta_s, \quad (5.40)$$

which explicitly verifies our Eq. (5.33) [as generally derived from the invariance equation (5.31a) under \mathbb{Z}_2^s] for the current NMO scheme. This is an explicit proof up to NLO that for a general NMO scheme the $\mu-\tau$ symmetric mass-matrix $M_\nu^{(s)} = M_\nu^{(0)} + \delta M_\nu^{(s)}$ does hold the \mathbb{Z}_2^s symmetry.

Then, using the $\mu-\tau$ anti-symmetric elements (5.39d)-(5.39e), we derive the ratio,

$$-\sqrt{2} \frac{\delta B_a}{\delta C_a} = -\frac{e^{-i\delta_D} \delta_x}{\delta_a - \frac{i}{2}(\delta\alpha_2 - \delta\alpha_3)} = \tan \theta_s, \quad (5.41)$$

where in the last step we have used Eq. (5.34) under the assumption that \mathbb{Z}_2^s symmetry also holds for the $\mu-\tau$ anti-symmetric mass-matrix $M_\nu^{(a)}$, i.e., the validity of the invariance equation (5.31b). Analyzing the real and imaginary parts of (5.41), we deduce two relations,

$$\delta_a = -\delta_x \cot \theta_s \cos \delta_D, \quad (5.42a)$$

$$\delta\alpha_2 - \delta\alpha_3 = 2 \tan \delta_D \delta_a. \quad (5.42b)$$

These are in perfect agreement with (5.26) and (5.27b), which are generally derived under a single assumption that the \mathbb{Z}_2^s symmetry persists in the presence of $\mu-\tau$ breaking. But, as will be shown in Sec. 5.3.2, this assumption does not generally hold, and the current $\mu-\tau$ blind seesaw (Sec. 2.2) provides a nontrivial counter example.

♦ Reconstruction Analysis for General Inverted Mass-Ordering Scheme

For the inverted mass-ordering (IMO), the light neutrinos have the spectrum $m_2 \gtrsim m_1 \gg m_3$, so we can define the small ratios,

$$z_1 \equiv \frac{m_1 - m_0}{m_1}, \quad z_2 \equiv \frac{m_2 - m_0}{m_1}, \quad z_3 \equiv \frac{m_3}{m_1}, \quad (5.43)$$

where we have $z_1 = z$ and $z_2 \simeq z + \frac{1}{2}y'$ in connection to the NLO parameters (y', z) introduced in Eqs. (3.7)-(3.9) of Sec. 3.2. Then we have the independent NLO parameters for the IMO analysis, $(z_1, z_2, z_3, \delta_a, \delta_x, \delta\alpha_i, \delta\phi_i)$. Expanding them perturbatively, we derive the LO form of the symmetric mass-matrix M_ν ,

$$M_\nu^{(0)} = m_0 \begin{pmatrix} 1 & 0 & 0 \\ & \frac{1}{2} & \frac{1}{2} \\ & \frac{1}{2} & \end{pmatrix}, \quad (5.44)$$

with $\alpha_{10} = \alpha_{20} = \alpha_{30} = \alpha_0$, $\phi_{10} = \phi_{20} = -\alpha_0$, and the NLO elements of M_ν ,

$$\delta A = m_0 [c_s^2 z_1 + s_s^2 z_2 - i2(c_s^2 \delta\phi_1 + s_s^2 \delta\phi_2 + \delta\alpha_1)], \quad (5.45a)$$

$$\delta B_s = \frac{1}{2\sqrt{2}} m_0 \sin 2\theta_s [z_1 - z_2 - i2(\delta\phi_1 - \delta\phi_2)], \quad (5.45b)$$

$$\delta C_s + \delta D = m_0 [s_s^2 z_1 + c_s^2 z_2 - i(2s_s^2 \delta\phi_1 + 2c_s^2 \delta\phi_2 + \delta\alpha_2 + \delta\alpha_3)], \quad (5.45c)$$

$$\delta B_a = -\frac{1}{\sqrt{2}} m_0 e^{i\delta_D} \delta_x, \quad (5.45d)$$

$$\delta C_a = -m_0 [\delta_a + \frac{i}{2}(\delta\alpha_2 - \delta\alpha_3)]. \quad (5.45e)$$

From (5.44), we have $B_s^{(0)} = 0$ and $A_s^{(0)} - (C_s^{(0)} + D^{(0)}) = 0$. So using the $\mu - \tau$ symmetric NLO elements (5.45a)-(5.45c), we can compute the ratio,

$$\frac{2\sqrt{2} B_s}{A_s - (C_s + D)} = \frac{\sin 2\theta_s [z_1 - z_2 - i2(\delta\phi_1 - \delta\phi_2)]}{\cos 2\theta_s [z_1 - z_2 - i2(\delta\phi_1 - \delta\phi_2)] - i(2\delta\alpha_1 - \delta\alpha_2 - \delta\alpha_3)}, \quad (5.46)$$

from which we deduce the consistent solution,

$$\frac{2\sqrt{2} B_s}{A_s - (C_s + D)} = \tan 2\theta_s, \quad (5.47a)$$

$$2\delta\alpha_1 = \delta\alpha_2 + \delta\alpha_3, \quad (5.47b)$$

which explicitly verifies our Eq. (5.33) [as generally derived from the invariance equation (5.31a) under \mathbb{Z}_2^s] for the current IMO scheme. Also the above solution (5.47b) exactly coincide with the general Eq. (5.27). The above is an explicit proof up to NLO that for a general IMO scheme the $\mu - \tau$ symmetric mass-matrix $M_\nu^{(s)} = M_\nu^{(0)} + \delta M_\nu^{(s)}$ does hold the \mathbb{Z}_2^s symmetry.

Then, with the $\mu - \tau$ anti-symmetric elements (5.45d)-(5.45e), we further evaluate the ratio,

$$-\sqrt{2} \frac{\delta B_a}{\delta C_a} = -\frac{e^{i\delta_D} \delta_x}{\delta_a + \frac{i}{2}(\delta\alpha_2 - \delta\alpha_3)} = \tan \theta_s, \quad (5.48)$$

where in the last step we have applied (5.34) under *the assumption* that the $\mu - \tau$ anti-symmetric mass-matrix $M_\nu^{(a)}$ also respects the \mathbb{Z}_2^s symmetry, i.e., the invariance equation (5.31b) holds. Inspecting the real and imaginary parts of (5.48), we deduce the following,

$$\delta_a = -\delta_x \cot \theta_s \cos \delta_D, \quad (5.49a)$$

$$\delta\alpha_2 - \delta\alpha_3 = 2 \tan \delta_D \delta_a, \quad (5.49b)$$

which coincide with Eqs.(5.42a)-(5.42b) as we derived for the NMO scheme. We see that both (5.49a)-(5.49b) and (5.42a)-(5.42b) precisely agree to (5.26) and (5.27b) which are generally derived under *a single assumption that \mathbb{Z}_2^s is a symmetry of the full mass-matrix* $M_\nu = M_\nu^{(s)} + \delta M_\nu^{(a)}$ *including its $\mu-\tau$ breaking part* $\delta M_\nu^{(a)}$. But, as we will prove in Sec. 5.3.2, the above assumption is not generally true and for the $\mu-\tau$ blind seesaw with IMO (Sec. 2.2) the \mathbb{Z}_2^s symmetry is violated by $\delta M_\nu^{(a)}$.

So far we have explicitly proven the relations (5.26) and (5.27) for general NMO and IMO schemes via the general *model-independent* reconstruction formalism (Sec. 3.1), where the only assumption is that the \mathbb{Z}_2^s symmetry fully persists in the presence of $\mu-\tau$ breaking. In the next subsection, we will map the $\mathbb{Z}_2^{\mu\tau} \otimes \mathbb{Z}_2^s$ symmetry into the neutrino seesaw Lagrangian, and demonstrate that the hidden \mathbb{Z}_2^s symmetry is a *full symmetry* of our soft $\mu-\tau$ breaking model in Ref. [1] where the physical prediction (5.26) holds; while for the current $\mu-\tau$ blind seesaw model the \mathbb{Z}_2^s is only a *partial symmetry* (respected by the $\mu-\tau$ symmetric part $M_\nu^{(s)}$), and is violated by the $\mu-\tau$ anti-symmetric part $\delta M_\nu^{(a)}$, leading to our prediction of the modified new correlation (4.13) in Sec. 4.1, in contrast to (5.49a) or (5.26).

5.3. Mapping $\mathbb{Z}_2 \otimes \mathbb{Z}_2$ Hidden Symmetry into Neutrino Seesaw

Consider the general seesaw Lagrangian in the form of (2.2) with two or three right-handed neutrinos. After spontaneous electroweak symmetry breaking, consider the invariance of (2.2) under the residual symmetry transformations,

$$\nu_L \rightarrow G_j \nu_L, \quad \mathcal{N} \rightarrow G_j^R \mathcal{N}, \quad (5.50)$$

where G_j is 3-dimensional unitary matrix, and G_j^R is 2×2 or 3×3 matrix (depending on two or three right-handed neutrinos invoked in the neutrino seesaw). Accordingly, we have the following invariance equations for the Dirac and Majorana neutrino mass-matrices,

$$G_j^T m_D G_j^R = m_D, \quad (5.51a)$$

$$G_j^{R^T} M_R G_j^R = M_R, \quad (5.51b)$$

from which we deduce the invariance equation for the seesaw mass-matrix of light neutrinos,

$$G_j^T M_\nu G_j = M_\nu, \quad (5.52)$$

where $M_\nu = m_D M_R^{-1} m_D^T$. Let us diagonalize the Majorana mass-matrices M_ν and M_R as follows,

$$U_\nu^T M_\nu U_\nu = D_\nu, \quad U_R^T M_R U_R = D_R, \quad (5.53)$$

in which $D_\nu = \text{diag}(m_1, m_2, m_3)$ and $D_R = \text{diag}(M_1, \dots, M_n)$ with $n = 2$ for the minimal seesaw or $n = 3$ for three-neutrino-seesaw. Thus, from (5.51)-(5.53), we can express G_j and G_j^R as,

$$G_j = U_\nu d_\nu^{(j)} U_\nu^\dagger, \quad G_j^R = U_R d_R^{(j)} U_R^\dagger, \quad (5.54)$$

where kernel representation $\{d_\nu^{(j)}\}$ is given in (5.12), and corresponds to the product group $\mathbb{Z}_2^{\mu\tau} \otimes \mathbb{Z}_2^s$ via the *equivalent flavor representation* $\{G_j\}$ for the light neutrino sector. For $d_R^{(j)}$ in (5.54), we give its nontrivial forms,

$$d_R^{(1)} = \text{diag}(-1, 1), \quad (\text{for minimal seesaw}), \quad (5.55\text{a})$$

$$d_R^{(1)} = \text{diag}(1, 1, -1), \quad d_R^{(2)} = \text{diag}(-1, 1, 1), \quad (\text{for 3-neutrino-seesaw}), \quad (5.55\text{b})$$

where $d_R^{(1)}$ forms a \mathbb{Z}_2' symmetry for right-handed neutrinos in the minimal seesaw, and $\{d_R^{(1)}, d_R^{(2)}\}$ form a product group $\mathbb{Z}_2'^{\mu\tau} \otimes \mathbb{Z}_2'^s$ for right-handed neutrinos in the three-neutrino-seesaw. The trivial case with $d_R^{(j)}$ equal to unity matrix is not listed here which corresponds to the singlet representation $G_j^R = \mathcal{I}$. Since the low energy oscillation data do not directly enforce a $\mathbb{Z}_2'^{\mu\tau}$ symmetry for heavy right-handed neutrinos, we find two possibilities when mapping the $\mathbb{Z}_2'^{\mu\tau}$ to the seesaw sector: **(i)**. the right-handed neutrinos have correspondence with the light neutrinos in each fermion family and transform simultaneously with the light neutrinos under the $\mathbb{Z}_2'^{\mu\tau}$ to ensure the invariance equation (5.51a); this means $\mathbb{Z}_2'^{\mu\tau} = \mathbb{Z}_2^{\mu\tau}$. **(ii)**. the right-handed neutrinos are singlet of the usual $\mathbb{Z}_2^{\mu\tau}$ symmetry (called “ $\mu-\tau$ blind”), so the extra symmetry $\mathbb{Z}_2'^{\mu\tau}$ in the \mathcal{N} sector is fully independent of the $\mathbb{Z}_2^{\mu\tau}$ for light neutrinos; this means that under $\mathbb{Z}_2^{\mu\tau}$ the invariance equation (5.51a) has $G_1 \in \mathbb{Z}_2^{\mu\tau}$ for light neutrinos and $G^R = \mathcal{I}$ for right-handed neutrinos. As generally shown in Sec. 5.2, the \mathbb{Z}_2^s symmetry dictates the solar angle θ_s for light neutrinos. The extra group $\mathbb{Z}_2'^s$ in the right-handed neutrino sector also has two possibilities: one is $\mathbb{Z}_2'^s = \mathbb{Z}_2^s$, and another is for the right-handed neutrinos being singlet of the \mathbb{Z}_2^s symmetry with $G_s^R = \mathcal{I}$.

5.3.1. Neutrino Seesaw with Common Soft $\mu-\tau$ and CP Breaking

In Ref. [1], we studied the common soft $\mu-\tau$ and CP breaking in the minimal neutrino seesaw, where the right-handed neutrinos $\mathcal{N} = (N_\mu, N_\tau)^T$ obeying the same $\mathbb{Z}_2^{\mu\tau} (= \mathbb{Z}_2'^{\mu\tau})$ at the LO, and small soft $\mu-\tau$ breaking is uniquely constructed in M_R at the NLO. In the $\mu-\tau$ symmetric limit, we inferred that the diagonalization matrix U_R is a 2×2 orthogonal rotation with its rotation angle $\theta_R \equiv \theta_{23}^R = \frac{\pi}{4}$ [1], as expected. Thus, inputting (5.55a) for $d_R^{(1)}$, we deduce from (5.54),

$$G_{\mu\tau}^R = \begin{pmatrix} 0 & 1 \\ 1 & 0 \end{pmatrix}, \quad (5.56)$$

which is just the $\mathbb{Z}_2^{\mu\tau}$ transformation matrix for right-handed neutrinos. With the two right-handed neutrinos $\mathcal{N} = (N_\mu, N_\tau)^T$ shown above, there is no rotation angle θ_{12}^R and also no corresponding $\mathbb{Z}_2'^s$ symmetry. So the right-handed neutrinos can only belong to the singlet representation $G_s^R = \mathcal{I}_2$ under \mathbb{Z}_2^s symmetry, with $d_R^{(2)} = \mathcal{I}_2$. In our soft $\mu-\tau$ breaking model [1], the Dirac mass-matrix,

$$m_D = \begin{pmatrix} a & a \\ b & c \\ c & b \end{pmatrix}, \quad (5.57)$$

exhibits the exact $\mathbb{Z}_2^{\mu\tau}$ symmetry, so it should obey the hidden \mathbb{Z}_2^s as well,

$$G_s^T m_D G_s^R = m_D, \quad (5.58)$$

where $G_s = G_s^0$ is given by (5.19) and $G_s^R = \mathcal{I}_2$. This further leads to the invariance equation for the seesaw mass-matrix of light neutrinos,

$$G_s^T M_\nu G_s = M_\nu, \quad (5.59)$$

where $M_\nu = m_D M_R^{-1} m_D^T$, and the invariance equation for M_R is trivial here since $G_s^R = \mathcal{I}_2$. [Given the form of $G_s = G_s^0$ as constructed in (5.19), we can also explicitly verify the equations (5.58) and (5.59).] Hence, the group parameter k of \mathbb{Z}_2^s and the corresponding solar angle θ_s via Eq. (5.21) are fully fixed by the elements of the $\mu-\tau$ symmetric m_D , and is independent of the soft $\mu-\tau$ breaking in M_R (which is the \mathbb{Z}_2^s singlet). This is a general proof based on group theory, without relying on making any expansion of the $\mu-\tau$ breaking terms in M_R . As can be explicitly solved from Eq. (5.58) above, we have [1],

$$\tan \theta_s = |k| = \frac{\sqrt{2}|a|}{|b+c|}. \quad (5.60)$$

As another nontrivial check, we inspect the consistency condition (5.36). With the form of M_ν in Ref. [1], we explicitly verify that (5.36) indeed holds,

$$\tan 2\theta_s = \frac{2\sqrt{2} B_s}{A - (C_s + D)} = -\frac{2\sqrt{2} \delta B_a \delta C_a}{\delta C_a^2 - 2\delta B_a^2} = \frac{2\sqrt{2} a(b+c)}{2a^2 - (b+c)^2}, \quad (5.61)$$

where both the $\mu-\tau$ symmetric mass-matrix $M_\nu^{(s)}$ and the anti-symmetric part $\delta M_\nu^{(a)}$ determine the same solar angle θ_s . The last equality in (5.61) can be derived also from the solution (5.60) above, they are all consistent. Hence, the \mathbb{Z}_2^s is a full symmetry of the seesaw sector and the light neutrino mass-matrix M_ν in this soft $\mu-\tau$ breaking model.

We note that this \mathbb{Z}_2^s symmetry has a nice geometric interpretation. The two vectors, $u_1 = (a, b, c)^T$ and $u_2 = (a, c, b)^T$, in the Dirac mass-matrix $m_D = (u_1, u_2)$, determine a plane S , obeying the plane-equation,

$$x - \frac{k}{\sqrt{2}}(y + z) = 0, \quad (5.62)$$

where the parameter k is given in (5.21). As shown in Ref. [1], the 3-dimensional representation G_s is just the reflection transformation respect to the plane S . For the case of three-neutrino-seesaw, the $\mu-\tau$ symmetric Dirac mass is extended to a 3×3 matrix,

$$m'_D = \begin{pmatrix} a' & a & a \\ b' & b & c \\ b' & c & b \end{pmatrix} = (u_0, u_1, u_2). \quad (5.63)$$

Thus, to hold m'_D invariant under the \mathbb{Z}_2^s symmetry, we just need to require its first column $u_0 = (a', b', b')^T$ to lie in the S plane, i.e.,

$$\frac{a'}{\sqrt{2}b'} = \frac{\sqrt{2}a}{b+c} = k, \quad (5.64)$$

where $k = \tan \theta_s$ as in (5.21). This means that the Dirac mass matrix (5.63) only contains one more independent parameter than that of the minimal seesaw; furthermore, m'_D is rank-2 and thus $\det M_\nu = (\det m'_D)^2 (\det M_R)^{-1} = 0$ always holds, as in the minimal seesaw.

5.3.2. $\mu-\tau$ Blind Seesaw with Common $\mu-\tau$ and CP Breaking

As constructed in Sec. 2, the $\mu-\tau$ blind seesaw defines the right-handed neutrinos \mathcal{N} as singlet of $\mathbb{Z}_2^{\mu\tau}$ symmetry. This means that we must have the $\mathbb{Z}_2^{\mu\tau}$ transformation matrix $G_{\mu\tau}^R = \mathcal{I}_2$ and $d_R^{\mu\tau} = d_R^{(2)} = \mathcal{I}_2$. Consider the general Dirac and Majorana mass-matrices in the minimal seesaw,

$$\tilde{m}_D = \begin{pmatrix} \tilde{a} & \tilde{a}' \\ \tilde{b}_1 & \tilde{c}_1 \\ \tilde{b}_2 & \tilde{c}_2 \end{pmatrix}, \quad \widetilde{M}_R = \begin{pmatrix} M_{11} & M_{12} \\ M_{12} & M_{22} \end{pmatrix}. \quad (5.65)$$

The Majorana mass-matrix \widetilde{M}_R can be diagonalized by the unitary rotation U_R ,

$$U_R^T \widetilde{M}_R U_R = M_R \equiv \text{diag}(M_1, M_2), \quad (5.66)$$

Then we can derive the seesaw mass-matrix for light neutrinos,

$$M_\nu \simeq \tilde{m}_D \widetilde{M}_R^{-1} \tilde{m}_D^T = m_D M_R^{-1} m_D^T, \quad (5.67)$$

where $m_D = \tilde{m}_D U_R$ takes the form as in (2.17). For the $\mu-\tau$ blind seesaw with \mathcal{N} being $\mathbb{Z}_2^{\mu\tau}$ singlet, we can always start with the mass-eigenbasis of \mathcal{N} with $M_R = \text{diag}(M_1, M_2)$, which means that the rotation U_R becomes automatically diagonal and real, $U_R = \mathcal{I}_2$. Then, the extra symmetry \mathbb{Z}'_2 of M_R must be independent of the $\mathbb{Z}_2^{\mu\tau}$ of light neutrinos, i.e., $\mathbb{Z}'_2 \neq \mathbb{Z}_2^{\mu\tau}$. So the natural choice is $\mathbb{Z}'_2 = \mathbb{Z}_2^s$. The \mathbb{Z}'_2 can have a nontrivial $d_R^s = d_R^{(1)} = \text{diag}(-1, 1)$ as in (5.55a). Thus, the corresponding symmetry transformation for \widetilde{M}_R is

$$G_s^R = U_R d_R^s U_R^\dagger = d_R^{(1)} = \text{diag}(-1, 1). \quad (5.68)$$

There is also a singlet representation of \mathbb{Z}'_2 , corresponding to $d_R = \mathcal{I}_2$.

Then, let us inspect the possible \mathbb{Z}_2^s symmetry for the Dirac mass-matrix by including the $\mu-\tau$ breaking effects [cf. (2.17) and (2.18) in Sec. 2.2]. This means to hold the invariance equations in (5.51),

$$G_s^T \tilde{m}_D G_s^R = \tilde{m}_D, \quad G_s^{R^T} \widetilde{M}_R G_s^R = \widetilde{M}_R, \quad (5.69)$$

which will become, in the mass-eigenbasis of right-handed neutrinos,

$$G_s^T m_D d_R^s = m_D, \quad d_R^{s^T} M_R d_R^s = M_R. \quad (5.70)$$

Since M_R and d_R are both diagonal, the invariance equation for M_R always holds. So we can rewrite the above invariance equation for m_D as,

$$G_s^T \overline{m}_D d_R^s = \overline{m}_D, \quad (5.71)$$

where $\overline{m}_D \equiv m_D(\widehat{m}_0 M_R)^{-\frac{1}{2}}$. [The $\mu-\tau$ symmetric form of \overline{m}_D was given in Eq. (2.8).] Using the notation \overline{m}_D , we can reexpress the seesaw mass-matrix, $M_\nu = \widehat{m}_0 (\overline{m}_D \overline{m}_D^T)$. So we can further deduce the invariance equations under G_s and d_R^s , respectively,

$$G_s^T \overline{m}_D \overline{m}_D^T G_s = \overline{m}_D \overline{m}_D^T, \quad d_R^s{}^T \overline{m}_D^T \overline{m}_D d_R^s = \overline{m}_D^T \overline{m}_D. \quad (5.72)$$

Next, we inspect the two equations in (5.72) to check the validity of the \mathbb{Z}_2^s symmetry after embedding the $\mu-\tau$ breaking into m_D [such as those constructed in (2.18) for instance]. From (5.72), we will explicitly prove that the G_s is a symmetry only for the $\mu-\tau$ symmetric part of $M_\nu \propto (\overline{m}_D \overline{m}_D^T)$; while d_R^s is violated by the $\mu-\tau$ breaking terms in $\overline{m}_D^T \overline{m}_D$. Hence, the \mathbb{Z}_2^s symmetry is only a *partial symmetry* of the light neutrinos, valid for the $\mu-\tau$ symmetric part $M_\nu^{(s)}$.

We can write down the mass-matrix \overline{m}_D with the most general $\mu-\tau$ breaking,

$$\begin{aligned} \overline{m}_D &= \begin{pmatrix} a & a' \\ b_1 & c_1 \\ b_2 & c_2 \end{pmatrix} = \begin{pmatrix} a & a' \\ b & c \\ b & c \end{pmatrix} + \begin{pmatrix} 0 & 0 \\ -\frac{\delta b_1 + \delta b_2}{2} & -\frac{\delta c_1 + \delta c_2}{2} \\ -\frac{\delta b_1 + \delta b_2}{2} & -\frac{\delta c_1 + \delta c_2}{2} \end{pmatrix} + \begin{pmatrix} 0 & 0 \\ -\frac{\delta b_1 - \delta b_2}{2} & -\frac{\delta c_1 - \delta c_2}{2} \\ +\frac{\delta b_1 - \delta b_2}{2} & +\frac{\delta c_1 - \delta c_2}{2} \end{pmatrix} \\ &= \overline{m}_D^{(0)} + \delta \overline{m}_D^{(s)} + \delta \overline{m}_D^{(a)} = \overline{m}_D^{(s)} + \delta \overline{m}_D^{(a)} \end{aligned} \quad (5.73)$$

where $b_1 \equiv b - \delta b_1$, $b_2 \equiv b - \delta b_2$, $c_1 \equiv c - \delta c_1$, and $c_2 \equiv c - \delta c_2$.

For the symmetric mass-matrix product, $\overline{m}_D \overline{m}_D^T = M_\nu / \widehat{m}_0 \equiv \overline{M}_\nu$, we compute, up to the NLO,

$$\begin{aligned} \overline{m}_D \overline{m}_D^T &= \begin{pmatrix} 1 & 0 & 0 \\ \frac{1}{2} & \frac{1}{2} & \frac{1}{2} \\ \frac{1}{2} & \frac{1}{2} & \frac{1}{2} \end{pmatrix} - (\delta b_1 + \delta b_2) \begin{pmatrix} 0 & \frac{a}{2} & \frac{a}{2} \\ b & b & b \end{pmatrix} - (\delta c_1 + \delta c_2) \begin{pmatrix} 0 & \frac{a'}{2} & \frac{a'}{2} \\ c & c & c \end{pmatrix} \\ &\quad - (\delta b_1 - \delta b_2) \begin{pmatrix} 0 & \frac{a}{2} & -\frac{a}{2} \\ b & 0 & -b \end{pmatrix} - (\delta c_1 - \delta c_2) \begin{pmatrix} 0 & \frac{a'}{2} & -\frac{a'}{2} \\ c & 0 & -c \end{pmatrix} \\ &\equiv \overline{M}_\nu^{(0)} + \delta \overline{M}_\nu^{(s)} + \delta \overline{M}_\nu^{(a)} = \overline{M}_\nu^{(s)} + \delta \overline{M}_\nu^{(a)}. \end{aligned} \quad (5.74)$$

where the $\overline{M}_\nu^{(s)}$ denotes the sum of the first three matrices and $\delta \overline{M}_\nu^{(a)}$ equals the sum of the last two matrices. For deriving the LO matrix $\overline{M}_\nu^{(0)}$ in (5.74) we have used the relations (2.14) for the IMO scheme. There exist two basic realizations for the common breaking of $\mu-\tau$ and CP symmetries in m_D or \overline{m}_D : one is for $\delta b_1 = \delta b_2 = 0$ and $(\delta c_1, \delta c_2) = c(\zeta', \zeta e^{i\omega})$, which corresponds to m_D in (2.18); and another is for $\delta c_1 = \delta c_2 = 0$ and $(\delta b_1, \delta b_2) = b(\zeta', \zeta e^{i\omega})$, which corresponds to m_D in (2.23). As we pointed out earlier, the invariance of the product (5.74) under $G_s \in \mathbb{Z}_2^s$ [cf. (5.72)] would be justified so long as our general consistency condition (5.36) could hold. So, with (5.74) we can explicitly compute $\tan 2\theta_s$ from the two expressions in (5.36) including the $\mu-\tau$ symmetric and anti-symmetric mass-matrix elements, respectively. We thus arrive at

$$\tan 2\theta_s^{(s)} = \frac{2\sqrt{2} B_s}{A - (C_s + D)} = -\frac{a'}{\sqrt{2} c}, \quad (5.75a)$$

$$\tan 2\theta_s^{(a)} = -\frac{2\sqrt{2}\delta B_a\delta C_a}{\delta C_a^2 - 2\delta B_a^2} = \frac{2\sqrt{2}a'c}{a'^2 - 2c^2} = \tan 4\theta_s^{(s)}, \quad (5.75b)$$

for $\delta b_1 = \delta b_2 = 0$, and

$$\tan 2\theta_s^{(s)} = \frac{2\sqrt{2}B_s}{A - (C_s + D)} = -\frac{a}{\sqrt{2}b}, \quad (5.76a)$$

$$\tan 2\theta_s^{(a)} = -\frac{2\sqrt{2}\delta B_a\delta C_a}{\delta C_a^2 - 2\delta B_a^2} = \frac{2\sqrt{2}ab}{a^2 - 2b^2} = \tan 4\theta_s^{(s)}, \quad (5.76b)$$

for $\delta c_1 = \delta c_2 = 0$. The above explicitly demonstrates the inequality $\theta_s^{(a)} \neq \theta_s^{(s)}$, and thus proves the violation of the consistency condition (5.36). This is because the $\mu - \tau$ anti-symmetric mass-matrix $\delta M_\nu^{(a)} = \hat{m}_0 \delta \bar{M}_\nu^{(a)}$ in (5.74) breaks the \mathbb{Z}_2^s symmetry. Hence, \mathbb{Z}_2^s is not a full symmetry of the mass-matrix M_ν . Nevertheless, we find that the $\mu - \tau$ symmetric part $M_\nu^{(s)} = \hat{m}_0 \bar{M}_\nu^{(s)}$ in (5.74) does respect the \mathbb{Z}_2^s symmetry, and its invariance equation (5.31a) leads to the correct solution (5.33) and thus (5.75a) for the solar angle θ_s . Substituting (5.21) into (5.75a) or (5.76a), we derive the equation, $k^2 + \frac{2}{r_0}k - 1 = 0$, with $r_0 \equiv \frac{a'}{\sqrt{2}c}$ corresponding to (5.75a), or $r_0 \equiv \frac{a}{\sqrt{2}b}$ corresponding to (5.76a). So we can fix the \mathbb{Z}_2^s group parameter k in terms of the ratio of seesaw mass-parameters in m_D ,

$$k = -1 \pm \sqrt{1 + r_0^2}. \quad (5.77)$$

Finally, we compute the other symmetric product $\bar{m}_D^T \bar{m}_D$, up to the NLO,

$$\bar{m}_D^T \bar{m}_D = \begin{pmatrix} 1 & 0 \\ 0 & 1 \end{pmatrix} - (\delta b_1 + \delta b_2) \begin{pmatrix} 2b & c \\ c & 0 \end{pmatrix} - (\delta c_1 + \delta c_2) \begin{pmatrix} 0 & b \\ b & 2c \end{pmatrix}. \quad (5.78)$$

The last two matrices of (5.78) arise from the $\mu - \tau$ breaking, which make $\bar{m}_D^T \bar{m}_D$ *non-diagonal* at the NLO, and thus explicitly violate the second invariance equation of (5.72). This violation of \mathbb{Z}_2^s does not directly lead to observable effect at low energies since the seesaw mass-matrix M_ν for light neutrinos is given by the first product $\bar{m}_D \bar{m}_D^T$ in Eq. (5.74). Also, we could choose to assign the right-handed neutrinos to be *singlet* under the \mathbb{Z}_2^s from the light neutrinos, i.e., $d_R = \mathcal{I}_2$, then the invariance equation for $\bar{m}_D \bar{m}_D^T$ becomes trivial. But the first invariance equation in (5.72) under $G_s \in \mathbb{Z}_2^s$ is still broken by the $\mu - \tau$ anti-symmetric mass-matrix $\delta M_\nu^{(a)} = \hat{m}_0 \delta \bar{M}_\nu^{(a)}$ in (5.74) for light neutrinos, as shown by Eq. (5.75) or (5.76) above.

From the analyses above, we conclude that the hidden symmetry \mathbb{Z}_2^s is a *partial symmetry* of the present model, respected by the $\mu - \tau$ symmetric part $M_\nu^{(s)}$ of the light neutrino mass-matrix, and thus determines the solar angle θ_s as in Eqs. (5.75a) and (5.77). This also agrees to the result (2.15) [Sec. 2.1] or (4.5) [Sec. 4.1] which we derived earlier. As a final remark, we stress that the violation of the hidden \mathbb{Z}_2^s symmetry by the $\mu - \tau$ anti-symmetric mass-matrix $\delta M_\nu^{(a)} = \hat{m}_0 \delta \bar{M}_\nu^{(a)}$ in (5.74) has an important physical impact: it predicts a *modified new correlation* (4.13), and can be *experimentally distinguished from Eq. (5.26)* as predicted before by our soft $\mu - \tau$ breaking of neutrino seesaw [1].

6. Conclusion

In this work, we have studied the common origin of $\mu-\tau$ breaking and CP violations in the neutrino seesaw with right-handed Majorana neutrinos being $\mu-\tau$ blind. The oscillation data strongly support $\mu-\tau$ symmetry as a good approximate symmetry in the light neutrino sector, leading to the zeroth order pattern, $(\theta_{23}, \theta_{13}) = (45^\circ, 0^\circ)$. Hence the $\mu-\tau$ breakings, together with the associated CP violations, are generically small. For the $\mu-\tau$ blind seesaw, we have convincingly formulated their common origin into Dirac mass matrix m_D (Sec. 2.2), leading to the unique inverted mass-ordering (IMO) of light neutrinos and distinct neutrino phenomenology. This is parallel to our previous work [1] where the common origin of $\mu-\tau$ and CP breaking arises from the Majorana mass matrix of the singlet right-handed neutrinos and uniquely leads to the normal mass-ordering (NMO) of light neutrinos.

In Sec. 3, we gave the model-independent reconstruction of low energy $\mu-\tau$ and CP breakings with inverted neutrino mass-spectrum. With this we derived various predictions of the $\mu-\tau$ blind neutrino seesaw in Sec. 4. In particular, we deduced a *modified new correlation* (4.13) between the two small $\mu-\tau$ breaking observables $\theta_{23} - 45^\circ$ and $\theta_{13} - 0^\circ$, as depicted in Fig. 2 and is very different from that in Ref. [1]. Eq. (4.13) is shown to also hold for the general three-neutrino seesaw in Sec. 4.3. This correlation can be experimentally tested against Eq. (4.15a) as deduced from our soft $\mu-\tau$ breaking seesaw mechanism [1]. As shown in Fig. 2 and Fig. 6, our predicted range of θ_{13} can saturate its present experimental upper bound. Imposing the current upper limit on θ_{13} , we derived a restrictive range of the deviation, $-4^\circ \leq \theta_{23} - 45^\circ \leq 4^\circ$ at 90% C.L., in Eq. (4.22). In Sec. 4.2, we have further generated the observed matter-antimatter asymmetry (the baryon asymmetry) from thermal leptogenesis in the $\mu-\tau$ blind seesaw. Under the successful leptogenesis, we derived the constrained correlation between $\theta_{23} - 45^\circ$ and $\theta_{13} - 0^\circ$, as presented in Fig. 6. This figure predicts a lower bound on the key mixing angle, $\theta_{13} \gtrsim 1^\circ$, which will be explored soon by the on-going reactor neutrino experiments at Daya Bay [10], Double-Chooz [12] and RENO [13]. Fig. 7(a) further constrains the Jarlskog invariant J into the negative range, $-0.037 \lesssim J \lesssim -0.0035$, while Fig. 7(b) predicts the range of neutrinoless $\beta\beta$ -decay observable, $45.5 \text{ meV} \lesssim M_{ee} \lesssim 50.7 \text{ meV}$, which can be probed by the on-going neutrinoless $\beta\beta$ -decay experiments [3]. A lower bound on the leptogenesis scale M_1 is inferred from Fig. 4, $M_1 > 3.5 \times 10^{13} \text{ GeV}$, and is given in Eq. (4.40). The correlations of the leptogenesis scale M_1 with the reactor angle θ_{13} and the Jarlskog invariant J are analyzed in Fig. 9(a)-(b).

Finally, we have studied the determination of solar mixing angle θ_{12} and its connection to a hidden flavor symmetry \mathbb{Z}_2^s and its possible breaking in Sec. 5. The general model-independent $\mathbb{Z}_2 \otimes \mathbb{Z}_2$ symmetry structure of light neutrino sector was analyzed in Sec. 5.2.1. We first reconstructed the 3-dimensional representation G_s^0 for \mathbb{Z}_2^s group in the $\mu-\tau$ symmetric limit as in Eq. (5.19). We proved that *hidden symmetry \mathbb{Z}_2^s holds for any $\mu-\tau$ symmetric mass-matrix M_ν of light neutrinos* and determines the solar angle θ_{12} via its group parameter, $k = \tan \theta_{12}$, as in Eq. (5.21). Then,

requiring that \mathbb{Z}_2^s persists *in the presence of general $\mu-\tau$ breaking*, i.e., $G_s = G_s^0$ as in (5.25), we deduce a unique correlation equation (5.26) which strikingly coincides with Eq. (4.15a), as predicted by our soft $\mu-\tau$ breaking seesaw [1]. In Sec. 5.2.2, we further analyzed the validity of \mathbb{Z}_2^s symmetry from general model-independent reconstructions of light neutrino mass-matrix M_ν . We derived the general consistency condition (5.36) for the validity of \mathbb{Z}_2^s symmetry in the presence of all possible $\mu-\tau$ breakings. Under this condition, we derived the nontrivial correlation (5.42a) or (5.49a) between the two $\mu-\tau$ breaking observables $\theta_{23} - 45^\circ$ and $\theta_{13} - 0^\circ$, which agrees to Eq. (5.26) as derived earlier from pure group theory approach. We stress that the agreement between (5.26) [or (5.42a)] and the prediction (4.15a) from our soft $\mu-\tau$ breaking seesaw is not a coincidence. As we explained in Sec. 5.3.1, the true reason lies in the fact that the soft $\mu-\tau$ breaking is uniquely embedded in the right-handed Majorana mass-matrix M_R which is a singlet of the \mathbb{Z}_2^s group and thus does not violate \mathbb{Z}_2^s . On the other hand, for the $\mu-\tau$ blind seesaw, the $\mu-\tau$ breaking is solely confined in the Dirac mass-matrix m_D which would have nontrivial transformation (5.70) or (5.72) *if* \mathbb{Z}_2^s could actually hold. As we have verified in Sec. 5.3.2, the invariance equation (5.72) hold only for the $\mu-\tau$ symmetric part of the light neutrino mass-matrix M_ν , and is *partially violated by its $\mu-\tau$ anti-symmetric part* [cf. Eq. (5.74)]. In consequence, we found: (i) the solar mixing angle θ_{12} is dictated by the group parameter k of the hidden symmetry \mathbb{Z}_2^s acting on the $\mu-\tau$ symmetric mass-matrix $M_\nu^{(s)}$ [cf. Eqs. (5.75a) and (5.77)]; (ii) the consistency condition (5.36) no longer holds, and we predicted a *modified new correlation* (4.13), which can be experimentally distinguished from Eq. (4.15a) as predicted by our soft $\mu-\tau$ breaking seesaw [1]. In contrast to our previous prediction (4.15a), Fig. 6 points to an important feature of the new correlation (4.13) by showing a more rapid increase of θ_{13} as a function of $\theta_{23} - 45^\circ$ [cf. also (4.20a)]; *this allows θ_{13} to saturate the current experimental upper limit*, and confines the deviation $\theta_{23} - 45^\circ$ into a more restrictive range, $-4^\circ \leq \theta_{23} - 45^\circ \leq 4^\circ$ at 90% C.L., as in Eq. (4.22). These distinctive predictions of the present $\mu-\tau$ blind seesaw can be systematically tested against those of our previous soft $\mu-\tau$ breaking seesaw [1], by the on-going and upcoming neutrino experiments.

Note Added in Proof:

After the submission of this paper to arXiv:1104.2654 on April 14, 2011, two long-baseline accelerator experiments newly announced evidences for θ_{13} via the $\nu_\mu \rightarrow \nu_e$ appearance channel, one by the T2K Collaboration [58] on June 14, 2011 and another by the Minos Collaboration [59] on June 24, 2011. Minos reported 62 e -like events above an estimated background of 49 events, and favors a nonzero θ_{13} at 1.5σ level. The resultant confidence interval yields, $0 \leq \sin^2 2\theta_{13} < 0.12$ (0.19) at 90% C.L. for NMO (IMO) with $\delta_D = 0$; and the best-fit value is $\sin^2 2\theta_{13} = 0.04$ (0.08) for NMO (IMO). On the other hand, the T2K experiment observed 6 e -like events with an estimated background of 1.5 events, indicating a nonzero θ_{13} at 2.5σ level. This gives the 90% C.L. limits, 0.03 (0.04) $< \sin^2 2\theta_{13} < 0.28$ (0.34) for NMO (IMO) with $\delta_D = 0$; and the best-fit value is $\sin^2 2\theta_{13} = 0.11$ (0.14)

for NMO (IMO). These new data indicate a relatively large θ_{13} mixing angle,

$$\text{T2K: } 5.0^\circ < \theta_{13} (9.7^\circ) < 16.0^\circ, \quad (\text{for NMO}), \quad (6.1\text{a})$$

$$5.8^\circ < \theta_{13} (11.0^\circ) < 17.8^\circ, \quad (\text{for IMO}); \quad (6.1\text{b})$$

$$\text{Minos: } 0^\circ \leq \theta_{13} (5.8^\circ) < 10.1^\circ, \quad (\text{for NMO}), \quad (6.1\text{c})$$

$$0^\circ \leq \theta_{13} (8.2^\circ) < 12.9^\circ, \quad (\text{for IMO}); \quad (6.1\text{d})$$

at 90% C.L., where the central values are shown in the parentheses. We would like to point out that *the new data from T2K and Minos further support our theory predictions* which give the unique inverted mass-ordering (IMO) and favors a naturally larger θ_{13} even for a rather small deviation of $\theta_{23} - 45^\circ$, as shown in Eq. (4.20a) and our Fig. 2 (Sec. 4.1) or Fig. 6 (Sec. 4.2).

Shortly afterwards, a new global analysis of oscillation data has been performed [60] to include the latest T2K and Minos data. With this we can update our Table-1 accordingly, and translate the improvements [60] into the new Table 2.

Parameters	Best Fit	90% C.L.	99% C.L.	1σ Limits	3σ Limits
$\Delta m_{21}^2 (10^{-5}\text{eV}^2)$	7.58	7.15 – 7.94	7.07 – 8.09	7.32 – 7.80	6.99 – 8.18
$\Delta m_{13}^2 (10^{-3}\text{eV}^2)$	2.35	2.20 – 2.55	2.10 – 2.63	2.26 – 2.47	2.06 – 2.67
θ_{12}	33.6°	$32.0^\circ – 35.4^\circ$	$31.0^\circ – 36.4^\circ$	$32.6^\circ – 34.7^\circ$	$30.6^\circ – 36.8^\circ$
θ_{23}	40.4°	$37.5^\circ – 47.9^\circ$	$36.3^\circ – 51.3^\circ$	$38.6^\circ – 45.0^\circ$	$35.7^\circ – 53.1^\circ$
θ_{13}	8.3°	$5.09^\circ – 10.4^\circ$	$3.5^\circ – 11.6^\circ$	$6.5^\circ – 9.6^\circ$	$1.8^\circ – 12.1^\circ$

Table 2: The updated global analysis [60] by including the latest data from Minos [59] and T2K [58] long-baseline accelerator experiments. (Using the new reactor fluxes will slightly shift the mixing angles θ_{12} and θ_{13} a bit as shown in [60].)

With Table-2, we have systematically updated our numerical analyses in Sec. 4. We find that the predictions of Fig. 2, Fig. 6 and Fig. 4 exhibit more constrained parameter space in an interesting way, while the other figures remain largely the same as before. For comparison, we use the updates in Table-2 and replot Figs. 2, 6, 4 as new Fig. 10, Fig. 11 and Fig. 12, respectively. In Figs. 10 and 11, we see that the updated 90% C.L. constraint on θ_{13} (yellow area) just picks up the central region of our predicted theory parameter-space. Comparing the two plots in Figs. 10-11, we see that imposing successful leptogenesis in Fig. 11 makes the parameter space more centered along the two wings, and the region around $\theta_{23} \sim 45^\circ$ is clearly disfavored. Since the new global fit of Table-2 gives the 90% C.L. limits, $-7.5^\circ < \theta_{23} - 45^\circ < 2.9^\circ$, with a central value $\theta_{23} - 45^\circ = -4.6^\circ$, it is clear that the left-wing of the theory parameter-space is more favored over the right-wing. Furthermore, imposing the θ_{23} and θ_{13} limits from Table-2 on our parameter-space in Fig. 11, we deduce the allowed range at 90% C.L., $-4.8^\circ < \theta_{23} - 45^\circ < 2.9^\circ$, which is shifted towards the negative side by about 1° as compared to Eq. (4.22).

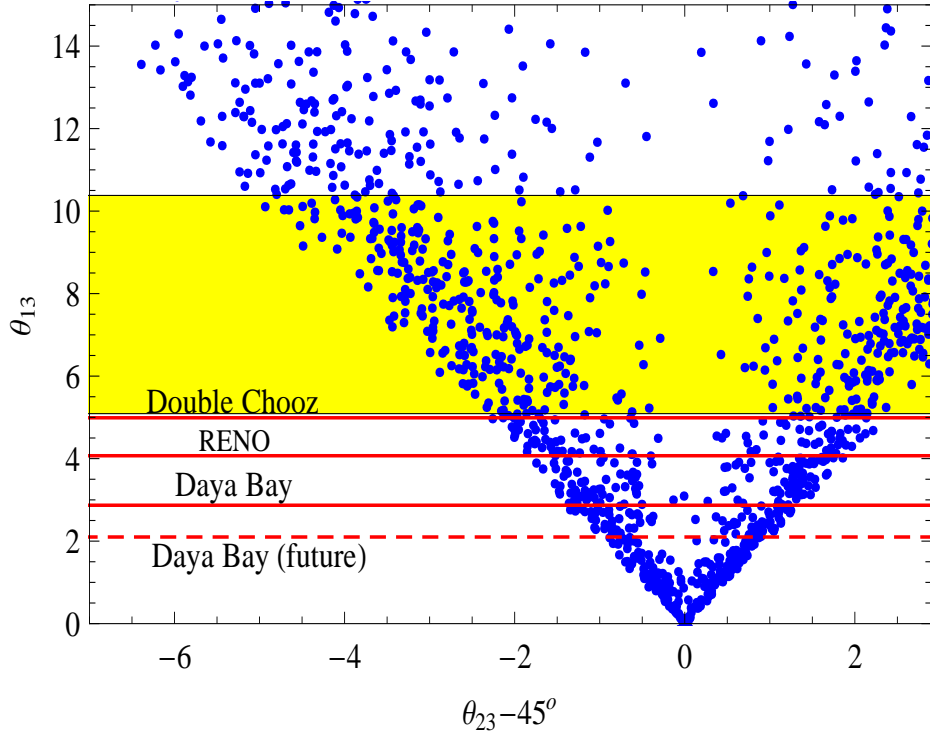


Figure 10: Update of Fig. 2 (Sec. 4.1) by using the improved global fit in Table-2, with 2000 samples. The shaded region (yellow) shows the updated constraint on θ_{13} at 90% C.L.

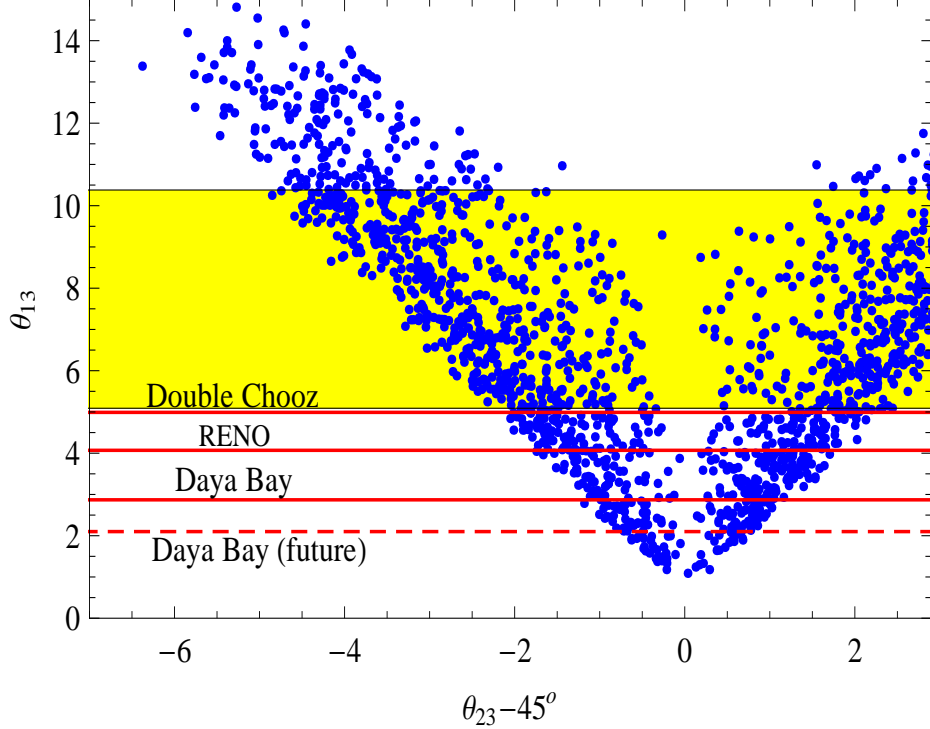


Figure 11: Update of Fig. 6 (Sec. 4.2) by using the improved global fit in Table-2, with 2000 samples. The shaded region (yellow) shows the updated constraint on θ_{13} at 90% C.L.

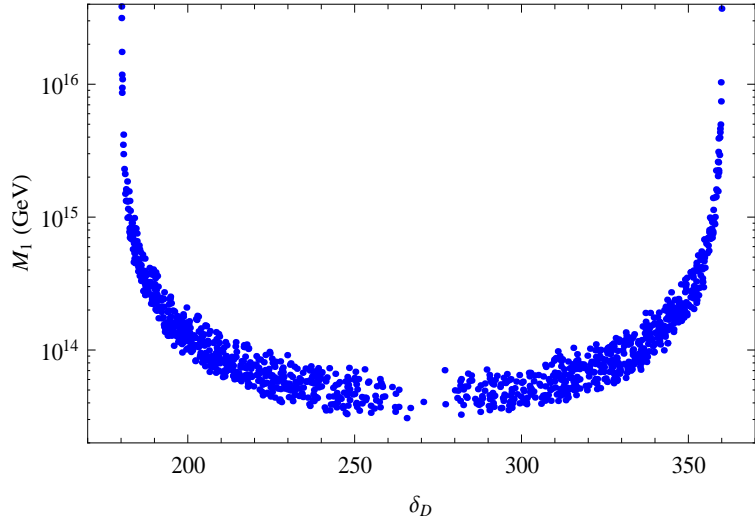


Figure 12: Update of Fig. 4 (Sec. 4.2) by using the improved global fit in Table-2, with 1200 samples.

Then, Fig. 12 shows that the predicted parameter region in the $M_1 - \delta_D$ plane is much more centered along the two edges in Fig. 4, and a high leptogenesis scale $M_1 > 10^{15}$ GeV is strongly excluded except for the tiny regions of the CP-angle δ_D very close to 180° and 360° .

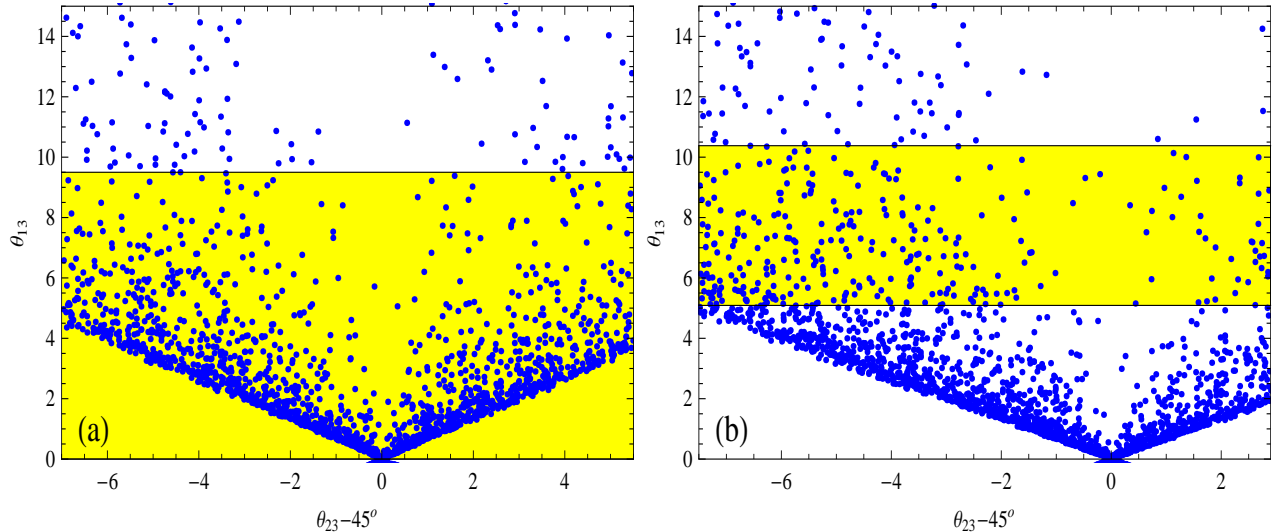


Figure 13: Correlation of θ_{13} and $\theta_{23} - 45^\circ$ as predicted by our Eq. (5.26) [Sec. 5.2] without seesaw and under the assumption of exact \mathbb{Z}_2^s symmetry. Plot-(a) shows the correlation by using the global fit in Table-1, while plot-(b) depicts the correlation under the improved global fit in Table-2, with 2000 samples in each plot. The shaded regions (yellow) give the allowed 90% C.L. ranges by the corresponding global fit.

Finally, as a comparison, we further analyze the prediction from our Eq. (5.26) [Sec. 5.2] which we derived for light neutrinos alone (without invoking seesaw) and under the assumption of an exact \mathbb{Z}_2^s symmetry. As we already proved in Sec. 5.3, this \mathbb{Z}_2^s only holds in a class of models including our soft $\mu - \tau$ and CP breaking model in Ref. [1], but can be violated in other class of models including the current $\mu - \tau$ blind seesaw model. Hence, *the \mathbb{Z}_2^s symmetry cannot generally hold in a model*

independent way. With Eq. (5.26), we plot the correlation between the $\mu - \tau$ breaking parameters θ_{13} and $\theta_{23} - 45^\circ$ in Fig. 13(a)-(b). In plot-(a) we show the correlation by using the global fit in Table-1, while in plot-(b) we depict the correlation under the improved global fit in Table-2. Each plots contains 2000 samples. The shaded regions (yellow) display the allowed 90% C.L. parameter space by the corresponding global fit. Note that Eq. (5.26) holds for both normal mass ordering and inverted mass ordering of light neutrinos. Fig. 13 shows that our predicted parameter space can easily saturate the current upper limit on θ_{13} , and thus accommodates a relatively large θ_{13} as indicated by the new data from T2K [58] and Minos [59]. The prediction of Fig. 13 differs from the above Fig. 10 significantly, because the coefficient in Eq. (4.18a) [corresponding to Fig. 10] has a nontrivial suppression factor relative to that of Eq. (4.18b) or Eq. (5.26) [corresponding to Fig. 13]. Furthermore, we note that the above Fig. 13 should also be compared to our previous Fig. 2 in Ref. [1] because the correlation (5.26) applies to both of them. But there are large differences between these two figures, the major reason is that we input the parameter $\theta_{23} - 45^\circ$ in Fig. 13 according to the oscillation data (Table-1 or Table-2) and without invoking seesaw, while the $\theta_{23} - 45^\circ$ in the Fig. 2 of Ref. [1] was derived as a function of fundamental $\mu - \tau$ and CP breaking parameters in the seesaw Lagrangian which were scanned within their theoretically allowed ranges. This also leads to a stronger upper limit of $\theta_{13} \lesssim 6^\circ$ in Ref. [1].

Note Added-2 :

After the publication of this paper in Phys. Rev. D 84 (2011) 033009, Daya Bay and RENO collaborations announced new measurements of nonzero θ_{13} on March 8, 2012 [61] and April 8, 2012 [62], respectively. Daya Bay experiment made a 5.2σ discovery of nonzero θ_{13} [61], $\sin^2 2\theta_{13} = 0.092 \pm 0.016(\text{stat}) \pm 0.005(\text{syst})$; and RENO found a nonzero θ_{13} at 4.9σ level [62], $\sin^2 2\theta_{13} = 0.113 \pm 0.013(\text{stat}) \pm 0.019(\text{syst})$. These give the following 3σ ranges of nonzero θ_{13} ,

$$\text{Daya Bay: } 5.7^\circ < \theta_{13} (8.8^\circ) < 11.1^\circ, \quad (6.2a)$$

$$\text{RENO: } 5.9^\circ < \theta_{13} (9.8^\circ) < 12.6^\circ, \quad (6.2b)$$

where the numbers in the parentheses $\theta_{13} = 8.8^\circ$ and $\theta_{13} = 9.8^\circ$ correspond to the central values.

Then, we can re-plot the Fig. 10, Fig. 11 and Fig. 13(b) as the new Fig. 14, Fig. 15 and Fig. 16, respectively. In these new plots, we have scanned the experimental inputs within 3σ ranges. For the successful leptogenesis, we find that the lower bound on the leptogenesis scale M_1 becomes, $M_1 > 2 \times 10^{13}$, at 3σ level. The successful leptogenesis in Fig. 15 further requires, $\theta_{13} \gtrsim 1^\circ$.

To compare with our predictions, we have displayed the 3σ range of θ_{13} from the new Daya Bay measurement [61] in the green shaded region. Furthermore, we show the 3σ lower and upper limits of θ_{13} from the new RENO data [62] by the horizontal red-lines. The horizontal black dashed-lines in each plot denote the 3σ limits from the global fit [60]. From Figs. 14-15, we see that the new limits from Daya Bay [61] and RENO [62] experiments nicely pick up the central regions of our predicted

parameter space of θ_{13} .

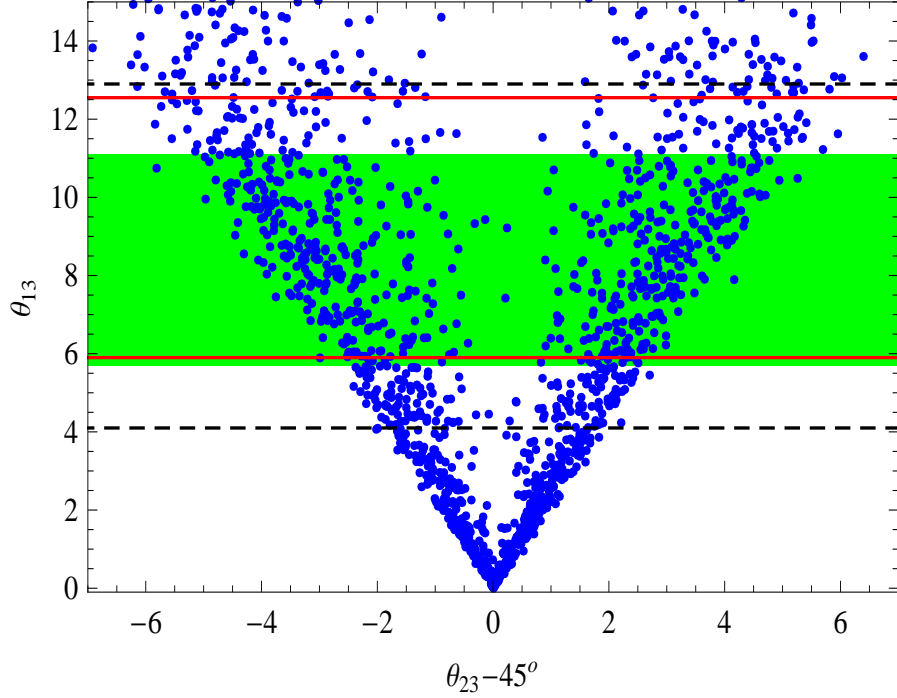


Figure 14: Update of Fig. 10, with 2000 samples. The experimental inputs are scanned within 3σ ranges. The 3σ ranges of the new Daya Bay data [61] are shown as the green shaded region; and the 3σ limits of the new RENO data [62] are depicted by the horizontal red-lines. The horizontal black dashed-lines denote the 3σ limits of the global fit [60].

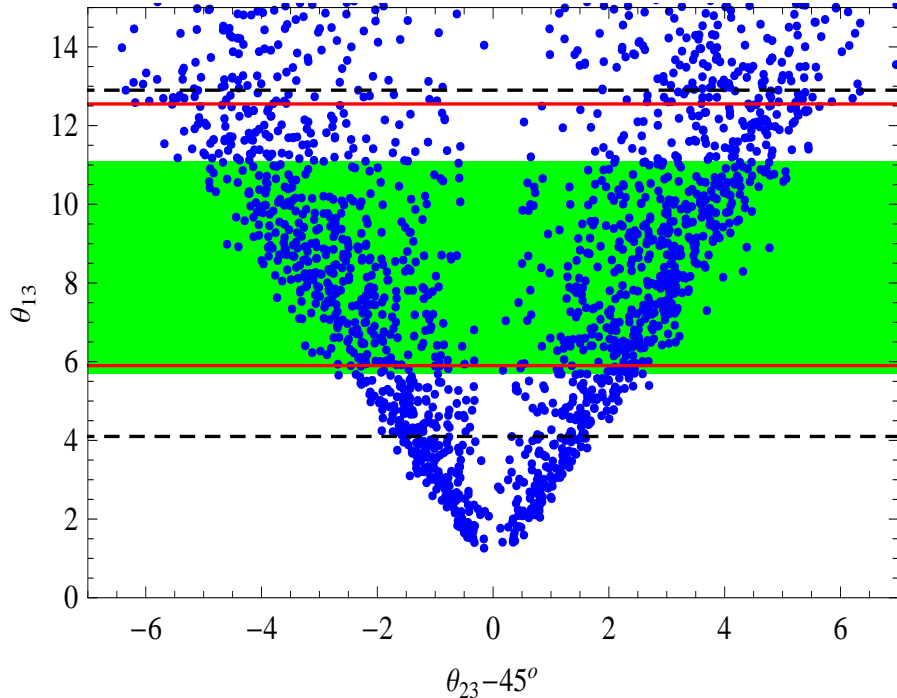


Figure 15: Update of Fig. 11, with 2000 samples. The experimental inputs are scanned within 3σ ranges. The 3σ ranges of the new Daya Bay data [61] are shown as the green shaded region; and the 3σ limits of the new RENO data [62] are depicted by the horizontal red-lines. The horizontal black dashed-lines denote the 3σ limits of the global fit [60].

Finally, Fig. 16 shows the correlation of θ_{13} and $\theta_{23} - 45^\circ$ as predicted by our Eq. (5.26) [Sec. 5.2] under the assumption of an exact \mathbb{Z}_2^s symmetry and without invoking seesaw. We have scanned the 3σ ranges of θ_{12} in (5.26). We see that the new data of Daya Bay [61] and RENO [62] pick up the upper parts of our predicted parameter space of θ_{13} .

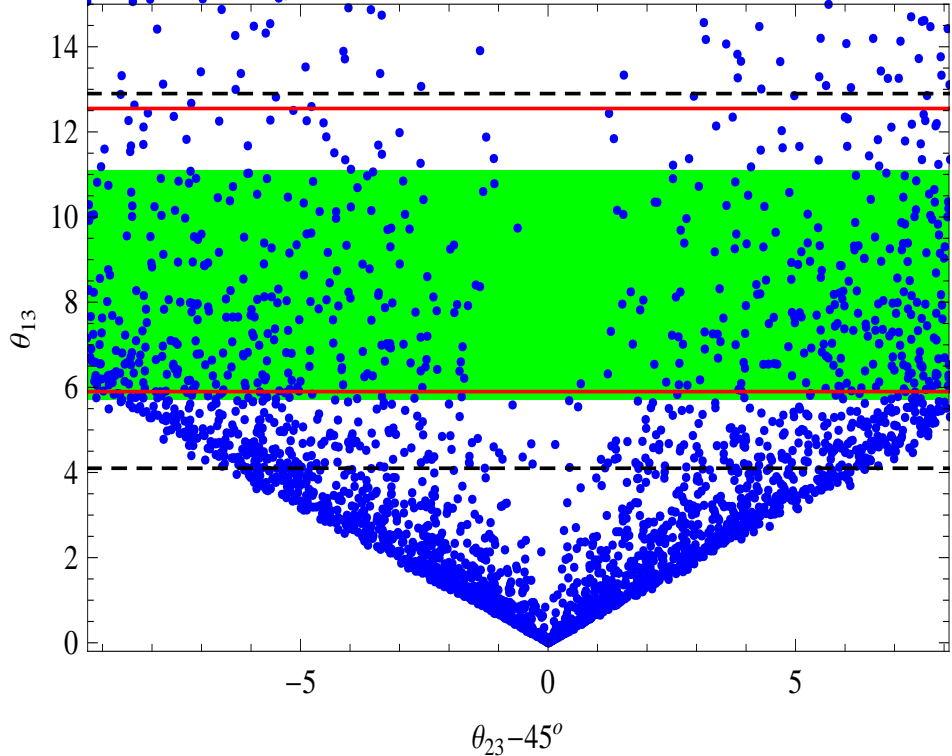


Figure 16: Correlation of θ_{13} and $\theta_{23} - 45^\circ$ as predicted by our Eq. (5.26) without seesaw and under the assumption of exact \mathbb{Z}_2^s symmetry, with 2000 samples. The experimental inputs are scanned within 3σ ranges. The 3σ ranges of the new Daya Bay data [61] are shown as the green shaded region; and the 3σ limits of the new RENO data [62] are depicted by the horizontal red-lines. The horizontal black dashed-lines denote the 3σ limits of the global fit [60].

Acknowledgments

We thank C. S. Lam, Rabindra N. Mohapatra, Werner Rodejohann and Alexei Yu. Smirnov for useful discussions on this subject, and Eligio Lisi for discussing the updated global fit [60] in connection with the new data from T2K [58] and Minos [59]. We are grateful to Yi-Fang Wang, Kam-Biu Luk and Jun Cao for discussing Daya Bay experiment [10]. We also wish to thank Profs. T. D. Lee and R. Friedberg for valuable correspondence and discussions on the comparison of θ_{13} predictions in our study and their work [36], which we showed at the end of Sec. 4.1 [cf. Eqs. (4.26)-(4.27)]. HJH thanks the Center for High Energy Physics at Peking University for kind hospitality and support. This research was supported by the NSF of China (under grants 10625522 and 10635030), the National Basic Research Program of China (under grant 2010CB833000), and by Tsinghua University.

References

- [1] S.-F. Ge, H.-J. He, F.-R. Yin, JCAP **05**, 017 (2010) [arXiv:1001.0940].
- [2] For recent reviews, *e.g.*, A. Yu. Smirnov, arXiv:1103.3461 and arXiv:0910.1778; G. Altarelli, arXiv:1011.5342 and arXiv:0905.3265; M. Dierckxens, arXiv:0911.1039 [hep-ex]; R. N. Mohapatra and A. Yu. Smirnov, Ann. Rev. Nucl. Part. Sci. **56**, 569 (2006) [arXiv:hep-ph/0603118]; A. Strumia and F. Vissani, arXiv:hep-ph/0606054; and references therein.
- [3] For reviews on neutrinoless double-beta decays, *e.g.*, W. Rodejohann, “Neutrinoless Double Beta Decay and Particle Physics”, arXiv:1106.1334 [hep-ph]; P. Vogel, arXiv:0807.1559 [hep-ph]; S. R. Elliott and P. Vogel, Ann. Rev. Nucl. Part. Sci. **52**, 115 (2002) [arXiv:hep-ph/0202264]; and references therein. For more recent studies, *e.g.*, A. Dueck, W. Rodejohann and K. Zuber, arXiv:1103.4152; J. Menendez, D. Gazit and A. Schwenk, arXiv:1103.3622; S. M. Bilenky, A. Faessler, W. Potzel and F. Simkovic, arXiv:1104.1952; and references therein.
- [4] M. C. Gonzalez-Garcia, M. Maltoni, J. Salvado, JHEP **1004**, 056 (2010) [arXiv:1001.4524]; JHEP **1008**, 117 (2010) [arXiv:1006.3795]; and references therein.
- [5] G. L. Fogli, E. Lisi, A. Marrone, A. Palazzo, and A. M. Rotunno, Phys. Rev. Lett. **101**, 141801 (2008) [arXiv:0806.2649] and arXiv:0809.2936 [hep-ph]; G. L. Fogli *et al.*, arXiv:0805.2517v3 [hep-ph] and Phys. Rev. D **78**, 033010 (2008); J. Phys. Conf. Ser. **203**, 012103 (2010); and references therein.
- [6] A. Yu. Smirnov, private communication; M. C. Gonzalez-Garcia, M. Maltoni and A. Yu. Smirnov, Phys. Rev. D **70**, 093005 (2004) [arXiv:hep-ph/0408170]; O. L. G. Peres and A. Yu. Smirnov, Phys. Rev. D **79**, 113002 (2009) [arXiv:0903.5323].
- [7] P. Adamson *et al.*, [MINOS Collaboration], arXiv:arXiv:0909.4996 and Phys. Rev. Lett. **101**, 131802 (2008) [arXiv:0806.2237].
- [8] Y. Itow *et al.*, [T2K Collaboration], arXiv:hep-ex/0106019; K. Abe *et al.*, [T2K Collaboration], Nucl. Instrum. Meth. A **659**, 106 (2011) [arXiv:1106.1238 [hep-ex]].
- [9] For a nice recent review, M. Mezzetto and T. Schwetz, “ θ_{13} : Phenomenology, Present Status and Prospect”, J. Phys. G **37**, 103001 (2010) [arXiv:1003.5800v2].
- [10] Y.-F. Wang [Daya Bay Collaboration], arXiv:hep-ex/0610024; J. Cao [Daya Bay Collaboration], Nucl. Phys. Proc. Suppl. **155**, 229 (2006); X. Guo *et al.* [Daya Bay Collaboration], arXiv:hep-ex/0701029; W. Wang [Daya Bay Collaboration], arXiv:0910.4605 [hep-ex]; M.-C. Chu [Daya Bay Collaboration], arXiv:0810.0807 [hep-ex]; C.-J. Lin [Daya Bay Collaboration], PoS (ICHEP 2010) 305 [arXiv:1101.0261 [hep-ex]]; Y.-F. Wang, K.-B. Luk, J. Cao, private communications. For the web link to Daya Bay Experiment (China-USA Collaboration), <http://dayawane.ihep.ac.cn>.
- [11] The Daya Bay reactor neutrino experiment is going to start data-taking by the middle of 2011 [10].
- [12] C. Palomares, [Double-Chooz Collaboration], EPS-HEP-2009, arXiv:0911.3227; F. Ardellier *et al.*, [Double Chooz Collaboration], arXiv:hep-ex/0606025; F. Ardellier *et al.*, arXiv:hep-ex/0405032. C. Bauera *et al.*, arXiv:1104.0758.

- [13] S. B. Kim [RENO Collaboration], AIP Conf. Proc. **981**, 205 (2008) [J. Phys. Conf. Ser. **120**, 052025 (2008)].
- [14] D. S. Ayres *et al.*, [NO ν A Collaboration], hep-ex/0503053. R. Roy [NO ν A Collaboration], J. Phys. (Conf. Series) **136**, 022019 (2008).
- [15] J. Peltoniemi, arXiv:0911.4876 [hep-ex], and references therein.
- [16] E. Komatsu *et al.*, [WMAP Collaboration], “Seven-Year WMAP Observations: Cosmological Interpretation”, Astrophys. J. Suppl. **192**, 18 (2011) [arXiv:1001.4538].
- [17] Particle Data Group, K. Nakamura *et al.*, J. Phys. G **37**, 075021 (2010).
- [18] The data already slightly favored a smaller θ_{23} than its maximal value back in 2004 [6]. Although this small deviation $\theta_{23} - 45^\circ < 0$ is not yet statistically significant, the tendency of having a negative $\theta_{23} - 45^\circ$ is found to be robust, due to the excess of e -like atmospheric neutrino events in the sub-GeV sample [6].
- [19] E.g., R. N. Mohapatra and A. Yu. Smirnov in Ref. [2] for a recent review covering this topic, and references therein. For a partial list of some recent studies, T. Fukuyama and H. Nishiura, hep-ph/9702253; R. N. Mohapatra and S. Nussinov, Phys. Rev. D **60**, 013002 (1999) [hep-ph/9809415]; C. S. Lam, Phys. Lett. B **507**, 214 (2001) [hep-ph/0104116]; W. Grimus and L. Lavoura, JHEP **0107**, 045 (2001) [hep-ph/0105212]; E. Ma, Phys. Rev. D **66**, 117301 (2002) [hep-ph/0207352]; P. F. Harrison and W. G. Scott, Phys. Lett. B **547**, 219 (2002) [hep-ph/0210197]; W. Grimus and L. Lavoura, Phys. Lett. B **572**, 189 (2003) [hep-ph/0305046]; R. N. Mohapatra and S. Nasri, Phys. Rev. D **71**, 033001 (2005) [hep-ph/0410369]; W. Grimus, A. S. Joshipura, S. Kaneko, L. Lavoura, H. Sawanaka, M. Tanimoto, Nucl. Phys. B **713**, 151 (2005) [hep-ph/0408123]; R. N. Mohapatra, JHEP **0410**, 027 (2004) [hep-ph/0408187]; C. S. Lam, Phys. Rev. D **71**, 093001 (2005) [hep-ph/0503159]; T. Kitabayashi and M. Yasue, Phys. Lett. B **621**, 133 (2005) [hep-ph/0504212]; R. N. Mohapatra and W. Rodejohann, Phys. Rev. D **72**, 053001 (2005) [hep-ph/0507312]; W. Grimus, S. Kaneko, L. Lavoura, H. Sawanaka, M. Tanimoto, JHEP **0601**, 110 (2006) [hep-ph/0510326]; K. Fuki and M. Yasue, Phys. Rev. D **73**, 055014 (2006) [hep-ph/0601118]; R. N. Mohapatra, S. Nasri, H. B. Yu, Phys. Lett. B **636**, 114 (2006) [hep-ph/0603020]; T. Ota and W. Rodejohann, Phys. Lett. B **639**, 322 (2006) [hep-ph/0605231]; Z. Z. Xing, Phys. Rev. D **74**, 013009 (2006) [hep-ph/0605219]; T. Baba and M. Yasue, Prog. Theor. Phys. **123**, 659 (2010) [arXiv:1003.1438]; Phys. Rev. D **77**, 075008 (2008) [arXiv:0710.2713]; Phys. Rev. D **75**, 055001 (2007) [hep-ph/0612034]; B. Adhikary, A. Ghosal, P. Roy, JHEP **0910**, 040 (2009) [arXiv:0908.2686]; M. Abbas and A. Yu. Smirnov, Phys. Rev. D **82**, 013008 (2010) [arXiv:1004.0099]; B. Adhikary, A. Ghosal, P. Roy, JCAP **1101**, 025 (2011) [arXiv:1009.2635]; T. Araki and C. Q. Geng, Phys. Lett. B **694**, 113 (2010) [arXiv:1006.0629]; S. Antusch, S. F. King, C. Luhn, M. Spinrath, Nucl. Phys. B **850**, 477 (2011) [arXiv:1103.5930]; and references therein.
- [20] J. N. Abdurashitov *et al.*, Phys. Rev. C **80**, 015807 (2009) [arXiv:0901.2200].
- [21] P. Minkowski, Phys. Lett. B **67**, 421 (1977); T. Yanagida, in Proceedings of Workshop on Unified Theories and Baryon Number in the Universe, p.95, eds. O. Sawada and A. Sugamoto, Japan, Feb. 13-14, 1979; S. L. Glashow, in Proceedings of the 1979 Cargese Summer Institute on Quarks and Leptons, p.687, eds. M. Levy, *et al.*, Cargese, July 9-29, 1979; M. Gell-Mann, P. Ramond, and R. Slansky, in Supergravity, p.315, eds. D. Freedman, *et al.*; R. N. Mohapatra and G.

Senjanovic, Phys. Rev. Lett. **44**, 912 (1980); J. Schechter and J. W. F. Valle, Phys. Rev. D **22**, 2227 (1980).

- [22] P. H. Frampton, S. L. Glashow, T. Yanagida, Phys. Lett. B **548**, 119 (2002) [arXiv:hep-ph/0208157]; M. Raidal and A. Strumia, Phys. Lett. B **553**, 72 (2003) [arXiv:hep-ph/0210021]. For reviews, *e.g.*, S. L. Glashow, arXiv:hep-ph/0306100; W. L. Guo, Z. Z. Xing, S. Zhou. Int. J. Mod. Phys. E**16**, 1 (2007); and references therein.
- [23] V. Barger, D. A. Dicus, H.-J. He, T. Li, Phys. Lett. B **583**, 173 (2004) [arXiv:hep-ph/0310278].
- [24] E.g., C. S. Lam, Phys. Rev. D **78**, 073015 (2008); G. Altarelli and F. Feruglio, Rev. Mod. Phys. **82**, 2701 (2010) [arXiv:1002.0211]; A. Yu. Smirnov, arXiv:1103.3461; and references therein.
- [25] E.g., S. Antusch, J. Kersten, M. Lindner, M. Ratz, Nucl. Phys. B **674**, 401 (2003) [arXiv:hep-ph/0305273]; S. Antusch, *et al.*, JHEP **0503**, 024 (2005) [arXiv:hep-ph/0501272]; J. A. Casas, J. R. Espinosa, A. Ibarra, I. Navarro, Nucl. Phys. B **573**, 652 (2000) [arXiv:hep-ph/9910420]; P. H. Chankowski, W. Krolkowski, S. Pokorski, Phys. Lett. B **473**, 109 (2000) [arXiv:hep-ph/9910231]; P. H. Chankowski and Z. Pluciennik, Phys. Lett. B **316**, 312 (1993); and references therein.
- [26] Here the RHS of (3.17) also contains flavor-dependent terms which are suppressed at least by the square of tau-lepton Yukawa coupling, $y_\tau^2 = \mathcal{O}(10^{-4})$, relative to the universal $\hat{\alpha}$ -term, and thus completely negligible for the present study.
- [27] For recent reviews of electroweak precision fit, *e.g.*, J. Erler, arXiv:0907.0883; P. Langacker, arXiv:0901.0241; and references therein.
- [28] B. Pontecorvo, Sov. Phys. JETP **6**, 429 (1957); Z. Maki, M. Nakagawa and S. Sakata, Prog. Theor. Phys. **28**, 870 (1962).
- [29] N. Cabibbo, Phys. Rev. Lett. **10**, 531 (1963); M. Kobayashi and T. Maskawa, Prog. Theor. Phys. **49**, 652 (1973).
- [30] T. D. Lee, Phys. Rev. D **8**, 1226 (1973); Phys. Rept. **9**, 143 (1974).
- [31] H.-J. He and F.-R. Yin, work in preparation.
- [32] P. Huber, M. Lindner, T. Schwetz, and W. Winter, JHEP **0911**, 044 (2009) [arXiv:0907.1896].
- [33] E.g., see the report “Physics at a future neutrino factory and super-beam facility”, [The ISS Physics Working Group], arXiv:0710.4947; D. M. Kaplan, arXiv:physics/0507023 [physics.acc-ph], in the proceedings of Lepton-Photon-2005 Conference, Uppsala, Sweden.
- [34] S. K. Agarwalla, P. Huber, J. Tang, W. Winter, “Optimization of the Neutrino Factory, revisited”, JHEP **1101**, 120 (2011) [arXiv:1012.1872]; and references therein.
- [35] C. Jarlskog, Phys. Rev. Lett. **55**, 1039 (1985); Z. Phys. C **29**, 491 (1985).
- [36] R. Friedberg and T. D. Lee, Chin. Phys. C **34**, 1547 (2010) [arXiv:1008.0453].
- [37] M. Fukugita and T. Yanagida, Phys. Lett. B **174**, 45 (1986).
- [38] For a recent review, W. Buchmuller, R. D. Peccei, T. Yanagida, Ann. Rev. Nucl. Part. Sci. **55**, 311 (2005) [arXiv:hep-ph/0502169]; and references therein.

- [39] For reviews, A. Riotto and M. Trodden, Ann. Rev. Nucl. Part. Sci. **49**, 35 (1999); M. Trodden, arXiv:hep-ph/0411301; and references therein.
- [40] A. D. Sakharov, Sov. Phys. JETP Lett. **5**, 24 (1967).
- [41] N. S. Manton, Phys. Rev. D **28**, 2019 (1983); V. Kuzmin, V. A. Rubakov, M. E. Shaposhnikov, Phys. Lett. **155B**, 36 (1985); J. Ambjorn, T. Askgaard, H. Porter, M. E. Shaposhnikov, Nucl. Phys. B **353**, 346 (1991).
- [42] G. 't Hooft, Phys. Rev. Lett. **37**, 8 (1976); Phys. Rev. D **14**, 3432 (1976).
- [43] J. A. Harvey and M. S. Turner, Phys. Rev. D **42**, 3344 (1990); S. Y. Khlebnikov and M. E. Shaposhnikov, Nucl. Phys. B **308**, 885 (1988).
- [44] W. Buchmuller, P. Di Bari, M. Plumacher, Annals Phys. **315**, 305 (2005) [arXiv:hep-ph/0401240]; New J. Phys. **6**, 105 (2004) [arXiv: hep-ph/0406014]; Nucl. Phys. B **643**, 367 (2002) [arXiv:hep-ph/0205349]; and references therein.
- [45] G. F. Giudice, A. Notari, M. Raidal, A. Riotto, and A. Strumia, Nucl. Phys. B **685**, 89 (2004) [arXiv:hep-ph/0310123]; A. Strumia, arXiv:hep-ph/0608347; and references therein.
- [46] A. Giuliani, [CUORE Collaboration], J. Phys. Conf. Ser. **120**, 052051 (2008).
- [47] V. E. Guiseppe *et al.*, [Majorana Collaboration], arXiv:0811.2446 [nucl-ex], in *Proceedings of 2008 IEEE Nuclear Science Symposium and Medical Imaging Conference*, Oct. 18-25, 2008, Dresden, Germany.
- [48] A. A. Smolnikov, [GERDA Collaboration], arXiv:0812.4194 [nucl-ex], in *Proceedings of 14th International School on Particles and Cosmology*, Baksan Valley, Russia, April 16-21, 2007.
- [49] B. Aharmin *et al.*, [SNO Collaboration], arXiv:0910.2984.
- [50] S. Abe *et al.*, [KamLand Collaboration], Phys. Rev. Lett. **100**, 221803 (2008).
- [51] These NLO elements are also generally given by the *model-independent reconstructions* in Sec. 3.2 with $m_3 = 0$ [cf. Eqs. (3.15a) and (3.16)], and in Sec. 5.2.2 with $m_3 \neq 0$ [cf. Eqs. (5.45a)-(5.45c)].
- [52] As we will further demonstrate in Sec. 5.3, this consistency condition is not always ensured in a given seesaw model, and thus the \mathbb{Z}_2^s symmetry could be partially broken, leading to modified correlation between the $\mu-\tau$ breaking observables.
- [53] W. Grimus and L. Lavoura, JHEP **0107**, 045 (2001) [arXiv:hep-ph/0105212].
- [54] For instance, a simple choice of such $d_\ell^{(j)}$ is, $d_\ell^{(1)} = \text{diag}(1, \eta, \eta^2) \in \mathbb{Z}_3$ with $\eta = \exp(i\frac{2\pi}{3})$, and \mathbb{Z}_3 is a subgroup of the general symmetry $\mathbb{G}_\ell = U(1) \otimes U(1)$ of lepton mass-matrix. The invariance of lepton mass-matrix $M_\ell M_\ell^\dagger$ under the transformation $F_1 = d_\ell^{(1)}$ automatically ensures left-handed leptons in their mass-diagonal basis.
- [55] The 3-dimensional representation (5.19b) of \mathbb{Z}_2^s was derived in Eq. (6.26) of Ref. [1] for our soft $\mu-\tau$ breaking seesaw model where the group parameter k (re-denoted as k' here) is related to the current k of (5.19b) by a simple notational conversion, $k' \equiv -\sqrt{2}/k$.

- [56] P. F. Harrison, D. H. Perkins and W. G. Scott, Phys. Lett. B **458**, 79 (1999); Phys. Lett. B **530**, 167 (2002); L. Wolfenstein, Phys. Rev. D **18**, 958 (1978).
- [57] C. S. Lam, Phys. Rev. D **78**, 073015 (2008) [arXiv:0809.1185]; Phys. Rev. Lett. **101**, 121602 (2008) [arXiv:0804.2622]; and references therein.
- [58] K. Abe *et al.*, [T2K Collaboration], “Indication of Electron Neutrino Appearance from an Accelerator-Produced Off-Axis Muon Neutrino Beam”, (June 14, 2011), arXiv:1106.2822 [hep-ex].
- [59] L. Whitehead, [Minos Collaboration], “Recent Results from Minos”, presentation at Joint Experimental-Theoretical Seminar, June 24, 2011, Fermilab, USA [http://theory.fnal.gov/jetp/talks/MINOSNue_2011June24.pdf]. The formal publication newly appeared on July 29, 2011, P. Adamson *et al.*, [Minos Collaboration], “Improved Search for Muon-Neutrino to Electron-Neutrino Oscillations in Minos”, arXiv:1108.0015 [hep-ex].
- [60] G. L. Fogli, E. Lisi, A. Marrone, A. Palazzo, and A. M. Rotunno, “Evidence of $\theta_{13} > 0$ from Global Neutrino Data Analysis”, arXiv:1106.6028 [hep-ph].
- [61] F. P. An *et al.*, [Daya Bay Collaboration], arXiv:1203.1669 [hep-ex].
- [62] J. K. Ahn *et al.*, [RENO Collaboration], arXiv:1204.0626.v2 [hep-ex].